UNIVERSITY OF SÃO PAULO
SCHOOL OF ANIMAL SCIENCE AND FOOD ENGINEERING

CARLOS ALBERTO VALENTIM JUNIOR

Fractional mathematical oncology: cancer-related dynamics under an interdisciplinary viewpoint

Pirassununga
2023

CARLOS ALBERTO VALENTIM JUNIOR

Fractional mathematical oncology: cancer-related dynamics under an interdisciplinary viewpoint

Corrected Version

Doctoral thesis presented to the Graduate Program in Engineering and Science of Materials at the School of Animal Science and Food Engineering, University of São Paulo, as a partial requirement for obtaining the title of Doctor of Science.

Area of concentration: Development, characterization and application of materials towards the agroindustry

Supervisor: Prof. Dr. José Antonio Rabi
Co-supervisor: Prof. Dr. Sergio Adriani David

Pirassununga
2023

Ficha catalográfica elaborada pelo
Serviço de Biblioteca e Informação, FZEA/USP,
com os dados fornecidos pelo(a) autor(a)

V155f

Valentim Jr., Carlos Alberto
Fractional mathematical oncology: cancer-related dynamics under an interdisciplinary viewpoint / Carlos Alberto Valentim Jr. ; orientador José Antonio Rabi ; coorientador Sergio Adriani David. -- Pirassununga, 2023.
136 f.

Tese (Doutorado - Programa de Pós-Graduação em Engenharia e Ciência de Materiais) -- Faculdade de Zootecnia e Engenharia de Alimentos, Universidade de São Paulo.

1. Matemática aplicada. 2. Oncologia. 3. Simulação. 4. Interdisciplinaridade. 5. Cálculo diferencial e integral. I. Rabi, José Antonio, orient. II. David, Sergio Adriani, coorient. III. Título.

To my parents, for their unwavering love and support, instrumental in making this achievement possible.

To Natalia, for being my anchor and source of strength throughout all these years.

ACKNOWLEDGEMENTS

First and foremost, I would like to express my sincerest gratitude to my supervisor, José Rabi, and my cosupervisor, Sergio David, for their invaluable guidance, mentorship, and support throughout my research. Their ever-present feedback, constructive criticism, and companionship have helped me shape not only this thesis but also my career and character.

I would also like to extend my gratitude to my friends, who have provided me with support, inspiration, enthusiastic discussions, and so many happy times.

I'm honored to acknowledge my peers and professors for all their insightful comments and feedback, which contributed to this work.

I owe a lot to my partner, Natalia Migueletti, whose unwavering love has been my constant source of strength and inspiration. Her encouragement and support have been instrumental in keeping me motivated and focused throughout this process. I am truly grateful for her presence in my life.

Last but not least, I'd like to thank my siblings, Carol and Gabriel Valentim, for their support and encouragement throughout my studies. I am deeply indebted to my parents, Carlos and Rosa Valentim, for their sacrifices and guidance in all stages of my life. Their belief in my abilities have been the driving force behind my story and shaped who I am.

This study was financed in part by the Coordenação de Aperfeiçoamento de Pessoal de Nível Superior - Brasil (CAPES) - Finance Code 001.

ABSTRACT

VALENTIM JR., C. A. **Fractional mathematical oncology: cancer-related dynamics under an interdisciplinary viewpoint**. 2023. 136p. Doctoral Thesis - School of Animal Science and Food Engineering, University of São Paulo, Pirassununga, 2023.

Mathematical Oncology, an interdisciplinary field incorporating concepts from biology to materials science, employs mathematical models to gain a comprehensive understanding of cancer-related phenomena. Fractional calculus, a branch of mathematical analysis, offers tools to describe complex phenomena and enables models the potential to provide better insights into oncological characteristics. This thesis surveys and explores Fractional Mathematical Oncology, presenting new models and reviewing recent developments. The thesis demonstrates the advantages of using fractional models in tumor growth prediction, specifically in ODE-based population models. Analytical solutions for five such models are derived and compared against extant (still scarce) clinical data, highlighting their superior performance and potential for further exploration. Additionally, a multistep exponential model with a fractional variable-order is proposed to represent tumor evolution. Model parameters are fine-tuned based on variable fractional order profiles, and results demonstrate its superior ability to fit clinical time series data, offering new perspectives for modeling tumor growth. Moreover, the thesis introduces cellular-automata simulation strategies in the context of tumor growth and dynamic models. This agent-based computational model allows for monitoring independent single parameters that vary in time and space. The model captures both single-cell and cluster-cell behaviors, representing various complex tumor features through different parameter settings. The proposed stochastic cellular automaton model effectively simulates different scenarios of tumor growth, serving as a valuable in silico tool for mathematical oncology research, potentially facilitating improved diagnosis and personalized treatment options. By integrating fractional calculus, physics-based models and cellular-automata simulations, the thesis contributes to the advancement of mathematical oncology, exploring promising avenues for understanding cancer dynamics, suggesting prospective research and potentially aiding decision-making in areas of interest in clinical oncology.

Keywords: Mathematical oncology. Fractional calculus. Differential equations. Variable-order calculus. Cellular automata. Stochastic models.

RESUMO

VALENTIM JR., C. A. **Oncologia matemática fracionária: a dinâmica do câncer sob uma visão interdisciplinar**. 2023. 136p. Tese (Doutorado) - Faculdade de Zootecnia e Engenharia de Alimentos, Universidade de São Paulo, Pirassununga, 2023.

A Oncologia Matemática, um campo interdisciplinar que incorpora conceitos da biologia à ciência dos materiais, utiliza modelos matemáticos para obter uma compreensão abrangente de fenômenos relacionados ao câncer. O cálculo fracionário, um ramo da análise matemática, oferece ferramentas para descrever fenômenos complexos e permite que modelos forneçam melhores *insights* sobre características oncológicas. Esta tese examina e explora a Oncologia Matemática Fracionária, apresentando novos modelos e revisando os desenvolvimentos recentes. A tese demonstra as vantagens do uso de modelos fracionários na previsão do crescimento tumoral, especificamente em modelos populacionais baseados em EDOs (equações diferenciais ordinárias). Soluções analíticas para cinco desses modelos são derivadas e comparadas com dados clínicos existentes (ainda escassos), destacando seu desempenho superior e potencial para exploração adicional. Além disso, é proposto um modelo exponencial de múltiplos estágios com uma ordem fracionária variável para representar a evolução de um tumor. Os parâmetros do modelo são ajustados com base em perfis de ordem fracionária variável, e os resultados demonstram sua habilidade superior em ajustar dados clínicos de séries temporais, oferecendo novas perspectivas para a modelagem do crescimento tumoral. Ademais, o estudo introduz estratégias de simulação de autômatos celulares no contexto de modelos dinâmicos de crescimento tumoral. Esse modelo computacional baseado em agentes permite monitorar parâmetros individuais independentes que variam no tempo e no espaço. O modelo captura comportamentos de células individuais e de grupos de células, representando várias características complexas de tumores por meio de diferentes configurações de parâmetros. O modelo estocástico proposto de autômato celular simula de forma eficaz diferentes cenários de crescimento tumoral, servindo como uma ferramenta valiosa *in silico* para pesquisa em oncologia matemática, potencialmente facilitando melhorias no diagnóstico e opções de tratamento personalizadas. Ao integrar cálculo fracionário, modelos fenomenológicos e simulações de autômatos celulares, esta tese contribui para o avanço da oncologia matemática, explorando perspectivas promissoras para compreender a dinâmica do câncer, sugerindo pesquisas prospectivas e potencialmente auxiliando na tomada de decisão em áreas de interesse da oncologia clínica.

Key-words: Oncologia Matemática. Cálculo fracionário. Equações diferenciais. Cálculo de ordem váriavel. Autômato celular. Modelos estocásticos.

LIST OF FIGURES

LIST OF TABLES

LIST OF ABBREVIATIONS AND ACRONYMS

2D	Bi-dimensional
BIRADS	Breast Imaging Reporting and Data System
CA	Cellular automata
CCT	Cycle cell time
FC	Fractional calculus
HCA	Hybrid cellular automata
ML	Mittag-Leffler
ODE	Ordinary differential equation
PDE	Partial differential equation
ROC	Receiver Operating Characteristic
RMSD	Root mean squared deviation
RTC	Regular tumor cell
SMAPE	Symmetric mean absolute percentage error
SSR	Sum of squared residuals
STC	Stem tumor cell
STD	Standard deviation
TCIA	The Cancer Imaging Archive

LIST OF SYMBOLS

α	Arbitrary order of fractional models
$\alpha(t)$	Variable arbitrary order of fractional models
α_n	Polynomial coefficient of order n
c	Oxygen concentration
(z)	Gamma function of z
	Tissue strain
$E_\alpha(z)$	Mittag-Leffler of order α
$E_\alpha\ \ (z)$	Extended Mittag-Leffler of order α and
	Auxiliary variable for fractional operators
D	Diffusion coefficient
D^α	Derivative operator of order α
D_x^α	Derivative operator of order α regarding position x
D_t^α	Caputo derivative operator of order α regarding time t
${}_L D_+^\alpha$	Left-handed Liouville derivative operator
${}_L D_-^\alpha$	Right-handed Liouville derivative operator
${}_{LC} D_+^\alpha$	Left-handed Caputo-Liouville derivative operator
${}_{LC} D_-^\alpha$	Right-handed Caputo-Liouville derivative operator
${}_R D_+^\alpha$	Left-handed Riemann derivative operator
${}_R D_-^\alpha$	Right-handed Riemann derivative operator
${}_{RC} D_+^\alpha$	Left-handed Caputo derivative operator
${}_{RC} D_-^\alpha$	Right-handed Caputo derivative operator
G	Elastic modulus
${}_a I$	Integral operator in the a-domain
${}_L I_+^\alpha$	Left-handed Liouville integral operator

${}_L I_-^\alpha$	Right-handed Liouville integral operator
${}_R I_+^\alpha$	Left-handed Riemann integral operator
${}_R I_-^\alpha$	Right-handed Riemann integral operator
C_n	Series constant coefficients
N	Number of replicate simulations
R^2	Coefficient of determination
$V(t)$	Tumor volume in respect of time t
a, b	Growth related constants
V_0	Initial tumor volume
V_∞	Maximum tumor volume
λ	Tumor growth rate of the exponential model
$\mathcal{M}_1$	Fractional exponential model with constant α
$\mathcal{M}_2$	Fractional exponential model with variable $\alpha(t)$
	Viscosity coefficient
t	Time step of the cellular automaton model
p_{max}	Maximum proliferation potential of tumor cells
p	Current proliferation potential of tumor cells
μ	Migration potential of tumor cells
P_A	Probability of cell apoptosis
P_P	Probability of proliferation
P_S	Probability of stem cell generation
P	Probability of migration
P_Q	Probability of quiescence
T	Total simulation steps of the cellular automaton model
R	Radius of convergence of a solution
	Stress

CONTENTS

1 INTRODUCTION

Cancer embodies a group of diseases that emerge from abnormally mutated cells and can appear in almost any body organ or tissue. It is the second leading cause of death worldwide and survival rates are profoundly related to timely access to quality diagnosis and treatment. It caused almost 10 million deaths only in 2020, indirectly being responsible for an annual cost reaching trillion dollar figures (WORLD HEALTH ORGANIZATION, 2021; INTERNATIONAL AGENCY FOR RESEARCH ON CANCER, 2020). Experimental oncology, techniques involving molecular biology and, more recently, genetics have dominated most research projects on the subject, increasing the knowledge on malignancies characterization, diagnosis and treatment (GATENBY; MAINI, 2003). In the last few decades, physics and mathematics have been increasingly applied to cancer-related problems, thus giving rise to a new research area (BYRNE, 2010; ROCKNE et al., 2019).

Mathematical Oncology broadens the development and application of models to manifold phenomena including tumor growth dynamics, anticancer therapies and personalized treatment (JACKSON; KOMAROVA; SWANSON, 2014; D'ONOFRIO; GANDOLFI, 2014). While this research field has rapidly evolved in the wake of increasing data availability from the recent expansion of bioinformatics (KHOURY; IOANNIDIS, 2014; MEYER et al., 2014), it still lacks theoretical models to understand, organize and apply clinical data (GATENBY; MAINI, 2003). As strategic advantage, the often called in silico models can test and reproduce several scenarios, which could be unfeasible or even impossible through in vitro experiments. It then becomes a powerful analysis tool as clinical tests in humans are time and resource consuming. Furthermore, in research activities know-why' has been progressively desired over know-how', contributing to the development of models that suitably combine data-oriented and phenomenological approaches (SAGUY, 2016).

Also called physics-based or mechanistic modeling, the phenomenological approach to oncological processes is a complex and interdisciplinary task, not only because tumors are multi-faceted organisms, but also due to governing equations being generally formulated by invoking concepts from different areas. Accordingly, Mathematical Oncology under phenomenological approaches remains largely an under-explored research niche (ANDERSON; QUARANTA, 2008) as a result of complex aspects such as variable compositions, heterogeneity and moving borders.

In this context, the present doctorate thesis aims at reviewing, proposing, analyzing and simulating cancer-related models under a holistic interdisciplinary viewpoint. As Figure 1 illustrates, Mathematical Oncology can benefit from approaches conveying engineering, physics, biosystems and nanothecnology. For instance, population dynamics and computational biology can be employed to analyze tumor growth (WODARZ; KO-

MAROVA, 2014), fluid mechanics and reaction-diffusion phenomena can determine nutrient availability around cells, material science can characterize external forces and stresses on tissue surrounding neoplasms (MATOZ-FERNANDEZ et al., 2017), and nanomedicine can enhance clinical translation of oncology (KASHKOOLI et al., 2021) and minimally invasive treatment approaches (CAVALCANTE et al., 2018; FLEURY ROSA; ISHIHARA; GAIDOS ROSERO, 2019).

Figure 1 – Sketch of possible interdisciplinary approaches to Mathematical Oncology and related keywords.

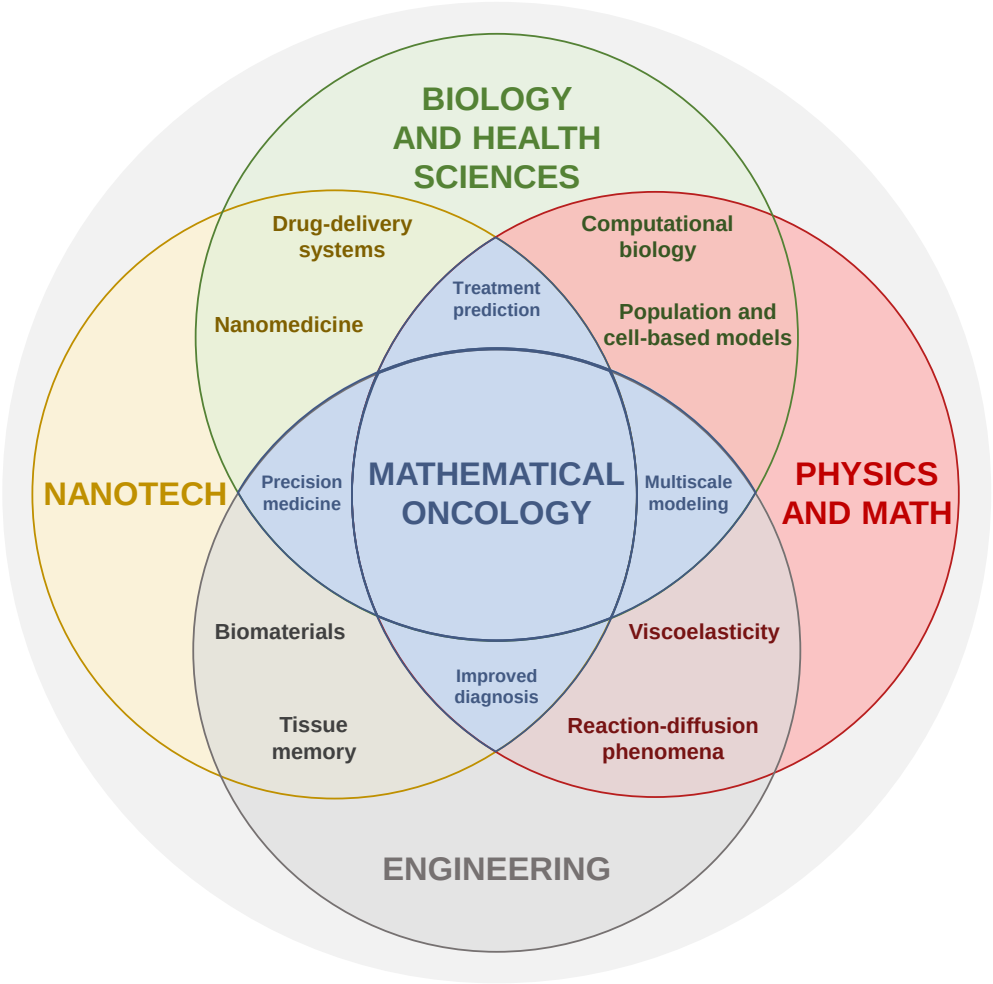

Source: Valentim, Rabi and David (2021)

The research described in this doctorate aims to explore fundamental concepts and follow mathematical approaches able to maintain deductive-reducionist model features without mischaracterizing eventual complexities. One promising alternative is modeling via fractional calculus – an area of mathematical analysis that employs non-integer order differential and integral calculus (OLDHAM; SPANIER, 1974; DAVID; LINARES; PALLONE, 2011; TEODORO; OLIVEIRA; CAPELAS DE OLIVEIRA, 2017; LUCHKO; KOCHUBEI, 2019). Fractional models are characterized by the presence of an arbitrary order (i.e. not necessarily integer) of differentiation (or integration). This feature widely amplifies the

application scope since it enables the model to present distinct behavior according to such fractional order, enhancing its ability to deal with properties from different scales regarding both fractal structure and memory of biological tissue (MAGIN et al., 2008; WEST, 2014; WEST, 2021; WEST, 2022) For this and other remarkable attributes, fractional models may be optimal to model biological phenomena (CRAIEM; ARMENTANO, 2007) and have been successfully applied towards Mathematical Oncology (HASSANI et al., 2021; SWEILAM et al., 2021; SWEILAM et al., 2020; YILDIZ; ARSHAD; BALEANU, 2018; IONESCU et al., 2017).

Notwithstanding, computational approaches in the context of Mathematical Oncology are also investigated, with the development and testing of an agent-based stochastic cellular automaton model capable of virtualizing several distinct case scenarios of tumor dynamics. The utilization of such model is also considered within the application of a comprehensive hybrid model, which employs the automaton as the central piece of a framework integrating different approaches – phenomenological, data-based, deterministic, and stochastic.

Hence, this thesis offers a holistic view to Mathematical Oncology as an interdisciplinary theme with a focus on fractional calculus and phenomenological modeling, symbiotically combining physics, mathematics, biology, and computational science. The text is organized in distinct major chapters as sketched in Figure 2, and while each chapter functions as independent papers, they also build upon concepts from previous ones thus increasing complexity progressively. Chapters 3 to 6 were already fully published in peer-reviewed journals and reproduce the content of corresponding papers with minor adaptations (e.g., trimming introductions and texts to mitigate unnecessary repetition and reading fatigue). All bibliographical entries referenced in each paper/chapter are presented at the end of the thesis.

Chapter 3 is the bibliographical revision of the thesis and is mostly adapted from a paper published during the doctorate, which is probably the first review article on Mathematical Oncology to include non-integer order calculus as a central discussion point, coining the term "fractional oncology" or "fractional Mathematical Oncology" (VALENTIM; RABI; DAVID, 2021). Next, Chapter 4 explores analytical solutions for fractional versions of classical tumor growth models, fitting them with extant clinical data to assess their predictive capabilities (VALENTIM et al., 2020). Chapter 5 proposes a novel interpretation for multi-step tumor models by using variable fractional orders as memory indexes (VALENTIM et al., 2021).

On the other hand, Chapter 6 follows a different approach, leaving deterministic models for a stochastic model while still retaining phenomenological aspects (VALENTIM; RABI; DAVID, 2023). An agent-based cellular automaton model is implemented and discussed under both biological and computational aspects. Case scenarios are analyzed to assess the capabilities of the model and the implementation code is made available online.

Finally, Chapter 7 presents a framework of prospective development of a model that not only combines elements of all aforementioned approaches, but also leverages the recent turn on methods concerning data science and computational intelligence.

Figure 2 – thesis organization: chapters are classified as deterministic, stochastic or hybrid approaches.

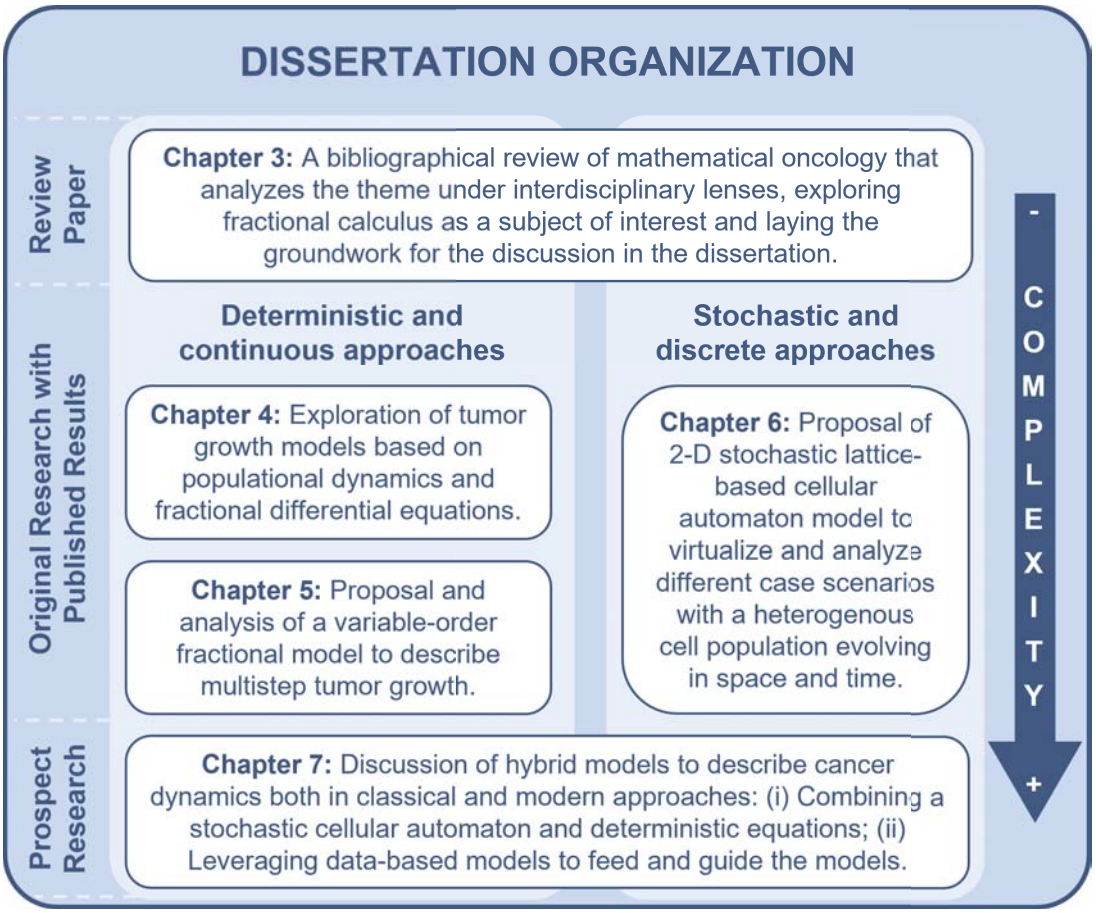

Source: Own authorship.

In short, while this thesis explores some complex mathematical approaches, it also vouches for simplicity. For instance, the comprehensive hybrid framework discussed in the last chapter involves well-defined reductionist concepts that become complex when incorporated together which is analogous, for instance, to emergent cancer phenomena. In fact, Byrne (2010) supports that it is the collaboration between theoreticians and modelers, i.e. the interplay among different areas, that could start improving Mathematical Oncology towards its effective application to real problems and personalized care. As different mathematical approaches can reproduce the same experimental results, Byrne (2010) also claims that it might be suitable to apply Occam's razor concept in order to develop an oncology-applied model. In other words, a model should contain sufficient detail to describe the phenomenon of interest but not excessively to obscure it. Undoubtedly, this isn't an easy feat, but we hope that this doctorate research is a step in the right

direction and that it will hopefully contribute to foster Mathematical Oncology and help to improve the foundations towards applied translational research.

2 OBJECTIVES

The main goal of the present doctorate thesis is to explore and analyze cancer-related phenomena involving tumor growth and its evolving characteristics in a holistic way, relying mainly on fractional calculus modeling while under an interdisciplinary approach. The project thus develops and explores phenomenological modeling skills on Mathematical Oncology. Simulation (virtualization) results are expected to highlight both novelty and contribution of proposed models, which may potentially contribute as fundamental research to aid decision making in oncology-related areas.

As specific objectives, the following are considered:

(i) Contribute to the literature with an up-to-date review on fractional calculus applied to Mathematical Oncology;

(ii) Search and select pertinent models in Mathematical Oncology that apply physics-based concepts and/or are developed under a interdisciplinary approach, identifying their contributions according to complexity and approach;

(iii) Assess how fractional calculus can improve these models, adapting them into new generalized models and assessing their prediction capabilities;

(iv) Contribute with a novel interpretation on multi-step tumor growth using a variable fractional order as model memory index;

(v) Investigate lattice-based approaches and stochastic models in Mathematical Oncology;

(vi) Simulate solutions in order to investigate scenarios, exploring "what if" possibilities and capabilities of each model;

(vii) Analyze and interpret obtained results under an interdisciplinary viewpoint;

(viii) Analyze potential contributions of obtained results as fundamental research towards translation into decision-making in oncology-related areas such as understanding of tumor behavior, early diagnosis techniques, and personalized treatment therapies.

3 BIBLIOGRAPHICAL REVIEW: FRACTIONAL MATHEMATICAL ONCOLOGY

This chapter adapts the review paper titled "Fractional Mathematical Oncology: on the potential of non-integer order calculus applied to interdisciplinary models", which is part of the study conducted over the doctorate and was published in Biosystems journal (Elsevier) (VALENTIM; RABI; DAVID, 2021). It serves as a bibliographical review to this thesis since it offers a background on the main aspects underlying the following chapters, thus providing pertinent grounding theory.

In addition, besides reviewing Mathematical Oncology and surveying some recent well-succeeded implementations of fractional models, the present chapter prospectively explores approaches to reductionist models that could help understand and describe cancer-related phenomena and predictive oncology. In theory, an interdisciplinary approach symbiotically combining physics, material science, biology and fractional calculus could offer unpaired developments and distinct views on oncology phenomena.

Overall, this chapter is organized as follows: section 3.1 provides a brief contextualization on Mathematical Oncology; section 3.2 surveys some of the most relevant continuum cancer-related models; on the other hand, section 3.3 presents cell-based and stochastic models; fractional calculus main aspects and oncology models are explored in section 3.4; finally, section 3.5 delves into hybrid approaches, discussing prospect investigations.

3.1 An introduction to Mathematical Oncology

Cancer is the collective name given for a large group of over 100 diseases related to abnormal cell reproduction (JACKSON; KOMAROVA; SWANSON, 2014). The World Health Organization (2021) states that cancer is the second major cause of death worldwide, responsible for about 1 in 6 deaths. It is a disease that generally compromises health care systems mainly as a result of its lingering effects along with usually severe side-effects from lasting treatments. Whether combined or separately administered, chemotherapy, immunotherapy and radiation therapy are usually the most common interventions. Considering how cancer might develop very differently in each case while dose adaptation or fractionation are both subject to individual clinical responses, personalized therapy may require the support from mathematical models to optimize treatment strategies (ENDERLING et al., 2019; ROCKNE et al., 2019).

In that context, Mathematical Oncology develops and applies models to cancer-related phenomena, ranging from tumor dynamics analysis to personalized treatment (JACKSON; KOMAROVA; SWANSON, 2014; ABERNATHY et al., 2017; CRISTINI; KOAY; WANG, 2017). It is a research field that has been benefiting from recent increase in data availability as provided by quickly evolving biosensors and bioinformatics techniques (KHOURY; IOANNIDIS, 2014). Predictive oncology may contribute to person-

alized treatment procedures by means of numerically virtualized scenarios based on tumor dynamics and individual gene expression.

As all-inclusive modeling prospectively enhances creating and carrying out innovative cancer treatments, research endeavors have been concerned to apply mathematics and physics towards cancer onset and early growth as well as tumor and intercellular interactions (D'ONOFRIO; GANDOLFI, 2014). Mathematical Oncology indeed rises as a scientific area relying on the notion that (1) mathematics can be applied to improve biomedical knowledge of the disease and (2) that biology proposes new mathematical challenges, which generates enhanced mathematical tools' (CHAUVIERE et al., 2010). Accordingly, Mathematical Oncology claims for comprehensive theoretical models to understand, coordinate and employ clinical data in view of aiding decision-making in oncology (GATENBY; MAINI, 2003).

On that matter and to different extents and perspectives, Mathematical Oncology can encompass the so-called translational research, which bridges the gap between basic research and its final application in health systems (BARRETO et al., 2019; DOROSHOW; KUMMAR, 2014). Also referred to as blackboard-to-bedside' or bench-to-bedside' research, in the present case it concerns how mathematical models can go from complex theoretical frameworks to comprehensive personalized strategies to identify and treat specific cancers. Applications of interest refer to early diagnosis improvement, such as decision-making support systems based on prediction algorithms (CHAKRABORTY; DEBBOUCHE; ANTONOV, 2020) or molecular testing through real-time tissue acquisition and analysis (MITRI et al., 2018), and personalized medicine. On the latter, information combined from mathematical models and corresponding in silico experiments can build patient-specific tumor profiles and be implemented into preclinical and clinical use (HAMIS; POWATHIL; CHAPLAIN, 2019). Overall, Mathematical Oncology can provide the necessary theory to connect the unique biology of patient's tumor to tailored treatment routine or drug dosage, enabling true precision-guided therapy (HORMUTH et al., 2021a; NENOFF et al., 2020; SARHADDI; YAGHOOBI, 2020).

3.2 Deterministic and continuum models: Tumor growth described by di erential equations

In spite of usually evolving differently, solid cancers have a common inception on the progenitor mutated cell that originates a primary tumor. Aiming at this mutual point may help grasp important characteristics of early tumor dynamics. Recently, gene sequencing and molecular biology have progressively explored paths and signals leading to cancerous cell arise (GOLUB et al., 1999; EASTON et al., 2015); yet, it is equally important to understand mechanistic basis of tumor cells dynamics.

Population or ecological models are customary approaches in view of grasping phenomenological foundations concerning general avascular tumor growth, being usually

modeled in terms of ordinary differential equations (ODE) (SAVAGEAU, 1980; SACHS; HLATKY; HAHNFELDT, 2001; SARAPATA; DE PILLIS, 2014). Albeit more elementary than oncology models containing partial differential equations (PDEs), ODE-based approaches have advantages motivating their current employment (WODARZ; KOMAROVA, 2014). Their relative simplicity (compared to PDE) enables the derivation of analytical solutions, thus allowing mathematical description of phenomena evolution (SANTOS, 2007). Moreover, ODE-based models free parameters can be usually fine-tuned against clinical data in order to describe different tumor phases (BENZEKRY et al., 2014; HARTUNG et al., 2014), favoring their flexibility and consequent use to support clinical advice.

Being tailored towards specific experimental evidence and biological peculiarities, many ODE models have been elaborated to virtualize dynamic tumor growth. Most follow a sigmoidal law relying on two parameters, namely population growth rate and carrying capacity. Aforesaid definition is imposed so that models can capture the particular stages a primary tumor sustains in view of available resources such as neoplasm surface area and tissue heterogeneity (MARU' I et al., 1994).

Tumor progression often involves different stages such as random mutations, alterations in tissue biomechanics (FRITSCH et al., 2010; RAMIÃO et al., 2016) and epigenetic spontaneous cell changes (BOVERI, 2014; LOWENGRUB et al., 2010). Those features should be considered when modeling tumor development since they interfere with growth behavior, thus enabling a possibly better approach supported by multistage carcinogenesis (WODARZ; KOMAROVA, 2014). Accordingly, some authors proposed models that integrate and express multifactorial or multistep growth patterns (RODRIGUEZ-BRENES; KOMAROVA; WODARZ, 2013; TRACQUI, 2009; SPENCER et al., 2004) (e.g. alternated dormancy periods modeled as stepwise patterns).

Alternatively, there are other ODE-based approaches in Mathematical Oncology besides ecological models. Kinetic interactions between tumor and immune cells on different cellular and sub-cellular levels can be modeled by means of ODE system (DOLFIN; LACHOWICZ; SZYMA SKA, 2014). Other models can target the interaction between gene expression and population dynamics concerning different cell classes (PORTA; ZAPPERI, 2017).

However, Murphy, Jaafari and Dobrovolny (2016) claim that ODE models may be unable to fully consider the intricate tumor dynamic evolution and need to be carefully employed. For other authors, these models should necessarily be used to describe only general trends concerning neoplasm behavior, being inadequate to characterize specific cases (e.g. in personalized therapy) (WODARZ; KOMAROVA, 2014). Such drawback is often a result of irregular growth patterns and aforementioned genetic instabilities in these organisms (LOWENGRUB et al., 2010; FRITSCH et al., 2010; RAMIÃO et al., 2016).

A subsequent climbing step in the complexity ladder takes cancer models into the significantly more robust PDE domain, describing tumor growth and other related

phenomena in terms of not only dynamic variations (i.e. time dependence) but also gradients (i.e. spatial dependence), allowing a far-reaching description of reality. When employing PDE-based models, well-established conservation laws can be conveniently applied to incorporate a more mechanistic (i.e. phenomenological) approach to oncology modeling (WODARZ; KOMAROVA, 2014). For that reason, PDE approach is a more comprehensive choice when studying tumor growth into surrounding tissue.

Some models describe tumors as a fluid or a fluidized mixture, thus admissible of being modeled through transport equations. Byrne and Preziosi (2003) proposed an early two-phase model of an avascular tumor comprising cellular (solid) and interstitial (liquid) parts. Along with supplementary constitutive laws, mass and momentum equations were applied to investigate time-spatial dependence of cell proliferation rate on cellular stress. Through their findings, the authors related the impact of mechanical effects on tumors equilibrium size, identifying a critical value for proliferation rate influencing on tumors outcome behavior (either growth or elimination). Fasano et al. (2014) proposed other models based on conservation laws and considering a heterogeneous system. They also considered free boundaries, being an important particularity when treating expanding tumors and complex processes in multi-component neoplastic formation. Other models employ the transport equation for metastatic processes and beyond (HARTUNG et al., 2014; XU; VILANOVA; GOMEZ, 2016).

In a surrogate approach, the diffusion equation can be used to study the dynamic of cell population density across tissues (DEBBOUCHE et al., 2021; POLOVINKINA et al., 2021). In those studies, one may consider different combinations of population heterogeneity, possibly including stem and regular tumor cells, dead cells, healthy cells and even lymphocytes or similar (ADAM; MAGGELAKIS, 1990; PHAM et al., 2012; WONG et al., 2015). Stability and possible outcomes are frequently focused in those investigations since they allow the virtualization of general scenarios regarding tumor form such as dormancy, evanescence, or uncontrolled growth and invasion.

Other models (PORTA; ZAPPERI, 2017) target specific cell behavior such as tumor angiogenic factors or mitosis rates trying to describe the specific interior cell behaviors leading to the accumulation of genetic chances and consequently emerging Hanahan and Weinberg's (2011) hallmarks of cancer. A vast part of Mathematical Oncology also focuses on modeling treatment-related phenomena such as drug delivery, tumor-immune dynamics, optimal chemotherapy and radiotherapy dosage, cycle-specific oncolytic virotherapeutics, and their impacts on tumor and healthy cells (ELADDADI; KIM; MALLET, 2014). In those studies, not only PDEs are employed but also ODE systems and control techniques.

As cancer is a systemic disease, some authors argue that it requires an equally systemic model approach. With the help of PDEs, a commonly adopted approach relies on modeling tumor micro-environment (i.e., neoplasm surroundings), considering not only where cancerous cells arise and proliferate but also on how they react under certain

environmental conditions. In this context, the concept of dynamic capacity of the tissue bearing the tumor can be better approached by modeling factors such as nutrient availability (BENZEKRY et al., 2014), invasion tendencies (REJNIAK, 2016), biomechanical stresses (TALONI et al., 2014; AMBROSI et al., 2017) and anticancer therapies.

Nevertheless, using PDEs is mathematically more difficult and costly than employing ODEs due to the simultaneous dependence on more than one independent variable and often intricate boundary and initial conditions. Additionally (and quite paradoxically), an inherent limitation of models employing solely differential equations turns out to be exactly their characteristics of being continuous and deterministic. When a model invokes specific cellular structure and probabilistic nature involving cell proliferation, a different mathematical approach is required.

3.3 Cell-based and stochastic models: tumor growth governed by discrete models

Anderson, Chaplain and Rejniak (2007) claim that while continuum mathematical models have been successfully employed to describe several portions of matter, they are essentially particles, cells, thus discrete. In the wake of the impressive progress of biochemical and biological concepts on genetics, sub-cellular levels and their intricate mechanisms, computational-enhanced Mathematical Oncology faces the difficult task of transforming specific portion-sized data into complex information describing emergent higher-level multi-scale cellular phenomena. In recent years, many cell-based models have been proposed to face such challenge (WEERASINGHE et al., 2019).

Cell-based or discrete models are organized frameworks that keep track of fully independent individual parameters varying in time and space, reflecting the heterogeneity and complex, emerging, phenomena found in cancer. Computationally, they can rely on different approaches including Monte-Carlo simulations, energy minimization techniques, volume conservation laws, motion rules and others (ANDERSON; CHAPLAIN; REJNIAK, 2007).

If these models follow a structural or grid organization, they are mathematically treated as lattice-based models, which are categorized according to the number of cells that each lattice site can hold (METZCAR et al., 2019). Lattice-gas cellular automata models admit more than one cell per site (being suitable for larger systems). On the other hand, if a single cell allegedly occupies many spots, then it should be modeled as sub-cellular systems (JAMALI; AZIMI; MOFRAD, 2010). Finally, if each cell can occupy a single lattice, it can be modeled as a regular cellular automaton (CA) (METZCAR et al., 2019).

Virtualization (numerical simulations) involving cell-based models are often referred to as in-silico experimentations because of their similarity and logical extension of in-vitro counterpart (JEANQUARTIER et al., 2016). Concerning regular CA models, relatively simple implementations can go a long way in providing emergent complex behavior. Enderling et al. (2009) established a basic set of rules concerning proliferation and migration

rates for each type of tumor cell (regular or stem) in a CA model and investigated the virtualization of very different emergent scenarios when changing these rules, including cell clustering and tumor dormancy. Later, Poleszczuk and Enderling (2014) improved their model by implementing it with high-performance computational techniques.

3.4 Fractional Mathematical Oncology

3.4.1 Fractional calculus basic theory

Fractional calculus (FC) or calculus of arbitrary order may be considered an natural extension of traditional integer order calculus since it is a mathematical area of analysis that investigates and applies concepts of non-integer differential and integral calculus. It appeared for the first time in correspondences between L'Hospital and Leibniz in the end of the 17th century (ROSS, 1977). Despite its ancient origin, FC had a slow development when compared with its integer counterpart. Only over one hundred years after those letters, there was the first formal definition for a fractional derivative, accomplished by Laplace and Lacroix (DOMINGUES, 2005).

Later, Riemann's and Liouville's definitions became two of the most known and popular formulations for fractional integrals and derivatives (OLDHAM; SPANIER, 1974). Nevertheless, the scenario changed when Caputo (1967) suggested a new approach from Riemann definition by incorporating initial conditions of integer order in the resolution of fractional differential equations. Such change allowed a greater fidelity to physical phenomena modeled with fractional calculus, which widely disseminated Caputo's approach in applications ranging from physics to life sciences. Many other definitions have surfaced ever since, with different interpretations and particularities addressed to each one (SALES TEODORO; TENREIRO MACHADO; CAPELAS DE OLIVEIRA, 2019; ORTIGUEIRA; MACHADO, 2017). Main publications on the theme have only appeared in the beginning of the 20th century (MACHADO et al., 2010; MACHADO, 2010), whose major history and grounding concepts can be found in classical materials from Oldham and Spanier (1974), Ross (1977) and, more recently, in works by David, Linares and Pallone (2011), Capelas de Oliveira and Tenreiro Machado (2014), and Luchko and Kochubei (2019).

Considering that FC is a generalization of integer order calculus, its fundamental concepts can be introduced by relying on simpler conjectures. Therefore, just as it is possible to state that real numbers are generalizations of natural and integer numbers, the same can be applied to some mathematical tools (HERRMANN, 2014). Factorials, for instance, comprise only natural numbers, thus restricting its application domain. As factorial generalization, gamma function is introduced for any $(z) > 0$ as

$$(z) = \int_0^\infty t^{z-1} e^{-t} dt \tag{3.1}$$

On the same line of thought, exponential Euler function

$$e^z = \sum_{n=0}^{\infty} \frac{z^n}{n!} \tag{3.2}$$

can also be generalized by replacing its factorial component with a gamma function, yielding

$$e^z = \sum_{n=0}^{\infty} \frac{z^n}{(1+n)} \tag{3.3}$$

and thus introducing the so-called Mittag-Leffler (ML) function for $(\alpha) > 0$

$$E_\alpha(z) = \sum_{n=0}^{\infty} \frac{z^n}{(1+n\alpha)}, \tag{3.4}$$

which was extended to admit two parameters for $(\alpha) > 0$ by Wiman (1905)

$$E_\alpha \ (z) = \sum_{n=0}^{\infty} \frac{z^n}{(n\alpha + \ )} \tag{3.5}$$

ML function is as important for FC as are exponential functions for integer calculus since it is commonly employed to represent the solution of several fractional mathematical and physical problems. This is due to the fact that many simple and popular functions are particular cases of this generalization. Therefore, several researchers have long explored its uses and particularities (CAMARGO, 2009; VALÉRIO et al., 2013; GORENFLO et al., 2014).

Considering the basic notation of conventional (i.e. integer order) derivative, one writes

$$g(x) = \frac{d}{dx} f(x) \tag{3.6}$$

If, for instance, it is assumed $f(x) = x^k$ then

$$\frac{d}{dx} x^k = k x^{k-1}, \tag{3.7}$$

whose generalization for $n \quad \mathbb{N}$ is

$$\frac{d^n}{dx^n} x^k = \frac{k!}{(k \quad n)!} x^{k-n} \tag{3.8}$$

By considering that order n may be arbitrary to the point of including non-integer values, one may apply gamma function (as previously introduced) to extend Eq. (3.8) as

$$\frac{d^\alpha}{dx^\alpha} x^k = \frac{(1+k)}{(1+k \quad \alpha)} x^{k-\alpha} \quad x \quad 0, k = \quad 1, \quad 2, \quad 3, \quad , \tag{3.9}$$

in which $x \quad 0$ and k is positive to assure the singularity of fractional derivative definition in view of the convergence of the integral in Eq. (3.1) for any integer $z > 0$.

This intuitive approach has been long applied to several types of functions. Before formally defining fractional derivatives, it is more intuitive to present the definitions

regarding fractional integrals in line with Herrmann (2014). An integration of a function is considered as the inverse operation of its differentiation

$$\left(\frac{d}{dx}\right)({}_aI)f = f \tag{3.10}$$

In turn, one defines the conventional integrator ${}_aI$ operator in a domain as

$${}_aIf = \int_a^x f(\ )d \tag{3.11}$$

The definition of fractional integrals start with a multiple integral as

$${}_aI^n f = \int_a^{x_n} \int_a^{x_{n-1}} \quad \int_a^{x_1} f(x_0)dx_0 \quad dx_{n-1}, \tag{3.12}$$

which represents the successive anti-differentiation of a continuous function $f(x)$. From Cauchy's Integral Theorem and the Fundamental Theorem of Calculus it is possible (FOLLAND, 2002) to represent Eq. (3.12) in a more convenient way, thus writing integral Cauchy formulation:

$${}_aI^n f(x) = \frac{1}{(n \quad 1)!}\int_a^x (x \quad)^{n-1} f(\ )d \tag{3.13}$$

By employing gamma functions, Eq. (3.13) can be extended for the fractional case as

$${}_{RL}I_+^\alpha f(x) = \frac{1}{(\alpha)}\int_a^x (x \quad)^{\alpha-1} f(\ )d\ , \tag{3.14}$$

$${}_{RL}I_-^\alpha f(x) = \frac{1}{(\alpha)}\int_x^b (\quad x)^{\alpha-1} f(\ )d \tag{3.15}$$

In those equations, a and b respectively determine the lower and upper limits of the integral domain. While Eq. (3.14) is called left-handed and valid for $x > a$ since it collects function values for $< x$, Eq. (3.15) is called right-handed and applies for $x < b$, collecting function values where $> x$. The choice of a and b fundamentally sets apart two of the most used definitions of fractional calculus, namely Liouville's and Riemann's fractional integrals for $a =$ and $b = +$, and $a = 0$ and $b = 0$, respectively. Pragmatically, the distinction between those definitions may be observed from the differentiation of some specific functions that will result in significantly different solutions, depending on the chosen approach.

From the definition of fractional integrals one can obtain fractional derivatives. Thus, the fractional derivative operator

$$\frac{d^\alpha}{dx^\alpha} = D^\alpha \tag{3.16}$$

is used to introduce the concept of operation sequence between integrals and derivatives. For instance, one can consider the following operation:

$$D^\alpha = D^m D^{\alpha-m} = \frac{d^m}{dx^m}{}_aI^{m-\alpha} \quad m \quad \mathbb{N} \tag{3.17}$$

Such notation determines that a fractional derivative may be interpreted as a fractional integral followed by a conventional integral. Therefore, once non-integer integral is defined, so is the corresponding fractional derivative. Another possibility regards an inverse sequence of operators as

$$D^{\alpha} = D^{\alpha-m}D^{m} =_{a} I^{m-\alpha}\frac{d^{m}}{dx^{m}} \quad m \quad \mathbb{N}, \tag{3.18}$$

leading to an alternative decomposition of the fractional derivative into a conventional derivative followed by a non-integer order integral. One must note that each decomposition can lead to a different result.

From these definitions, it is possible to understand the non-locality mechanism in FC. The conventional derivative is the local operator and the fractional derivative can be interpreted as the inversion of the fractional integration, i.e. a non-local operation. As a result, both Liouville and Riemann approaches lead to different definitions of fractional derivatives depending on the adopted decomposition sequence. Therefore, for $0 < \alpha \leq 1$ one obtains Riemann-Liouville fractional derivatives by employing equations for integral operators in the sequence given in Eq. (3.17):

$${}_{RL}D^{\alpha}_{+}f(x) = \frac{d}{dx}{}_{RL}I^{1-\alpha}_{+}f(x) = \frac{d}{dx}\frac{1}{(1 \quad \alpha)}\int_{a}^{x}(x \qquad)^{-\alpha}f(\ )d\ , \tag{3.19}$$

$${}_{RL}D^{\alpha}_{-}f(x) = \frac{d}{dx}{}_{RL}I^{1-\alpha}_{-}f(x) = \frac{d}{dx}\frac{1}{(1 \quad \alpha)}\int_{x}^{b}(\qquad x)^{-\alpha}f(\ )d \tag{3.20}$$

If the operators sequence is inverted, as in Eq. (3.18), one obtains Caputo-Liouville or Caputo-Riemann derivatives:

$${}_{RLC}D^{\alpha}_{+}f(x) = {}_{RL}I^{1-\alpha}_{+}\frac{d}{dx}f(x) = \frac{1}{(1 \quad \alpha)}\int_{a}^{x}(x \qquad)^{-\alpha}\frac{df(\ )}{d}d\ , \tag{3.21}$$

$${}_{RLC}D^{\alpha}_{-}f(x) = {}_{RL}I^{1-\alpha}_{-}\frac{d}{dx}f(x) = \frac{1}{(1 \quad \alpha)}\int_{x}^{b}(\qquad x)^{-\alpha}\frac{df(\ )}{d}d \tag{3.22}$$

The fractional operator can also be written by stating the independent variable as subscript, i.e. D^{α}_{x}. It is worth mentioning that when the independent variable is time t, the definition given by Eq. (3.21) is also called causal derivative . Such name stems from the integral in the definition considering values smaller than t, i.e., considering what happened before that instant while defining time flow as causal (ORTIGUEIRA; MACHADO, 2017). In this case, the non-locality feature is called memory effect, being very important to model nonlinear phenomena history such as cancer-related phenomena as addressed in next section.

For the sake of simplicity, the left-handed Caputo-Riemann operator can be written as either D^{α}_{x} or D^{α}_{t}, depending on the independent variable, and given by the definition

$$D^{\alpha}_{x}f(x) = \frac{1}{(1 \quad \alpha)}\int_{0}^{x}(x \qquad)^{-\alpha}\frac{df(\ )}{d}d\ , \tag{3.23}$$

which is widely known as Caputo's derivative (CAPUTO, 1967). Its usefulness to model physical problems and solve generalized differential equations is recurrent because, if $f(x)$ is a constant, by applying Riemann's definition one obtains

$$ {}_{R}D_{+}^{\alpha} const = \frac{const}{(1 \quad \alpha)} x^{-\alpha}, \tag{3.24} $$

while in case of Caputo's definition

$$ D_{+}^{\alpha} const = 0, \tag{3.25} $$

which adheres to integer-order models with constant initial or boundary conditions, thus justifying its widespread use.

For their many remarkable characteristics, fractional models have been increasingly chosen and successfully applied in many other areas such as signal processing (MILJKOVI et al., 2017), thermoacoustics (VALENTIM, 2018), economy (DAVID et al., 2016; DAVID et al., 2021), robotics (LEYDEN; GOODWINE, 2016), food science (DAVID; KATAYAMA, 2013), chemical kinetics (SINGH; KUMAR; BALEANU, 2017), electromagnetism (MESCIA; BIA; CARATELLI, 2019), traffic control (KUMAR et al., 2018), among others (VALENTIM; RABI; DAVID, 2020; DAVID; RABI, 2020; DAVID et al., 2020; MAINARDI, 2018; DAVID; VALENTIM, 2015; HERNANDEZ; O'REGAN; BALACHANDRAN, 2010; HASSANI; TENREIRO MACHADO; MEHRABI, 2021).

3.4.2 Cancer-related fractional models

One may refer to Fractional Mathematical Oncology as the intersection between FC and Mathematical Oncology, wherein there are already many fields of application. For instance, concerning population or ecological models, the elevation of cancer cells may be interpreted as a population increase subjected to restrictions concerning substrate availability and competition (with healthy cells). Some works have applied FC as an attempt to generalize the main models for tumor growth. Effectively, arbitrary orders in differential equations might refine cell growth dynamics description, allowing a deeper understanding of investigated phenomena (VARALTA; GOMES; CAMARGO, 2014).

On that note, Valentim et al. (2020) generalized and analytically solved relevant ODE models for tumor growth towards fractional order extensions. The solutions were then fitted to an extent clinical data set of breast cancer evolution in mice. Resulting best-fitted models perform better as predictors compared to their traditional counterparts, suggesting that inclusion of fractional models could avoid misdirection when choosing potential predictors. Moreover Bolton et al. (2015) suggested that fractional models with a specific arbitrary order (namely 0.68) would better fit to experimental curves obtained from tumor growth in mice.

Stemming from ODE frameworks, Valentim et al. (2021) proposed fractional variable-order models to describe multi-stage tumor characteristics. Exploring the memory

effect in non-integer order models, the authors interpreted the variable order as indicative of tumor memory. Clinical data were employed to fit and analyze different mathematical behaviors relating to tumor particularities. Results suggested that variable order $\alpha(t)$ modeled as a periodic function can better describe tumor evolution regarding the fitted data, potentially capturing dormancy periods.

Within the viscoelastic scope, Magin (2010) developed a fractional rheological model that is not limited to particular definitions of Maxwell, Voigt and Kelvin. Thus the author managed to obtain better results when identifying benign and malign tumors in elastography data from MRI scans. Magin et al. (2008) also claim that fractional operators encode information about molecular interactions regarding the spin of water that is built in polymer structures and in the extracellular matrix of cells and tissues , being able to store extra information on the physical phenomena being modeled when compared to traditional integer order models.

Another featured application of FC in Mathematical Oncology refers to modeling the invasion of healthy systems by tumors as well as cancer cells transport throughout the organism, characterizing metastasis onset. Such processes are often modeled as diffusion phenomena in which several parameters must be taken into account in order to maintain the accuracy of the phenomenological description. In a non-integer order model, one can adjust the arbitrary order so that the system acquires sub-diffusive or super-diffusive behaviors, visualizing complex aspects that traditional (i.e. integer-order) counterparts cannot reproduce, as shown in a tumor diffusion model by Iyiola and Zaman (2014).

In continuous transport models, FC also allows to incorporate statistical randomness by combining a probability distribution function with a dynamic (i.e. time-dependent) random-walk model. Therefore, it is possible to simultaneously consider stochastic and deterministic natures when simulating tumor evolution, whose random-related mutations can suddenly lead to pivoting features favoring growth, movement or invasion of healthy tissue (IOMIN, 2006).

Regarding treatment therapies, Iomin (2014) investigated the effects of different mathematical functions to represent chemotherapeutic treatments in scenarios modeled through fractional kinetics. Namazi, Kulish and Wong (2015) proposed a new prediction method based on Hurst coefficient and fractional-diffusion equation aiming at modeling the effect of a specific drug in lung-cancer patients' DNA. The authors found that the new model could simulate drug effects with 3.21% mean difference from real sick patients' DNA. FC has also gained strength in exploring ideal combinations of chemotherapy and immunotherapy through optimal control to minimize cancerous cells with the lowest possible impact on healthy cells (YILDIZ; ARSHAD; BALEANU, 2018).

Other studies embrace treatment optimization methods (UCAR; ÖZDEMIR; ALTUN, 2019; KHAJANCHI; NIETO, 2019), control in invasion systems (MANIMARAN et al., 2019; DAI; LIU, 2019), bioengineering (IONESCU et al., 2017), and general tumor

growth (REN; YU; CHEN, 2018; SOWNDARRAJAN et al., 2019; FARAYOLA et al., 2020). From aforementioned studies, one can note the contemporary interest of the scientific community towards mathematical tools that suitably describe oncological models, improve the understanding of tumor mechanics and evolution, and expand diagnostic options and treatment routines. In this context, fractional oncology may play a promising and strategic role to allow more accurate and reliable virtualization devices.

3.5 Fractional hybrid models

Hybrid models are a recent category in which continuum characteristics are incorporated into discrete frameworks. Advantages of such approach are very clear for modeling multi-scale phenomena since the discrete part can focus on cell movements scale while the continuum methods can model events on larger scales (REJNIAK; ANDERSON, 2011). This capacity to bridge scale gaps while communicating aspects of very different magnitudes across the model makes hybrid approaches very interesting to describe several aspects of cancer phenomena (ANDERSON et al., 2007).

Accordingly, Anderson, Chaplain and Rejniak (2007) proposed a hybrid model comprising discrete methods to deal with tumor cells while considering continuous methods to model micro-environment factors such as host tissue, matrix-degradative enzymes and oxygens. Their model focused on micro-scale level to simulate tumor at tissue-scale and could be easily implemented to incorporate other scales (e.g. sub-cellular).

In the following years, many other hybrid models were proposed, each with their own characteristics and often involving either discrete or continuum tools (CHAMSEDDINE; REJNIAK, 2019). Zangooei and Habibi (2017) combined CA and machine learning methods to develop a vascular multi-scale framework capable of predicting cell phenotypes. In-silico results indicate that their model can represent key cancer features, such as angiogenesis, while presenting good agreement with biological behavior. Phillips et al. (2020) also proposed a hybrid model capable of describing the physical interaction between tumor and surrounding blood vessels, but focused on complementing cells' discrete behavior with a mathematical description of vascular endothelial growth factor (VEGF).

Additionally, Norton et al. (2019) reviewed agent-based and hybrid models that specifically handle the interplay between tumor immune micro-environment and cancer immune response, thoroughly discussing the importance of modeling tumor heterogeneity. Alemani et al. (2012) combined CA with lattice Boltzmann method to model multi-scale tumor dynamics considering nutrient diffusion and immune competition. The authors replaced PDEs with a statistic and stochastic approach claiming that such system combination could successfully capture cellular, molecular and continuum complexities.

On that context, coupled differential equations can help purely stochastic models cover some shortcomings. For instance, integrating a diffusion PDE to a hybrid model could tackle at least two problems at once. Firstly, if a CA disregards dead cells, it also

dismisses their remains, which could cause some sort of toxicity in tumor micro-environment. Secondly, it is known that tumors can react very differently depending on oxygen lack or abundance. By its nature, some cells can effectively change biomechanical characteristics in order to migrate from an oxygen-deprived environment. Therefore, a model that does not take tissue nutrient availability into account can overlook important tumor dynamics details.

Accordingly, the diffusion equation could be an important tool to model tumor micro-environment. It could mathematically describe diffusive transport of chemical species (e.g. oxygen and nutrients simultaneously with cell remains) through the tissue in which the tumor grows. By following transport laws (e.g. Fick's law), this part of the model would be completely deterministic while also depending on outcomes from stochastic CA (e.g. if a cell replicates, it will increase nutrient consumption in that lattice area, thus influencing the diffusion equation). On the other hand, at each time step the deterministic portion of the model would also affect probabilities generated from the CA (e.g. if nutrient availability is very low, the chance for local apoptosis is higher).

Moreover, the literature generally confirms that diffusion processes are better modeled with a time-fractional derivative (COSTA; CAPELAS DE OLIVEIRA, 2012; WU et al., 2015; AGRAWAL, 2002). These fractional models would be capable of presenting sub-diffusive and super-diffusive phenomena by only varying the arbitrary order of model time derivative. This feature could provide a much powerful tool to represent how nutrients are transported through tissue and affect tumor growth, possibly enhancing accuracy of the hybrid model.

On the other hand, CA models often disregard healthy cells, not establishing any stress relation between cells and their surrounding extracellular matrix. As an attempt to improve this characteristic on a hybrid framework, a differential equation to model viscoelasticity of both tumor and its surrounding tissue may be useful.

Furthermore, external stresses such as pressure and mechanical resistance can strongly affect tumor progression, malignancy and metastasis possibility (FRITSCH et al., 2010; RAMIÃO et al., 2016; PORTA; ZAPPERI, 2017). As a result, it becomes very important to account for these factors by modeling tumor (or its surrounding tissue) as either soft or viscoelastic material. As discussed in (MAGIN, 2012; MAGIN, 2004; CATANIA; SORRENTINO; FASANA, 2008), fractional approaches can generally provide more effective reductionist viscoelastic models, being a viable option to mathematically describe such phenomena.

On that note, a hybrid model could potentially contain at least two equations modeling tumor micro-environment, namely one dealing with nutrient diffusivity and the other tackling tissue stresses. A conceptual scheme of a prospective hybrid model as previously described is illustrated in Figure 3. Although there are other hybrid CA models developed in the literature, there are few that profoundly consider such aspects through

an interdisciplinary view. Moreover, even fewer (if any) rely on improved capabilities of fractional models to describe natural phenomena in differential equations constituting the deterministic part of these models. This could be a prospective research field in Mathematical Oncology that could potentially contribute to areas of interest such as understanding tumor evolution, early diagnosis techniques and personalized treatment therapies.

Figure 3 – Conceptual scheme for the hybrid model with fractional differential equations.

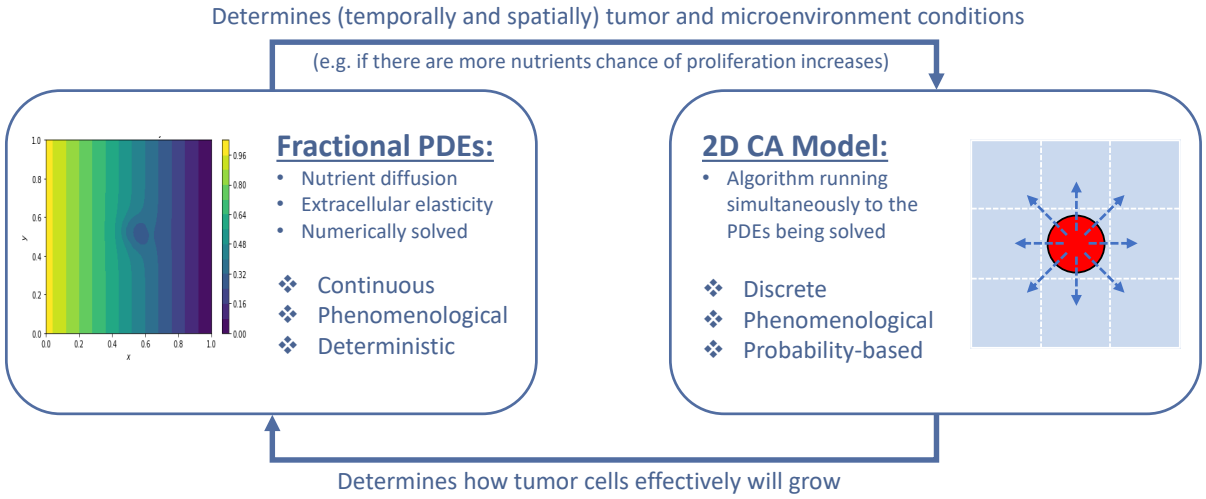

Source: Valentim, Rabi and David (2021).

3.6 Concluding remarks

There are tools in Mathematics (still) waiting to establish their way in Theoretical Biology and such is the case of fractional (i.e. non-integer order) calculus, whose historical and philosophical aspects have attracted growing interest. As addressed and discussed in the present review work, the application of fractional calculus indeed arises as powerful and strategic modeling approach in view of prospective challenges and opportunities in Mathematical Oncology. Besides well-known advantages of either testing or reproducing different in silico scenarios (which could be impractical or even impossible via corresponding in vitro experimentation), Fractional Mathematical Oncology can straightforwardly deal with heterogeneous scales, memory effects and/or dormancy periods related to tumor onset and development.

4 CAN FRACTIONAL CALCULUS HELP IMPROVE TUMOR GROWTH MODELS?

This chapter reproduces and adapts the paper entitled "Can fractional calculus help improve tumor growth models?", which is part of the study conducted over the doctorate and was published in the Journal of Computational and Applied Mathematics (Elsevier) (VALENTIM et al., 2020).

In the chapter, we explore ODE-based population models as viable tools to investigate tumor growth and support clinical evidence. By following a fractional approach, the study derives analytical solutions for five of these models, whose parameters are best-fitted against extant clinical data. In terms of tumor growth prediction, results show that fractional models not only have better performance, which is mostly wanted for decision-making in oncology, but also reveal interesting characteristics to be further explored.

Accordingly, section 4.1 firstly introduces ODE-based modeling in tumor dyamics while section 4.2 presents five of the most popular models in the category. Next, they are analytically solved using fractional power series method and compared to corresponding classical solutions. Experimental data are used to best-fit (i.e. fine-tune) free model parameters, including the fractional order α, in section 4.3. Solutions are numerically implemented and the capability of simulating future tumor behavior is assessed for both fractional and classical models, with main results being discussed. Finally, main conclusions are drawn in section 4.4.

4.1 Introduction

Despite being an exceptionally complex group of diseases, all solid cancers have a common origin on the growth of a primary tumor. Focusing on this mutual point may contribute to understand important features of early tumor growth. While gene sequencing and molecular biology have increasingly clarified paths and signals leading to cancerous cell arise (GOLUB et al., 1999; EASTON et al., 2015), it is equally important to understand phenomenological principles underlying tumor population cells growth. Approaches based on ecological models and expressed via ordinary differential equations (ODE) offer the possibility of broadening concepts and insights as far as general avascular tumor growth is concerned (SAVAGEAU, 1980; SACHS; HLATKY; HAHNFELDT, 2001; SARAPATA; DE PILLIS, 2014).

By including specific modifications to account for experimental observations and biological particularities, several ODE models have been developed to describe dynamic tumor growth. The majority of them follows a sigmoidal law relying on two parameters, namely growth rate and carrying capacity of the population. This behavior is justified by

the different stages that a primary tumor undergoes in view of available resources such as tumor surface area and medium heterogeneity (MARU' I et al., 1994).

Although simpler than oncology models including partial differential equations (PDEs), ODE-based approaches have conveniences that motivate their use until today (WODARZ; KOMAROVA, 2014). Their relative simplicity enables analytical solutions being deduced, as means to mathematically describe phenomena evolution (SANTOS, 2007). Besides, ODE-based models are flexible, an their free parameters can be fine-tuned against experimental data so as to describe different tumor phases (BENZEKRY et al., 2014; HARTUNG et al., 2014), which favors their use to support clinical advice. Nevertheless, there is not a consensus about choosing the most appropriate ODE-based model for a particular cancer. Unsuitable model choice may yield considerable differences in oncological predictions (MURPHY; JAAFARI; DOBROVOLNY, 2016), thus claiming for further research.

Accordingly, ODE models for tumor growth can be extended to better fit experimental data while keeping their deductive-reductionist aspects (i.e. they can be generalized so that complexity becomes embedded in simplicity). Amid mathematical alternatives, fractional calculus studies non-integer order differential and integral calculus (OLDHAM; SPANIER, 1974; HERRMANN, 2014; DAVID; LINARES; PALLONE, 2011; SALES TEODORO; TENREIRO MACHADO; CAPELAS DE OLIVEIRA, 2019; TARASOV; TARASOVA, 2019). Fractional models are characterized by the presence of an arbitrary order of differentiation (or integration), which expands the application scope to deal with distinct behavior according to such fractional order. This is a key aspect of non-integer order calculus, which makes it an interesting tool for reductionist approaches, even in relatively simpler models. Moreover, fractional calculus have inherent attributes that may improve ODE-based tumor models such as describing complex phenomena as long-term memory and/or spatial heterogeneity (WEST, 2014).

For their many remarkable characteristics, fractional models have been increasingly chosen and successfully applied in signal processing (MILJKOVI et al., 2017), thermoacoustics (VALENTIM, 2018), economy (DAVID et al., 2016), robotics (LEYDEN; GOODWINE, 2016), viscoelasticity (DAVID; KATAYAMA, 2013), chemical kinetics (SINGH; KUMAR; BALEANU, 2017), electromagnetism (MESCIA; BIA; CARATELLI, 2019), agricultural computing (DAVID et al., 2016), traffic control (KUMAR et al., 2018), among other areas (DAVID; RABI, 2020; DAVID et al., 2020; MAINARDI, 2018; HERNANDEZ; O'REGAN; BALACHANDRAN, 2010). In fact, what could be coined as "fractional mathematical oncology" already exists, with many recent studies deploying non-integer calculus to deal with cancer-related topics including chemotherapy, radiotherapy and immunotherapy dynamics (UCAR; ÖZDEMIR; ALTUN, 2019; YILDIZ; ARSHAD; BALEANU, 2018; FARAYOLA et al., 2020; KHAJANCHI; NIETO, 2019), numerical solution and control for invasion systems (MANIMARAN et al., 2019; DAI; LIU, 2019), bioengineering (IONESCU

et al., 2017), and tumor growth (SOWNDARRAJAN et al., 2019; SOLÍS-PÉREZ; GÓMEZ-AGUILAR; ATANGANA, 2019, 2019; REN; YU; CHEN, 2018; BOLTON et al., 2015). The increasing number of studies in this area might support fractional calculus as alternative reductionist phenomenological modeling (approach) to further investigate early avascular general tumor growth governed by ODEs.

Accordingly, to the best of our knowledge, a comparison of widely used ODE models for tumor growth and their fractional counterparts remains largely unattempted, especially if considering as evaluation criteria their prediction performance when fitted with a relatively long clinical time series. In view of that, the present study aims at assessing whether fractional models have advantages in relation to integer counterparts claimed as better alternatives for classical population-based tumor models.

4.2 Methodology

4.2.1 Extant tumor growth models

Tumor growth models governed by ODEs equations usually have the general form

$$\frac{dV(t)}{dt} = af(V(t)) \quad bg(V(t)), \tag{4.1}$$

where $V(t)$ is tumor volume at a given time t, $\frac{dV(t)}{dt}$ represents tumor growth rate, a is a parameter related to how tumor increases its size whereas b is a parameter limiting tumor size (WODARZ; KOMAROVA, 2014). Functions $f(V(t))$ and $g(V(t))$ dictate whether the model is exponential, logistic or other.

Being the simplest one to analyze tumor growth, the exponential model is characterized by growth rate linearly proportional to tumor size. The governing ODE is obtained by imposing $f(V(t)) = V(t)$ and $g(V(t)) = 0$ in Eq. (4.1). Being one of the earliest tumor models, the exponential model has been explored under the fractional calculus viewpoint (ATICI et al., 2015; IOMIN, 2006).

Sigmoidal cancer models are characterized by S-shaped growth curves, the most known being the logistic model or Verhulst equation. The main difference from the exponential model is that growth is bounded by a maximum (i.e. asymptotic) tumor size. Biologically speaking, this upper limit might, in principle, resemble real tumor dynamics, i.e. as tumor size increases so does its difficulty to absorb nutrients and oxygen via diffusion (by disregarding angiogenesis). The logistic model is obtained by imposing $f(V(t)) = V(t)$ and $g(V(t)) = V(t)^2$ in Eq. (4.1). Some fractional logistic models have been proposed and solved for several applications, including tumor growth (ORTIGUEIRA; BENGOCHEA, 2017; TARASOV, 2019; AREA; LOSADA; NIETO, 2016; D'OVIDIO; LORETI, 2018).

Another widely used ODE model for tumor dynamics is Gompertz Law (LAIRD, 1964), stating that growth rate decays exponentially, which biologically resonates very well with several types of tumor. Accordingly, this model is considered one of the best

predictors of tumor behavior among ODE-based models, specially for patients under chemotherapy (NORTON, 1988). It has been explored under several distinct approaches, including more recently fractional modeling (FRUNZO et al., 2019). Although Gompertz model has many parameterizations (TJØRVE; TJØRVE, 2017), in the present study we choose an approach (NORTON, 1988) that imposes $f(V(t)) = 0$ and $g(V(t)) = bV(t)\ln(V(t)\ V_\infty)$ in Eq. (4.1). This variation of Gompertz equation was chosen because it has the same number of parameters as in other ODE models (excluding the exponential variation).

The next model herein considered is the one proposed by Von Bertalanffy (VON BERTALANFFY, 1960), which accounts for allometric principles regarding tumor shape development (namely a sphere in the present study). According to this model, both tumor growth and degradation are proportional to a power of tumor size, which resonates very well with the idea that cells in different tumor layers have distinct access to nutrients, thus rendering distinct behavior. Bertalanffy model is obtained from the general form, Eq. (4.1), by setting $f(V(t)) = V(t)^{2\ 3}$ and $g(V(t)) = V(t)$.

Guiot-West model is also considered, which envisages an universal growth law as proposed by Guiot (GUIOT et al., 2003) while following complexity and scaling considerations from West (WEST; BROWN; ENQUIST, 2001). It mathematically resembles Bertalanffy model with a different power of tumor size. Having its roots in the fractal-like structure of energy distribution, 3/4 power is a recurring value in models of complex natural phenomena. From the general form, Eq. (4.1), Guiot-West model is obtained when $f(V(t)) = V(t)^{3\ 4}$ and $g(V(t)) = V(t)$.

Except for the exponential model, aforesaid ODE models have mutual similarities since they all follow sigmoidal laws with a growth rate parameter (either a or b) and a limiting parameter (V_∞). However, as previously stated, they also have distinct characteristics that emulate specific tumor growth nature, thus justifying the assessment of their predicting performance against experimental data. For convenience, the corresponding ODEs for each of those models are summarized in Table 1.

Table 1 – ODE-based tumor growth models considered in this study.

Model	Differential equation	Max. Size	Growth condition
Exponential	$\frac{dV(t)}{dt} = aV(t)$		$a > 0$
Logistic	$\frac{dV(t)}{dt} = aV(t)\left(1 \quad \frac{V(t)}{V_\infty}\right)$	$V_\infty = a\ \ b$	$a > 0$
Gompertz	$\frac{dV(t)}{dt} = bV(t)\ln\left(\frac{V_\infty}{V(t)}\right)$	$V_\infty = \ln^{-1}(a\ \ b)$	$b > 0$
Bertalanffy	$\frac{dV(t)}{dt} = aV(t)^{2\ 3} \quad bV(t)$	$V_\infty = (a\ \ b)^3$	$a > b$
Guiot-West	$\frac{dV(t)}{dt} = aV(t)^{3\ 4} \quad bV(t)$	$V_\infty = (a\ \ b)^4$	$a > b$

Source: Valentim et al. (2020).

4.2.2 Fractional analytical solutions

The governing differential equations presented in subsection 4.2.1 are analytically solved by the fractional power series method (TRUJILLO; RIBERO; BONILLA, 1999) whose application to exponentially-based ODEs is opportune. Such methodology has been applied (KILBAS; SRIVASTAVA; TRUJILLO, 2006) to similar ODEs, demonstrating good suitability in this context.

4.2.3 Fractional derivative operator to power series

In line with Eq. (3.23), Caputo's definition is used for a series representation as

$$f(x) = \sum_{n=0}^{\infty} C_n x^n$$

applied to a power series concerning tumor volume $V(t)$. Aiming at fractionally modeling time-dependent tumor growth, $x = t^\alpha$ is then set for $t \quad 0$ with $0 < x < R$ and $0 < t^\alpha < R^\alpha$, where R is the radius of convergence of the series for which such operations hold (TRUJILLO; RIBERO; BONILLA, 1999), yielding

$$D_t^\alpha V(t) = \sum_{n=0}^{\infty} C_n D_t^\alpha (t^{n\alpha}), \quad \text{with } V(t) = \sum_{n=0}^{\infty} C_n t^{n\alpha} \tag{4.2}$$

Bearing in mind that the fractional derivative of a power is given by Eq. (3.8) and according to Eq. (3.9), the fractional derivative of $V(t)$ can be extended to a power series such that Eq. (4.2) becomes

$$D_t^\alpha V(t) = \sum_{n=1}^{\infty} C_n \frac{(n\alpha + 1)}{[(n \quad 1)\alpha + 1]} t^{(n-1)\alpha} \tag{4.3}$$

for $n > 0$ and $D_t^\alpha V(t) = 0$ in case of $n = 0$.

Accordingly, Eq. (4.3) establishes the fractional derivative of time-dependent tumor volume $V(t)$ as represented by a fractional power series, Eq. (4.2). In what follows, a generalized (i.e. fractional) solution is proposed for each ODE-based tumor growth model considered in Table 1.

4.2.4 Fractional exponential model

The generalized representation of the exponential model is given by

$$D_t^\alpha V(t) \quad aV(t) = 0 \tag{4.4}$$

Since the expression for $D_t^\alpha V(t)$ is established, one can insert Eqs. (4.2) and (4.3) into Eq. (4.4)

$$\sum_{n=1}^{\infty} C_n \frac{(n\alpha + 1)}{[(n \quad 1)\alpha + 1]} t^{(n-1)\alpha} \quad a \sum_{n=0}^{\infty} C_n t^{n\alpha} = 0$$

After index adjustment and some manipulation, one obtains the recurring equation for a non-trivial solution

$$C_{n+1} = \frac{aC_n \ \ (n\alpha + 1)}{[(n+1)\alpha + 1]} \tag{4.5}$$

The first series coefficient C_0 is recovered by imposing the initial condition. Therefore, considering Eq. (4.2) for $t = 0$ and initial tumor volume V_0, one obtains $C_0 = V_0$. By applying such recurrence relations to Eq. (4.2), the solution for Eq. (4.4) then becomes

$$V(t) = V_0 + aV_0t^{\alpha} + \frac{a^2V_0}{(2\alpha+1)}t^{2\alpha} + \frac{a^3V_0}{(3\alpha+1)}t^{3\alpha} + \quad = V_0\sum_{n=0}^{\infty}\frac{a^nt^{n\alpha}}{(n\alpha+1)} \tag{4.6}$$

It is possible to represent such solution in a more elegant form using Mittag-Leffler function in Eq. (3.4), which yields

$$V(t) = V_0E_{\alpha}(at^{\alpha}) \tag{4.7}$$

It is worth remarking that the solution given by Eq. (4.6), or equivalently Eq. (4.7), is a generalization of the integer order model. In other words, when $\alpha = 1$ aforesaid equations recover the classical representations related to the integer order model, namely

$$V(t) = V_0\sum_{n=0}^{\infty}\frac{a^nt^n}{n!} = V_0e^{at} \tag{4.8}$$

4.2.5 Fractional logistic model

In order to solve the fractional version of the logistic model, the variable change $V(t) = 1 \ \ u(t)$ is proposed. Thereby, the governing ODE of such model is rewritten as

$$\frac{du(t)}{dt} + au(t) = \frac{a}{V_{\infty}},$$

whose derivative change to a fractional operator yields the generalized form

$$D_t^{\alpha}u(t) + au(t) = \frac{a}{V_{\infty}}, \tag{4.9}$$

with $u(t)$ being a fractional power series analogous to Eq. (4.2).

Bearing in mind the fractional power series representations for $D_t^{\alpha}u(t)$ and $u(t)$, as respectively given by Eqs. (4.3) and (4.2), Eq. (4.9) then becomes

$$\sum_{n=1}^{\infty}C_n\frac{(n\alpha+1)}{[(n \quad 1)\alpha+1]}t^{(n-1)\alpha} + a\sum_{n=0}^{\infty}C_nt^{n\alpha} = \frac{a}{V_{\infty}}$$

In order to obtain the recurrence relations to coefficients C_n, the previous equation is rewritten as

$$\left[\frac{C_1 \ \ (\alpha+1)}{(1)} + aC_0\right]t^0 + \sum_{n=1}^{\infty}\left[C_{n+1}\frac{[(n+1)\alpha+1]}{(n\alpha+1)} + aC_n\right]t^{n\alpha} = \frac{a}{V_{\infty}}t^0 + \sum_{n=0}^{\infty}0t^{n\alpha} \tag{4.10}$$

By retrieving C_0 from the initial condition $u_0 = 1\ V_0$, the recurrence relation for the first coefficient is

$$C_1 = \frac{a}{(\alpha+1)}\left(C_0 \quad \frac{1}{V_\infty}\right), \tag{4.11}$$

whereas for remaining coefficients

$$C_{n+1} = \frac{aC_n\ (n\alpha+1)}{[(n+1)\alpha+1]} \tag{4.12}$$

By applying such recurrence relations, one obtains a solution for Eq. (4.9) given by

$$u(t) = \frac{1}{V_0} + \left(\frac{1}{V_0} \quad \frac{1}{V_\infty}\right)\left(\ at^\alpha + \frac{a^2}{(2\alpha+1)}t^{2\alpha} + \quad\right) = \frac{1}{V_0} + \left(\frac{1}{V_0} \quad \frac{1}{V_\infty}\right)\sum_{n=1}^{\infty}\frac{(-a)^n t^{n\alpha}}{(n\alpha+1)} \tag{4.13}$$

A solution for the fractional logistic model is obtained by retrieving the original variable $V(t) = 1\ u(t)$

$$V(t) = \frac{V_\infty}{\frac{V_\infty}{V_0} + \left(\frac{V_\infty}{V_0} \quad 1\right)\sum_{n=1}^{\infty}\frac{(-a)^n t^{n\alpha}}{(n\alpha+1)}} = \frac{V_\infty}{1 + \left(\frac{V_\infty}{V_0} \quad 1\right)E_\alpha(\ at^\alpha)} \tag{4.14}$$

As in fractional solutions subsequently presented in this work, the second expression refers to the related Mittag-Leffler representation. Analogous to the fractional exponential solution, the classical representations are recovered when $\alpha = 1$ is imposed in Eq. (4.14)

$$V(t) = \frac{V_\infty}{\frac{V_\infty}{V_0} + \left(\frac{V_\infty}{V_0} \quad 1\right)\sum_{n=1}^{\infty}\frac{(-a)^n t^n}{n!}} = \frac{V_\infty}{1 + (V_\infty\ V_0 \quad 1)e^{-at}} \tag{4.15}$$

4.2.6 Fractional Gompertz model

In order to solve the fractional version of Gompertz model, the variable change $V(t) = V_\infty e^{-u(t)}$ is proposed. Thereby, the governing ODE is rewritten as

$$\frac{du(t)}{dt} = \quad bu(t),$$

so that changing the derivative for a fractional operator renders the generalized form

$$D_t^\alpha u(t) + bu(t) = 0, \tag{4.16}$$

with $u(t)$ being again a fractional power series analogous to Eq. (4.2).

Since Eq. (4.16) is very similar to Eq. (4.4), the solution procedure is analogous to the one concerning the exponential model. Therefore, for the sake of brevity, the solution for Eq. (4.16) is straightforwardly given by

$$u(t) = \ln\left(\frac{V_\infty}{V_0}\right)\left[1 + \quad bt^\alpha + \frac{b^2}{(2\alpha+1)}t^{2\alpha} + \quad\right] = \ln\left(\frac{V_\infty}{V_0}\right)\sum_{n=0}^{\infty}\frac{(\quad b)^n t^{n\alpha}}{(n\alpha+1)} \tag{4.17}$$

Changing back to variable $V(t) = V_\infty e^{-u}$ one obtains

$$V(t) = V_0 \exp\left[\ln\left(\frac{V_\infty}{V_0}\right)\left[1 \quad \sum_{n=0}^{\infty} \frac{(-b)^n t^{n\alpha}}{(n\alpha+1)}\right]\right] = V_0 \exp\left[\ln\left(\frac{V_\infty}{V_0}\right)[1 \quad E_\alpha(\ \ bt^\alpha)]\right] \tag{4.18}$$

Once more, classical representations are recovered by imposing $\alpha = 1$ in Eq. (4.18)

$$V(t) = V_0 \exp\left[\ln\left(\frac{V_\infty}{V_0}\right)\left[1 \quad \sum_{n=0}^{\infty} \frac{(\ \ b)^n t^n}{n!}\right]\right] = V_0 \exp\left[\ln\left(\frac{V_\infty}{V_0}\right)\left(1 \quad e^{-bt}\right)\right] \tag{4.19}$$

4.2.7 Fractional Bertalanffy model

In order to solve the fractional version of Bertalanffy model, the variable change $V(t) = u(t)^3$ is proposed. Thereby, the governing ODE is rewritten as

$$\frac{du(t)}{dt} + \frac{b}{3}u(t) = \frac{a}{3},$$

where changing the derivative to a fractional operator yields the generalized form

$$D_t^\alpha u(t) + \frac{b}{3}u(t) = \frac{a}{3}, \tag{4.20}$$

with $u(t)$ being a fractional power series analogous to Eq. (4.2).

As Eq. (4.20) is very similar to Eq. (4.9), the recurrence relations are given by

$$C_1 = \quad \frac{b}{3}\frac{1}{(\alpha+1)}\left(C_0 \quad \frac{a}{b}\right), \tag{4.21}$$

where C_0 is the initial condition $u_0 = V_0^3$, and

$$C_{n+1} = \quad \frac{b}{3}\frac{C_n \ \ (n\alpha+1)}{[(n+1)\alpha+1]} \tag{4.22}$$

From those recurrence relations, one finally obtains a solution for Eq. (4.20)

$$u(t) = V_0^{1\ 3} + \left(V_0^{1\ 3} \quad \frac{a}{b}\right)\left[\ \ \frac{b}{3}t^\alpha + \left(\frac{b}{3}\right)^2 \frac{t^{2\alpha}}{(2\alpha+1)} + \quad\right] = V_0^{1\ 3} + \left(V_0^{1\ 3} \quad \frac{a}{b}\right)\sum_{n=1}^{\infty}\left[\left(\ \ \frac{b}{3}\right)^n \frac{t^{n\alpha}}{(n\alpha+1)}\right] \tag{4.23}$$

By changing back to $V(t) = u(t)^3$ one obtains

$$V(t) = \left[V_0^{1\ 3} + \left(V_0^{1\ 3} \quad \frac{a}{b}\right)\sum_{n=1}^{\infty}\left[\left(\ \ \frac{b}{3}\right)^n \frac{t^{n\alpha}}{(n\alpha+1)}\right]\right]^3,$$

which has $a \ \ b = V_\infty^{1\ 3}$ to avoid division by zero while maintaining parameter homogeneity with previous models. One thus obtains a generalized solution to Bertalanffy model

$$V(t) = \left[V_0^{1\ 3} + \left(V_0^{1\ 3} \quad V_\infty^{1\ 3}\right)\sum_{n=1}^{\infty}\left[\left(\ \ \frac{b}{3}\right)^n \frac{t^{n\alpha}}{(n\alpha+1)}\right]\right]^3 = \left[V_\infty^{1\ 3} + \left(V_0^{1\ 3} \quad V_\infty^{1\ 3}\right) E_\alpha\left(\ \ \frac{b}{3}t^\alpha\right)\right]^3 \tag{4.24}$$

As expected, by imposing $\alpha = 1$ Eq. (4.24) recovers classical representations

$$V(t) = \left[V_0^{1\ 3} + \left(V_0^{1\ 3} \quad V_\infty^{1\ 3}\right)\sum_{n=1}^{\infty}\left[\left(\ \ \frac{b}{3}\right)^n \frac{t^n}{n!}\right]\right]^3 = \left[V_\infty^{1\ 3} + \left(V_0^{1\ 3} \quad V_\infty^{1\ 3}\right) e^{-\frac{b}{3}t}\right]^3 \tag{4.25}$$

4.2.8 Fractional Guiot-West model

The final model considered is the generalized version of Guiot-West model, in which the variable change $V(t) = u(t)^4$ is proposed. Thereby, one can rewrite the governing ODE as

$$\frac{du(t)}{dt} + \frac{b}{4}u(t) = \frac{a}{4},$$

whose derivative change to a fractional operator yields the generalized form

$$D_t^\alpha u(t) + \frac{b}{4}u(t) = \frac{a}{4} \tag{4.26}$$

The analytical steps to solve Eq. (4.26) are very similar to those solving Eq. (4.20). Accordingly, the solution for Eq. (4.26) is given by

$$u(t) = V_0^{1\ 4} + \left(V_0^{1\ 4} \quad \tfrac{a}{b}\right)\left[\ \tfrac{b}{3}t^\alpha + \left(\tfrac{b}{3}\right)^2 \tfrac{t^{2\alpha}}{(2\alpha+1)} + \quad \right] = V_0^{1\ 4} + \left(V_0^{1\ 4} \quad V_\infty^{1\ 4}\right)\sum_{n=1}^{\infty}\left[\left(\ \tfrac{b}{4}\right)^n \tfrac{t^{n\alpha}}{(n\alpha+1)}\right] \tag{4.27}$$

By changing back to $V(t) = u(t)^4$ one finds a generalized solution for Guiot-West model as

$$V(t) = \left[V_0^{1\ 4} + \left(V_0^{1\ 4} \quad V_\infty^{1\ 4}\right)\sum_{n=1}^{\infty}\left[\left(\ \tfrac{b}{4}\right)^n \tfrac{t^{n\alpha}}{(n\alpha+1)}\right]\right]^4 = \left[\tfrac{a}{b} + \left(V_0^{1\ 4} \quad V_\infty^{1\ 4}\right) E_\alpha\left(\ \tfrac{b}{4}t^\alpha\right)\right]^4 \tag{4.28}$$

By imposing $\alpha = 1$, Eq. (4.28) also recovers classical representations

$$V(t) = \left[V_0^{1\ 4} + \left(V_0^{1\ 4} \quad V_\infty^{1\ 4}\right)\sum_{n=1}^{\infty}\left[\left(\ \frac{b}{4}\right)^n \frac{t^n}{n!}\right]\right]^4 = \left[V_\infty^{1\ 4} + \left(V_0^{1\ 4} \quad V_\infty^{1\ 4}\right) e^{-\frac{b}{4}t}\right]^4 \tag{4.29}$$

In order to summarize the solutions derived in this section, Table 2 presents the fractional analytical solutions for each model along with their classical integer order counterparts. The proof of convergence is demonstrated by finding the radius of convergence R for each power series (as presented in appendix 4.5.1).

Additionally, it is important to state that in cases where variables are changed, the fractional equation solved for each model are Eqs. (4.13), (4.17), (4.23), and (4.27). Therefore, as presented in Table 2, the fractional solutions herein obtained refer to modified fractional versions of Logistic, Gompertz, Bertalanffy and Guiot-West models. While appendix 4.5.2 brings further comments on this issue, throughout the text those modified models will be referred to simply as models' for the sake of conciseness.

4.2.9 Numerical methods and clinical data

Experimental data to fine-tune the model parameters were extracted from Worschech et al. (2009), hereby listed in Table 3 and represented in Figure 4. These data refer to human breast cancer of cell line GI-101A reproduced by xenografts (i.e. inserted and grown in live animals, nude mice in this case) and comprise a time series of the 14 points, each representing tumor volume (in mm^3) at a specific time (in days). The time series

Table 2 – Representation of classical and fractional solutions for extant tumor growth ODE models for $0 < \alpha \leq 1$.

Model	Classical solution $V(t) =$	Modified-Fractional model	Var. change $V(t) =$	Fractional solution $V(t) =$
Exp.	$V_0 e^{a}$	$D_t^{\alpha} V(t) = aV(t)$		$V_0 E_{\alpha}(at^{\alpha})$
Log.	$\frac{V_{\infty}}{1+(V_{\infty}\ V_0-1)e^{-at}}$	$D_t^{\alpha} u(t) + au(t) = \frac{a}{V_{\infty}}$	$\frac{1}{u(t)}$	$\frac{V_{\infty}}{1+(V_{\infty}\ V_0-1)E_{\alpha}(-at^{\alpha})}$
Gom.	$V_0 \exp\left[\ln\left(\frac{V_{\infty}}{V_0}\right)\left(1 \quad e^{-bt}\right)\right]$	$D_t^{\alpha} u(t) + bu(t) = 0$	$V_{\infty} e^{-u(t)}$	$V_0 \exp\left[\ln\left(\frac{V_{\infty}}{V_0}\right)[1 \quad E_{\alpha}(\ \ bt^{\alpha})]\right]$
Ber.	$\left[V_{\infty}^{1\ 3} + \left(V_0^{1\ 3} \quad V_{\infty}^{1\ 3}\right) e^{-\frac{b}{3}t}\right]^3$	$D_t^{\alpha} u(t) + \frac{b}{3} u(t) = \frac{a}{3}$	$u(t)^3$	$\left[V_{\infty}^{1\ 3} + \left(V_0^{1\ 3} \quad V_{\infty}^{1\ 3}\right) E_{\alpha}\left(\ \ \frac{b}{3}t^{\alpha}\right)\right]^3$
G.W.	$\left[V_{\infty}^{1\ 4} + \left(V_0^{1\ 4} \quad V_{\infty}^{1\ 4}\right) e^{-\frac{b}{4}t}\right]^4$	$D_t^{\alpha} u(t) + \frac{b}{4} u(t) = \frac{a}{4}$	$u(t)^4$	$\left[V_{\infty}^{1\ 4} + \left(V_0^{1\ 4} \quad V_{\infty}^{1\ 4}\right) E_{\alpha}\left(\ \ \frac{b}{4}t^{\alpha}\right)\right]^4$

Source: Valentim et al. (2020).

statistically represents eight different patients, where it is assumed that the precision is identical for all points, with no uncertainty differences between experimental points affecting the curve fitting in any tests.

Furthermore, points were extracted using online tool *WebPlotDigitizer* and, as this is a manual procedure, it might involve some degree of inaccuracy. Consequently, while resulting error values and best-fitted parameters should not be identical to those in (MURPHY; JAAFARI; DOBROVOLNY, 2016), one can reproduce them by using the values in Table 3.

Table 3 – Clinical time series.

Time (days)	0 00	9 02	20 00	32 07	43 04	54 01	65 15
Volume (mm^3)	225 5	303 0	575 6	651 4	681 6	927 8	1211 8
Time (days)	76 04	82 04	87 10	93 00	97 99	106 96	114 03
Volume (mm^3)	1458 0	1897 3	2166 2	2557 0	2707 7	2916 8	3480 2

Source: Data extracted from Worschech et al. (2009).

The best-fitted model parameters were obtained using Mathematica and *FindMinimum/NMinimize* functions. A global-search algorithm was employed to minimize the sum of squared residuals (SSR) for different parameter combinations, which is here calculated as

$$SSR = \sum_{j=1}^{n} (V_j \quad V_j)^2, \tag{4.30}$$

where V_j are the experimental data, $n = 14$ stands for the total number of points, and V_j are the corresponding analytical approximations.

In each routine instance, 100 random start values were generated as constrained by the specific profile and model restrictions. Moreover, an internal interior-point method was executed in parallel to compare each model configuration against the available experimental data. Therefore, the local minima were identified and ranked in order to find the global minimum for each model configuration. Constraints were chosen to guarantee stability and closeness to real characteristics being simulated. Accordingly, growth rate

Figure 4 – Plot of clinical time series: evolution of tumor volume.

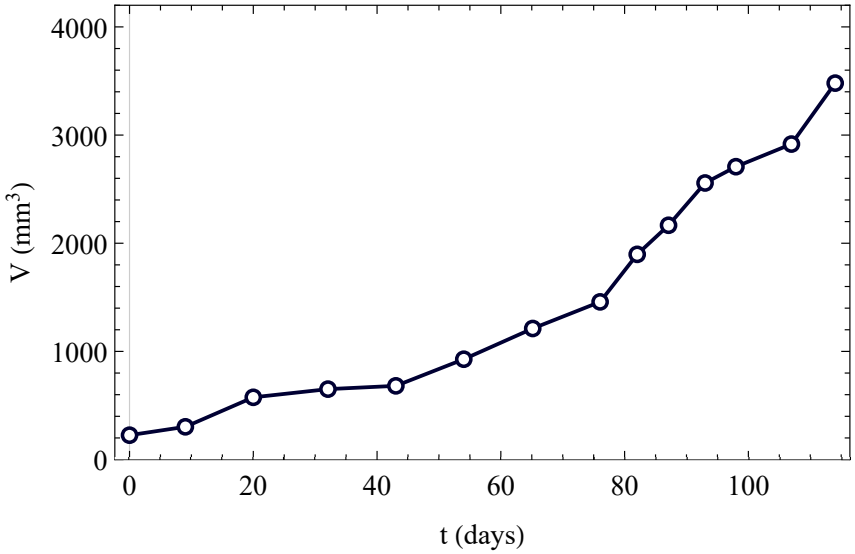

Source: Data extracted and plotted from Worschech et al. (2009).

parameters (a or b) were forced to be positive while maximum tumor size V_∞ was limited to values between 1000 and 1 10^7 mm^3. This upper bound was chosen based on (KHAJOTIA et al., 2014), which reported the extraction of an unusually large breast tumor of approximately $105,000$ mm^3 from a middle-aged patient. Fractional order evaluation was bounded as $0 < \alpha \leq 1$.

Either when the algorithm failed to find the global minimal SSR for a given profile or when the results were not accurate enough, the algorithm was re-calculated by changing the search range of each parameter. Processing was repeated until the minimum SSR for each model was found. After finding the parameter combinations yielding the lowest SSR, additional evaluation indexes were used to better assess the fitting of these parameters, namely the root mean squared deviation

$$RMSD = \sqrt{\frac{1}{n}\sum_{j=1}^{n}\left(V_j \quad V_j\right)^2} \tag{4.31}$$

and the coefficient of determination

$$R^2 = 1 \quad \frac{\sum_{j=1}^{n}(V_j \quad V_j)^2}{\sum_{j=1}^{n}(V_j \quad V)^2}, \tag{4.32}$$

where V is the mean of the experimental values. Finally, the symmetric mean absolute percentage error was evaluated as

$$SMAPE = \frac{100\%}{n}\sum_{j=1}\frac{V_j \quad V_j}{(\ V_j \ + \ V_j\ )\ \ 2} \tag{4.33}$$

Simulation results and best-fitted fractional ODE models are discussed in section 4.3.

4.3 Results and discussion

The first half of the experimental time series in Table 3 was used to best fit model parameters whereas the remaining points were used for prediction. Best-fitted model parameters are presented in Table 4 with 8-digit and 6-digit precision respectively used for model parameters and quality indicators. The first SSR column presents the error indicator referring to the first seven data values, i.e. the quality indicator used as minimizing objective function related to the best-fitted parameters. Along with other quality indicators, the second SSR column is calculated using best-fitted parameters while considering the entire time series. Therefore, these are the values to be analyzed when assessing which model can better predict tumor growth.

Results show that the fractional version of each model achieves better indicators in comparison to integer order counterparts. Although this outcome may be justified by the fact that all fractional models have an extra parameter, it is worth analyzing the arbitrary order power of each model. The exponential models were the best-fitted ones to experimental data whereas the integer order logistic model was by far the worst predictor. Results follow, at least proportionally, those obtained in (MURPHY; JAAFARI; DOBROVOLNY, 2016) for integer order models. Discrepancies might be attributed to possible disparity when extracting plot data as well as parameterization choice, e.g. we used two parameters in all models while Murphy, Jaafari and Dobrovolny (2016) opted for 3-parameter Gompertz version.

When choosing which model to adopt for tumor growth prediction, one should elect the model based on the lowest SSR for the first seven clinical values. As discussed by Murphy, Jaafari and Dobrovolny (2016), even best-fitted ODE models should be chosen very carefully and results in Table 4 suggest this is especially true if only integer order models are considered. In this case, one would choose Bertalanffy model even though it is not the best predictor. On the other hand, this misdirection does not occur if non-integer order models are considered, as one would choose the fractional exponential model, which has the best predicting performance (i.e. the lowest error indicators).

If one also considers fractional models instead of only their classical versions, the indicator for how close the best model replicates experimental data would rise from 67 5% to 88 8% - a very significant improvement. This reveals a major convenience of using fractional models as they keep a higher degree of information regarding the fitted time series, decreasing misfitting while still maintaining a relatively simple and reductionist form. Such advantage is mainly attributed to the memory effect, an inherent characteristic linked to the definition of fractional operators that allows models to consider not only elements at the evaluation instant but also those occurring before. This feature naturally favors fractional models to describe biological phenomena, as these generally involve complex and emergent behavior, with tumor growth being no exception.

SMAPE indexes provide immediate understanding of how significant error measures

Table 4 – Best-fitting results and quality indicators concerning prediction capabilities.

	Optimal parameters			Fitting (first 7 values)	Evaluation indicators (all 14 values)			
Model	α	a or b	V_∞	SSR	SSR	RMSD	SMAPE	R^2
Exp.	1	0 026262978		56015 1	1 90101 10^6	98 4837	10 91%	0 871367
	0 54461097	0 10866092		24538 9	1 65259 10^6	91 8235	13 46%	0 888177
Log.	1	0 037933924	1904 4308	38749 45	7 46890 10^6	195 209	25 19%	0 494611
	0 8260742	0 060601055	9 9999611 10^6	29423 4	4 60664 10^6	153 308	20 15%	0 688288
Gom.	1	0 013990651	3515 5192	33701 4	5 48662 10^6	167 311	21 69%	0 628744
	0 7420777	0 007056656	9 9999993 10^6	27105 3	3 37355 10^6	131 194	17 64%	0 771726
Ber.	1	0 01846817	7432 4834	32042 9	4 79927 10^6	156 480	20 39%	0 675254
	0 83361501	0 001867692	9 7941268 10^6	28525 2	4 23496 10^6	146 993	19 47%	0 713438
G.-W.	1	0 032431579	5650 8422	32450 8	4 96891 10^6	159 221	20 71%	0 663775
	0 80309314	0 004994717	9 9999988 10^6	28061 7	3 97308 10^6	142 376	18 93%	0 731159

Source: Valentim et al. (2020).

are relative to volume magnitude at each comparison. In models, relative errors range from 10 91% (exponential model) to 25 19% (logistic model). For all models but the exponential one, fractional models perform better than their integer order counterparts. This exception is probably due to the fact that the integer order exponential model predicts very well experimental points 9, 10 and 11 (compare Figure 5b and Figure 6b) while predicting very poorly points 13 and 14. As SMAPE indexes measure relative errors, they naturally tend to underweight errors in later tumor progression (as absolute values increase).

Regarding overall goodness of fit, the performance of each model can be depicted with the help of evaluation indicators in Table 4, particularly SMAPE and R^2 coefficient, which are relative indexes. Regardless of either fractional or integer order, exponential models seem to fare better (with lower SMAPE and R^2 closer to 1) while logistic models are the worst predictors for the fitted time series. Indexes ranges also indicate that the goodness of fit varies considerably among models. It is important to remind, though, that any fit is subject to uncertainties in experimental data, which is more complicated when data refer to living subjects since there are intrinsic ethical complexities in clinical trials that may impact data quality.

Nevertheless, even non-integer order models do not properly simulate values in the far future as suggested in Figure 5 and Figure 6, which compare experimental data respectively with best-fitted integer and fractional predictions. Yet, while aforesaid discrepancies claim for further studies using other data, (even slightly) better predictors may improve clinical assessment (e.g. by preventing overestimation or underestimation of chemotherapy dosage).

Overall, numerical results suggest that fractional models may play an important role in tumor prediction. The arbitrary order α has a very stark influence on each model analyzed in this study, being able to significantly alter the predicted volume growth dynamics. This feature is evidenced in Figure 7 to Figure 11 showing volume and volume change rate as plotted for different arbitrary orders about the best-fitted value for each model. In each figure, the surface on the left shows how tumor volume is dynamically

Figure 5 – Tumor growth: clinical data and numerical predictions from best-fitted fractional models.

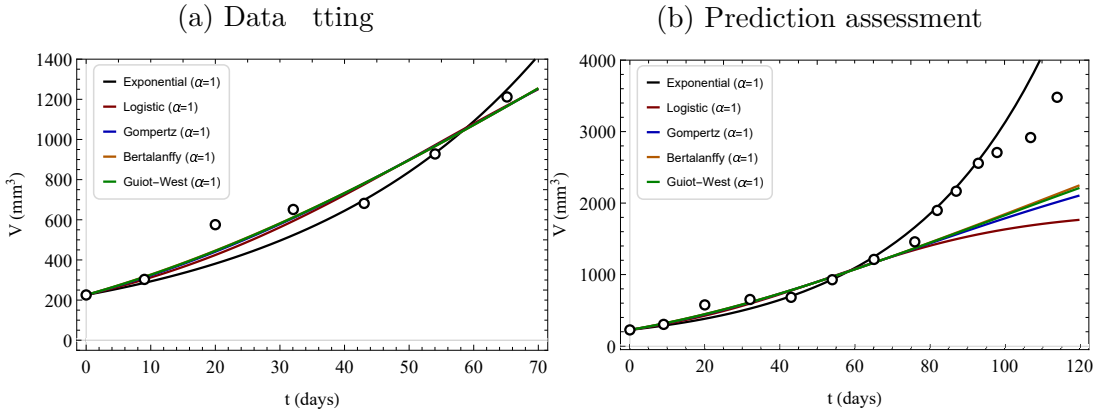

Source: Valentim et al. (2020).

Figure 6 – Tumor growth: clinical data and numerical predictions from best-fitted integer order models.

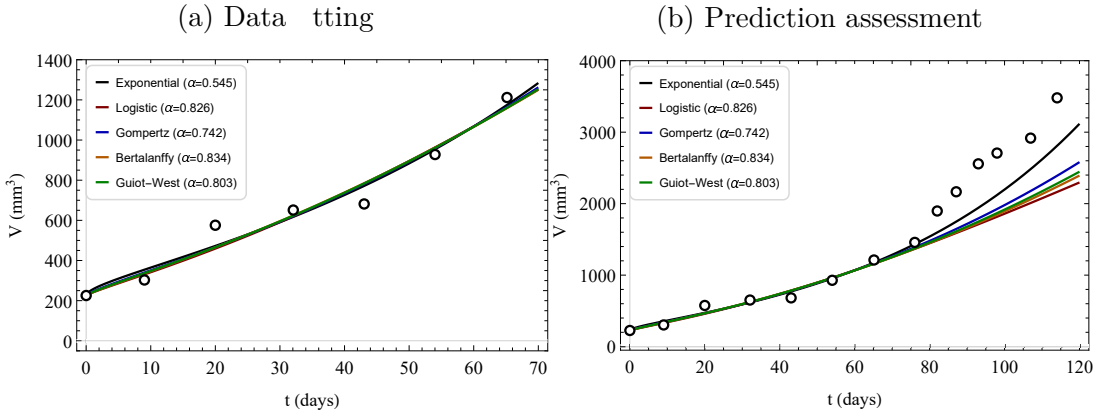

Source: Valentim et al. (2020).

modeled for different α indicating that larger or advanced-stage tumors might be better modeled with higher α values. Correspondingly, the contour plot on the right shows how more aggressive tumors (i.e. with higher volume change rate) might be better modeled with higher α as well. These figures reinforce the notion that more powerful (and useful) tumor growth models could be overruled if only integer order models are considered to support clinical advice.

Figure 7 – Tumor growth: simulations using best-fitted exponential model for different values of α and t.

(a) Tumor volume (mm^3) (b) Tumor volume variation (mm^3/day)

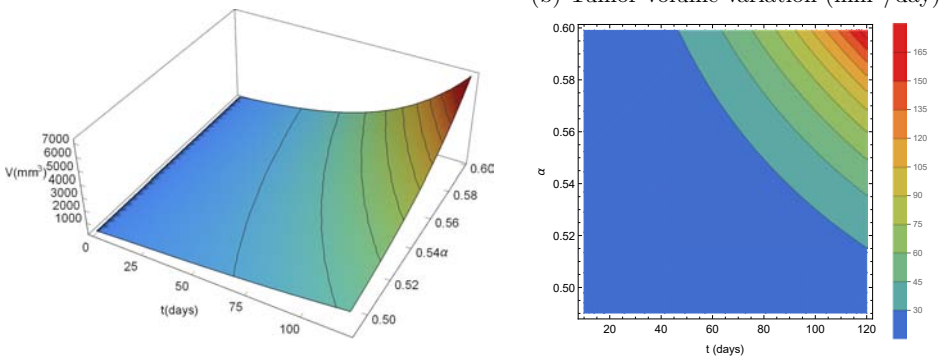

Source: Valentim et al. (2020).

Figure 8 – Tumor growth: simulations using best-fitted logistic model for different values of α and t.

(a) Tumor volume (mm^3) (b) Tumor volume variation (mm^3/day)

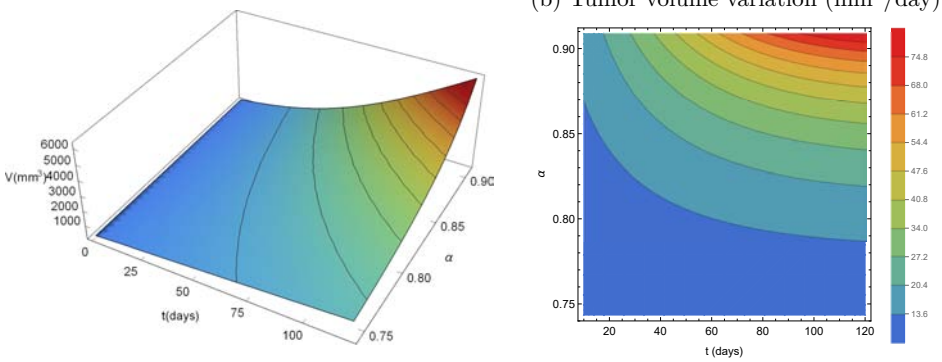

Source: Valentim et al. (2020).

Figure 9 – Tumor growth: simulations using best-fitted Gompertz model for different values of α and t.

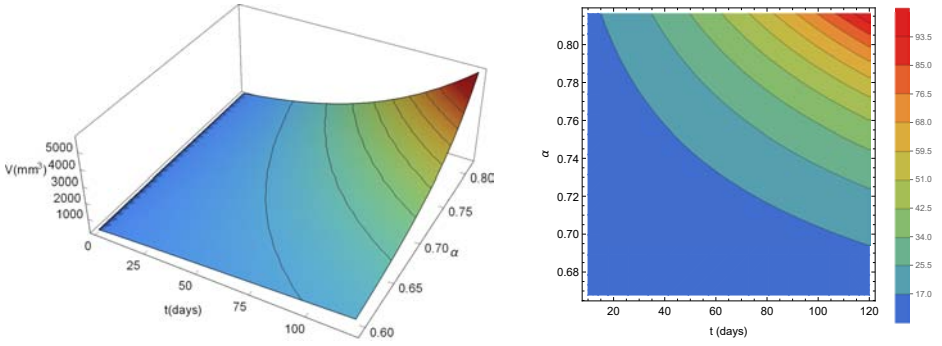

(a) Tumor volume (mm^3) (b) Tumor volume variation (mm^3/day)

Source: Valentim et al. (2020).

Figure 10 – Tumor growth: simulations using best-fitted Bertalanffy model for different values of α and t.

(a) Tumor volume (mm^3)

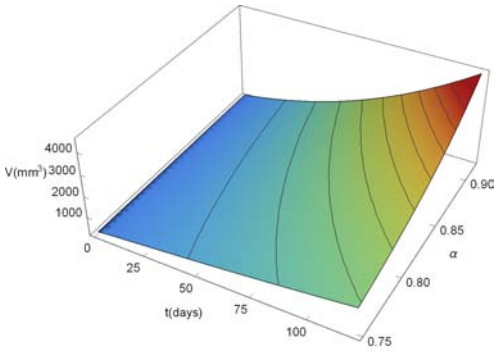

(b) Tumor volume variation (mm^3/day)

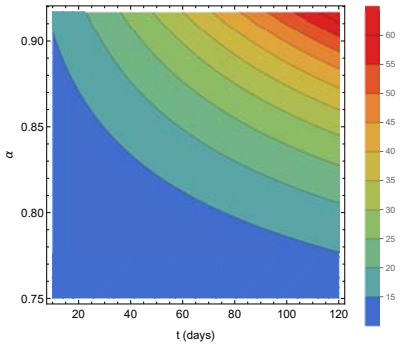

Source: Valentim et al. (2020).

Figure 11 – Tumor growth: simulations using best-fitted Guiot-West model for different values of α and t.

(a) Tumor volume (mm^3)

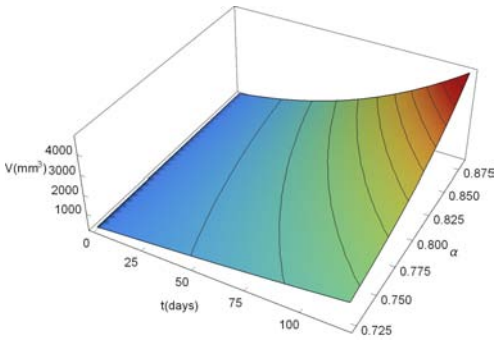

(b) Tumor volume variation (mm^3/day)

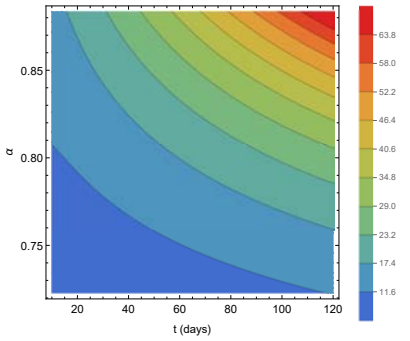

Source: Valentim et al. (2020).

4.4 Conclusions

In this chapter we derived generalized (fractional) solutions for five different ODE-based tumor growth models, using a straightforward analytical method of resolution and presenting intermediary steps to make the study more self-contained. We best-fitted those models against extant experimental data and assessed their performance and advantages in terms of predicting tumor growth - especially in comparison to their integer order counterparts. As stated in (MURPHY; JAAFARI; DOBROVOLNY, 2016), the choice of tumor growth model can lead to very different prediction outcomes, and the effect of choice should be considered very carefully. Our goal in this chapter was to investigate if fractional calculus could extend the number of adequate candidates, thus potentially improving decision making regarding the choice of an appropriate model for tumor prediction.

According to the obtained results for the particular experimental data used, one will have a lower chance of making a poor choice if he also considers the evaluation errors of non-integer order models, thus suggesting an improvement on the decision-making process. Additionally, results also reinforce the notion that fractional calculus should be a timely part of dynamic modeling regardless of the area of application.

We believe that fractional calculus have features and nuances that could be further explored in relation to tumor growth assessment. For instance, fractional models' better prediction performance may be related to the memory effect, inherent to the definition of the non-integer order derivative. Since tumors are constituted of cells accumulating several mutations and changes along their evolution, it is possible that fractional models are capable of taking these non-local (past) events into account. Another interesting trend is that higher fractional orders seem to better model larger, quickly growing, tumors. Therefore, aforesaid models should be considered to support clinical advice.

While those preliminary results and possible features are quite encouraging, further studies should be carried out, particularly regarding the versatility of arbitrary order α as well as testing these models against other experimental data sets.

4.5 APPENDIX: ODE solutions convergence tests and veri cation

4.5.1 Convergence tests

Considering that the fractional power series of the solutions for each model are convergent for a determined radius R, the proof of convergence will be demonstrated by finding such radius for each case.

The adopted procedure will consider the Cauchy-Hadamad Teorem, in which one applies the root test knowing that

$$\frac{1}{R} = \lim_{n\to\infty} (\ C_n{}^{\ 1\ n}), \tag{4.34}$$

where lim is the superior limit and C_n are the constant coefficients of a fractional power series in the form $V(t) = \sum_{n=0}^{\infty} C_n t^{n\alpha}$.

4.5.1.1 Fractional exponential model

Considering the solution given by Eq. (4.6) in the power series form, we have

$$C_n = \frac{a^n}{(n\alpha + 1)},$$

which by plugging in Eq. (4.34) yields

$$\frac{1}{R} = \lim_{n\to\infty} \left(\left| \frac{a^n}{(n\alpha + 1)} \right|^{1\ n} \right),$$

and after some manipulations

$$\frac{1}{R} = a \lim_{n\to\infty} \left(\frac{1}{(n\alpha + 1)^{\ 1\ n}} \right) = a \lim_{n\to\infty} \quad (n\alpha + 1)^{\ -1\ n}$$

Now, for finding such limit, we write

$$\frac{1}{R} = a \lim_{n\to\infty} \exp(\log(\quad (n\alpha + 1)^{\ -1\ n})) = a \exp\left(\lim_{n\to\infty} \frac{\log(\ \ (n\alpha + 1))}{n} \right)$$

By evaluating the limit with the L'Hôspital rule, one finds

$$\frac{1}{R} = a \exp\left(\lim_{n\to\infty} \frac{d(\log(\ \ (n\alpha + 1)))\ \ dn}{dn\ \ dn} \right) = a \exp\left(\lim_{n\to\infty} \frac{'(n\alpha + 1)}{(n\alpha + 1)} \right),$$

where $'$ is the derivative of the gamma function in respect of n, with such derivative being calculated by using the polygamma function $_0$ (HERRMANN, 2014). Therefore

$$\frac{1}{R} = a \exp\left(\lim_{n\to\infty} \alpha \quad _0(n\alpha + 1) \right) = a \exp(\qquad) = 0$$

and the radius of convergence is $R =$, that is, the solution given by Eq. (4.6) converges on the entire plan.

4.5.1.2 Other models

One can notice that all the fractional power series present in the solutions for the other models studied in section 4.2 have the form

$$C_n = \frac{(C)^n}{(n\alpha + 1)},$$

where $C =$ a, $C =$ b, $C = (\ \ b\ 3)$, and $C = (\ \ b\ 4)$ for Eqs. (4.13), (4.17), (4.23), and (4.27) respectively.

Plugging C_n for each of these cases in Eq. (4.34) and following a procedure analogous to the one described in 4.5.1.1 (omitted here for the sake of brevity), one can find for all cases that

$$\frac{1}{R} = 0 \qquad R =$$

Therefore, the solutions given by Eqs. (4.13), (4.17), (4.23), and (4.27) also converge on the entire plan.

4.5.2 On the modi ed fractional models

In order to find solutions for the fractional Logistic, Gompertz, Bertalanffy, and Guiot-West models subsection 4.2.5 to subsection 4.2.8), an exploratory approach has been attempted by relying on change of variables as a mean to solve simpler equations before changing back to the original ones.

Although such approach is frequently employed in traditional (i.e. integer order) with almost no caveats, not all typical rules may be directly invoked and used in fractional calculus (HERRMANN, 2014). For instance, there are several definitions of fractional derivative, each possibly yielding different results when applied to the same function. In this thesis, Caputo's definition (CAPUTO, 1967; SALES TEODORO; TENREIRO MACHADO; CAPELAS DE OLIVEIRA, 2019) has been used due to its recognized suitability in dealing with initial conditions when describing natural phenomena.

By changing variables, the actual fractional equation to be solved was altered, as indicated in Table 2. Nevertheless, although the fractional solutions obtained are strictly for modified fractional versions of their respective classical models, they are still valid and present common features of such models (e.g. sigmoidal behavior). They can also recover the known traditional solution for the integer order ODE when $\alpha = 1$ as seen in Figure 12, which compares classical solutions for integer order ODEs with integer-order power series solutions as well as fractional solutions obtained for each model in the chapter.

As suggested by curve overlapping in each figure, all these equations are actually equivalent solutions when $\alpha = 1$. As these simulations were carried for illustrative purposes, parameters were set as $a, b = 0\ 0246$, $V_\infty = 4800$, and $V_0 = 225\ 535$ in all simulations. For every solution depicted here, equations are the same as obtained throughout the chapter, conveniently summarized in Table 5.

Table 5 – Summary of solutions compared in Figure 12.

Model	Classical Solution	Power series solution	Fractional solution ($\alpha = 1$)
Log.	$\frac{V_\infty}{1+(V_\infty\ V_0-1)e^{-at}}$	$\frac{V_\infty}{\frac{V_\infty}{V_0}+\left(\frac{V_\infty}{V_0}-1\right)\sum_{n=1}^{\infty}\frac{(-a)^n t^n}{n!}}$	$\frac{V_\infty}{1+(V_\infty\ V_0-1)E_\alpha(-at^\alpha)}$
Gom.	$V_0 \exp\left[\ln\left(\frac{V_\infty}{V_0}\right)\left(1 \quad e^{-bt}\right)\right]$	$V_0 \exp\left[\ln\left(\frac{V_\infty}{V_0}\right)\left[1 \quad \sum_{n=0}^{\infty}\frac{(-b)^n t^n}{n!}\right]\right]$	$V_0 \exp\left[\ln\left(\frac{V_\infty}{V_0}\right)[1 \quad E_\alpha(\ -bt^\alpha)]\right]$
Ber.	$\left[V_\infty^{1\ 3}+\left(V_0^{1\ 3} \quad V_\infty^{1\ 3}\right)e^{-\frac{b}{3}t}\right]^3$	$\left[V_0^{1\ 3}+\left(V_0^{1\ 3} \quad V_\infty^{1\ 3}\right)\sum_{n=1}^{\infty}\left[\left(\ \frac{b}{3}\right)^n\frac{t^n}{n!}\right]\right]^3$	$\left[V_\infty^{1\ 3}+\left(V_0^{1\ 3} \quad V_\infty^{1\ 3}\right)E_\alpha\left(\ \frac{b}{3}t^\alpha\right)\right]^3$
G-W.	$\left[V_\infty^{1\ 4}+\left(V_0^{1\ 4} \quad V_\infty^{1\ 4}\right)e^{-\frac{b}{4}t}\right]^4$	$\left[V_0^{1\ 4}+\left(V_0^{1\ 4} \quad V_\infty^{1\ 4}\right)\sum_{n=1}^{\infty}\left[\left(\ \frac{b}{4}\right)^n\frac{t^n}{n!}\right]\right]^4$	$\left[V_\infty^{1\ 4}+\left(V_0^{1\ 4} \quad V_\infty^{1\ 4}\right)E_\alpha\left(\ \frac{b}{4}t^\alpha\right)\right]^4$

Source: Valentim et al. (2020).

Figure 12 – Comparison between classical, power series, and fractional solutions of ODE models with $\alpha = 1$.

(a) Logistic model

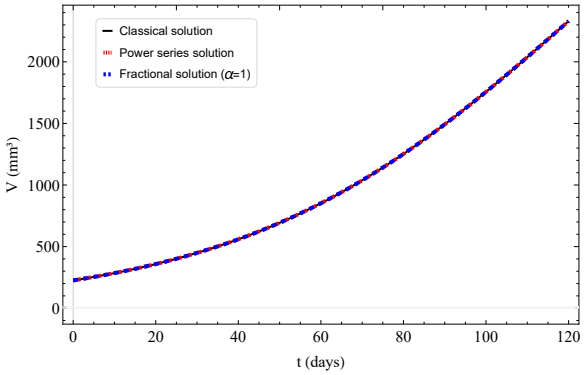

(b) Gompertz model

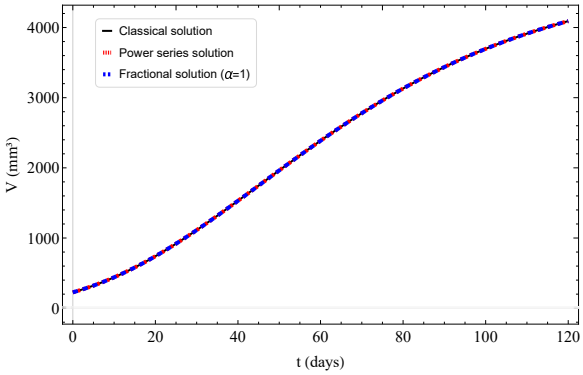

(c) Bertalan y model

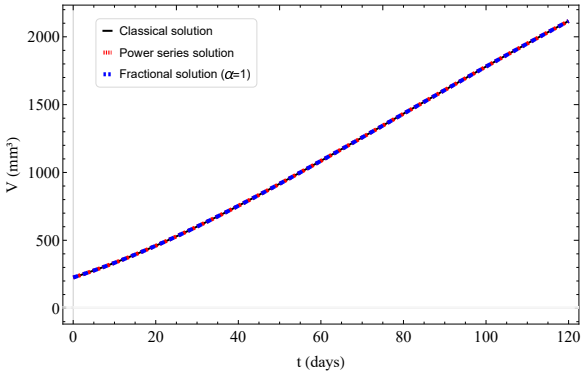

(d) Guiot-West model

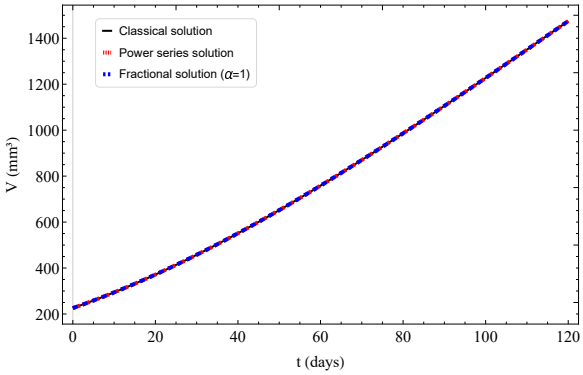

Source: Valentim et al. (2020).

5 ON MULTISTEP TUMOR GROWTH MODELS OF VARIABLE FRACTIONAL ORDER

This chapter reproduces and adapts the paper entitled "On multistep tumor growth models of fractional variable-order", which is part of the study conducted over the doctorate and was published in the journal Biosystems (Elsevier) (VALENTIM et al., 2021).

In the chapter, we propose a multistep exponential model with a variable fractional order representing the evolution history of a tumor. Model parameters are tuned according to variable fractional order profiles while assessing their capability of fitting a clinical time series. The results point to the superiority of the proposed model in describing the experimental data, thus providing new perspectives for modeling tumor growth.

Accordingly, section 5.1 introduces the subject while section 5.2 presents the model and variable-order considered in this study, while discussing their physical meaning. Additionally, the differences between variable growth rate and variable fractional order are also explored along with the numerical methodology. Section 5.3 analyzes the obtained solutions and the numerical results. Moreover, the section also explores the best-fitted variable-order model parameters against a clinical time series. Finally, section 5.4 draws the main conclusions.

5.1 Introduction

Strategies based on ecological models are often considered in order to understand phenomenological principles underlying general avascular tumor growth and are commonly expressed in terms of ordinary differential equations (ODE) (SARAPATA; DE PILLIS, 2014). These descriptions usually address simple characteristics, making ODE models flexible since they allow a parameter fine-tuning and can be analytically solved (BENZEKRY et al., 2014; HARTUNG et al., 2014; MARU' I et al., 1994), which favors their use for supporting clinical advice.

Nevertheless, while traditional ODE models provide an approximate idea of how tumors grow, experience shows that they are often unable to consider the full complexity of the dynamical evolution (MURPHY; JAAFARI; DOBROVOLNY, 2016). Some researchers also point that such laws should only be used to describe general tumor behavior, being unsuitable to characterize specific cases (WODARZ; KOMAROVA, 2014). One typical reason for this problem is the irregular growth patterns of these organisms. In fact, it is known that tumors go through many changes whilst advancing towards malignancy, accumulating different physical characteristics and admitting severe genetic (LOWENGRUB et al., 2010) and biomechanical modifications (FRITSCH et al., 2010; RAMIÃO et al., 2016).

A possible improved approach that avails these characteristics comes from multistep patterned growth models, resorting to multistage carcinogenesis concepts (WODARZ;

KOMAROVA, 2014). According to this notion, natural random mutations and epigenetic spontaneous changes in cancer cells should be considered when modeling tumor development (BOVERI, 2014), since they interfere with growth behavior. Indeed, some authors proposed models that incorporate and exhibit multifactorial or multistep growth patterns (RODRIGUEZ-BRENES; KOMAROVA; WODARZ, 2013; TRACQUI, 2009; SPENCER et al., 2004) (e.g., stepwise tumor growth to describe alternated dormancy periods).

Recent advances suggest that ODE models for tumor growth can be improved by adopting the tools of fractional calculus, a branch of mathematical analysis addressing non-integer order differentiation. Fractional calculus expands standard ODE to deal with complex behavior. This pivotal characteristic allows fractional models to describe phenomena such as long-term memory, non-locality and spatial heterogeneity (WEST, 2014), encouraging their application in several different areas. In fact, fractional mathematical oncology increasingly figures as a potential successful alternative approach for cancer-related topics such as treatment optimization (UCAR; ÖZDEMIR; ALTUN, 2019; YILDIZ; ARSHAD; BALEANU, 2018; FARAYOLA et al., 2020; KHAJANCHI; NIETO, 2019) and control in invasion systems (MANIMARAN et al., 2019; DAI; LIU, 2019; SOWNDARRAJAN et al., 2019).

5.2 Methodology

By generalizing both integration and differentiation to a variable-order (SAMKO; ROSS, 1993; ALMEIDA; TAVARES; TORRES, 2018), fractional models may rely on a governing fractional ODE where order α is time-dependent. To assess whether this feature can be explored in mathematical oncology, a variable-order fractional exponential model is here proposed with $\alpha(t)$ contributing to the description of a multistep tumor growth model. The variable-order acts as an index of memory (DU; WANG; HU, 2013), either considering or disregarding characteristics aggregated during tumor evolution. To the best of our knowledge, this concept was not yet employed to tumor growth and, therefore, it can be explored to describe tumor dynamics in relation to clinical data, thus potentially advancing decision-making schemes in oncology.

5.2.1 Variable order as an index of tumor memory

Figure 13 schematically illustrates a tumor evolution, accumulating genetic and biomechanical alterations towards malignancy. As a living organism, its composition and overall behavior change dramatically during its successive stages (PORTA; ZAPPERI, 2017). In material science, viscoelasticity memory has been successfully characterized by fractional derivatives, which also extended to biological modeling of tissues (MAGIN, 2010). More recently, the concept of memory index has been considered (DU; WANG; HU, 2013) in terms of memory phenomena possibly involving a short and a long stage. The

latter would be governed by a fractional derivative with order α indicating the level of memory retention: the higher the index, the slower the memory loss.

Figure 13 – Path to malignancy and tumor heterogeneity stages.

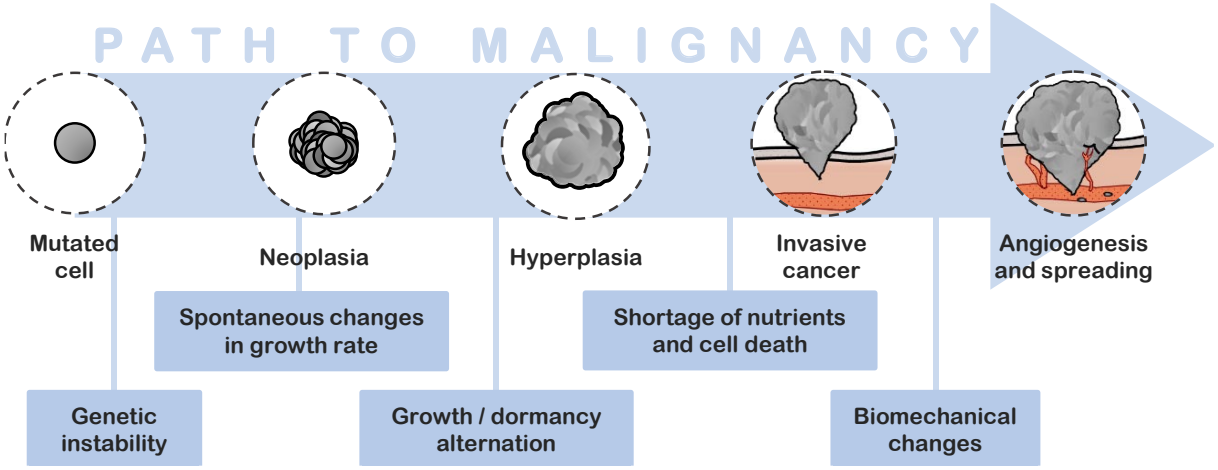

Source: Valentim et al. (2021).

Fractional derivatives capture possible scale deformations, diffusive phenomena, or they even take into account probabilistic effects (MACHADO, 2003; PODLUBNY, 2001). These concepts were also extended to the idea of memory and non-locality that occur in fractional models (HERRMANN, 2014; DU; WANG; HU, 2013). The dismissal of such aspect could be one major fact undermining the performance of current ODE models. Nonetheless, fractional models can still be incomplete inasmuch as a static (i.e. permanent) arbitrary order can potentially make them overlook tumor heterogeneity in time during its multiple stages. Accordingly, models are hereafter envisaged with a fractional variable-order potentially capturing specific time-dependent tumor features and stages.

5.2.2 The variable-order exponential model

Among extant tumor growth ODE models, the exponential model is probably the simplest one (WODARZ; KOMAROVA, 2014). In this model, if $V(t)$ is tumor volume at time t, then its growth rate is assumed as $D_t^1 V(t) = \lambda V(t)$, where D_t^1 is the classic first-order time-derivative and $\lambda > 0$ is a proportionality parameter. For a fractional derivative operator D_t^α, one can generalize this model as

$$\mathcal{M}_1 : D_t^\alpha V(t) = \lambda V(t) \tag{5.1}$$

for $0 < \alpha \leq 1$ and $t > 0$. $\mathcal{M}_1$ is a fractional model with a well-defined analytical solution (HERRMANN, 2014; GORENFLO et al., 2014) given by

$$V(t) = V_0 E_\alpha(\lambda t^\alpha), \tag{5.2}$$

where V_0 is initial volume and E_α is Mittag-Leffler function presented in Eq. (3.4). In order to deal with a multistep tumor growth model, the arbitrary order α may allegedly

equally vary with time such as

$$\mathcal{M}_2 : D_t^{\alpha(t)} V(t) = \lambda V(t), \tag{5.3}$$

where $\alpha(t)$ is a time profile.

Due to its suitability in tackling initial-value problems with respect to natural phenomena, Caputo definition of fractional derivative is selected. Particularly, the operator is defined by a type III variable-order left-hand Caputo derivative (ALMEIDA; TAVARES; TORRES, 2018)

$$D_t^{\alpha(t)} V(t) = {}_0^C D_t^{\alpha(t)} V(t) = \frac{1}{(1 \quad \alpha(t))} \int_0^t (t \qquad)^{-\alpha(t)} \frac{d}{d} V(\ \ ) d \ , \tag{5.4}$$

where is an auxiliary variable and is the gamma function. The fractional differentiation of power functions

$$D_t^{\alpha(t)} t \ \ = \frac{(\ \ + 1)}{(\qquad \alpha(t) + 1)} t^{\ -\alpha(t)} \tag{5.5}$$

can be applied when α is constant and also holds when $\alpha(t)$ is a time-dependent variable (VALÉRIO; COSTA, 2011). Hence, this section aims at applying constant-order fractional methods to solve Eq. (5.3), such as the power series method used in subsection 4.2.4.

Accordingly, if $\alpha(t)$ is assumed to vary slowly with respect to the sampling period while time is sub-divided in separate windows, then the solutions for $D_t^{\alpha} V(t) = \lambda V(t)$ hold approximately and a variable-order model can be written as

$$V(t) = V_0 E_{\alpha(t)}(\lambda t^{\alpha(t)}), \tag{5.6}$$

with $0 < \alpha(t) \leq 1$, $0 < t \leq T$, and the variable-order Mittag-Leffler function is given by

$$E_{\alpha(t)}(\lambda t^{\alpha(t)}) = \sum_{n=0}^{\infty} \lambda^n \frac{t^{n\alpha(t)}}{(n\alpha(t) + 1)}, \tag{5.7}$$

where $E_{\alpha(t)} = E_{\alpha(t)\,1}$ from the definition by Ortigueira, Valério and Machado (2019). Despite all simulations for $\mathcal{M}_2$ have been carried using Eq. (5.6), hereafter referred to as approximate analytical solution, a comparison with a numerical solution has been explored in appendix 5.5.1 for validation purposes.

For this model, $\alpha(t)$ allegedly describes some of specific time-dependent tumor features, even though such mathematical description is a priori unknown. Therefore, as an exploratory approach, $\alpha(t)$ is tentatively approximated by profiles with polynomials based on a Taylor series, namely $\alpha(t) = \alpha_0$ (equivalent to a fractional constant-order model), $\alpha(t) = \alpha_0 + \alpha_1 t$, $\alpha(t) = \alpha_0 + \alpha_1 t + \alpha_2 t^2$ and $\alpha(t) = \alpha_0 + \alpha_1 t + \alpha_2 t^2 + \alpha_3 t^3$ (i.e., zeroth, first, second and third order polynomials). Parameters α_0, α_1, α_2 and α_3 are obtained by means of a numerical routine (described in subsection 5.2.4) fitting aforementioned profiles to experimental data. After analyzing the behavior of the fitted polynomials while gaining insight into which mathematical functions better describe $\alpha(t)$, a new profile is proposed. The best-fitted $\alpha(t)$ profiles are analyzed in section 5.3 in terms of describing tumor growth behavior.

5.2.3 Fractional order pro les and variable growth rate

When coming across the present work, one may naturally inquire: why adopting a variable-order approach? Why employing fractional calculus, a more sophisticated tool, if one could simply use a variable growth rate $\lambda(t)$ in an exponential model to describe tumor evolution?

The concept of fractional order profile is used here under a perspective different from a simple growth rate parameter. It is true that, pragmatically, the value of α will ultimately dictate the growth rate, but the biophysical meaning of α is actually much deeper. While a parameter $\lambda(t)$ would only set a proportionality between tumor growth rate and its volume $V(t)$ at a given time t, the variable-order $\alpha(t)$ takes not only into account the tumor evolution but also to what extent it should be considered during the distinct growth stages. These ideas will be further explored in the analysis of the fitting results, in section 5.3.

It is also important to highlight that parameters $\lambda(t)$ and $\alpha(t)$ are mathematically distinct, i.e., they play very different roles in the governing ODE. As a result, a traditional (integer order) exponential model with distinct growth rates performs differently from the one adopting a fractional exponential model with distinct order values.

As an illustration of this distinct behavior, Fig. 14, compares the exponential model $\mathcal{M}_1$ of Eq. (5.2) with 10% perturbations in the parameters λ and α. In Fig. 14(a), a classical exponential model (i.e., with $\alpha = 1$) is simulated with λ changing about a reference λ_m. The relative differences between altered and unaltered parameters are calculated as

$$\text{Relative difference}(\%) = \frac{V_0 E_\alpha(\lambda_m t^\alpha) \quad V_0 E_\alpha(\lambda t^\alpha)}{V_0 E_\alpha(\lambda_m t^\alpha)} \quad 100\%$$

and rise up to 35% due to just a 10% increase in λ_m (i.e., $\lambda = 1\ 1\lambda_m$).

In Fig. 14(b), the same type of test is applied for the fractional order α_m while maintaining λ unaltered. The relative difference between the curves, herein calculated as

$$\text{Relative difference}(\%) = \frac{V_0 E_{\alpha_m}(\lambda t^\alpha) \quad V_0 E_\alpha(\lambda t^\alpha)}{V_0 E_{\alpha_m}(\lambda t^\alpha)} \quad 100\%$$

can be considerable (surpassing 150% between α_m and $1\ 1\alpha_m$), implying that variations in each parameter have different influence on the tumor growth curves. These comparisons indicate that a variable order model can achieve very different results (which is potentially interesting) from those exhibited by exponential models using a variable growth rate.

5.2.4 Numerical methods and clinical data

The clinical data used to best-fit the variable order models in subsection 5.2.2 are the same described in subsection 4.2.9. The algorithm routine used to fit the variable order model is schematized in Figure 15. The numerical method is practically equal to the one used before, with only a few modifications concerning the different parameters to be fitted.

Figure 14 – Comparing tumor growth described with $\mathcal{M}_1$ and Eq. (5.2) with 10% variation in the values λ (left) and α (right).

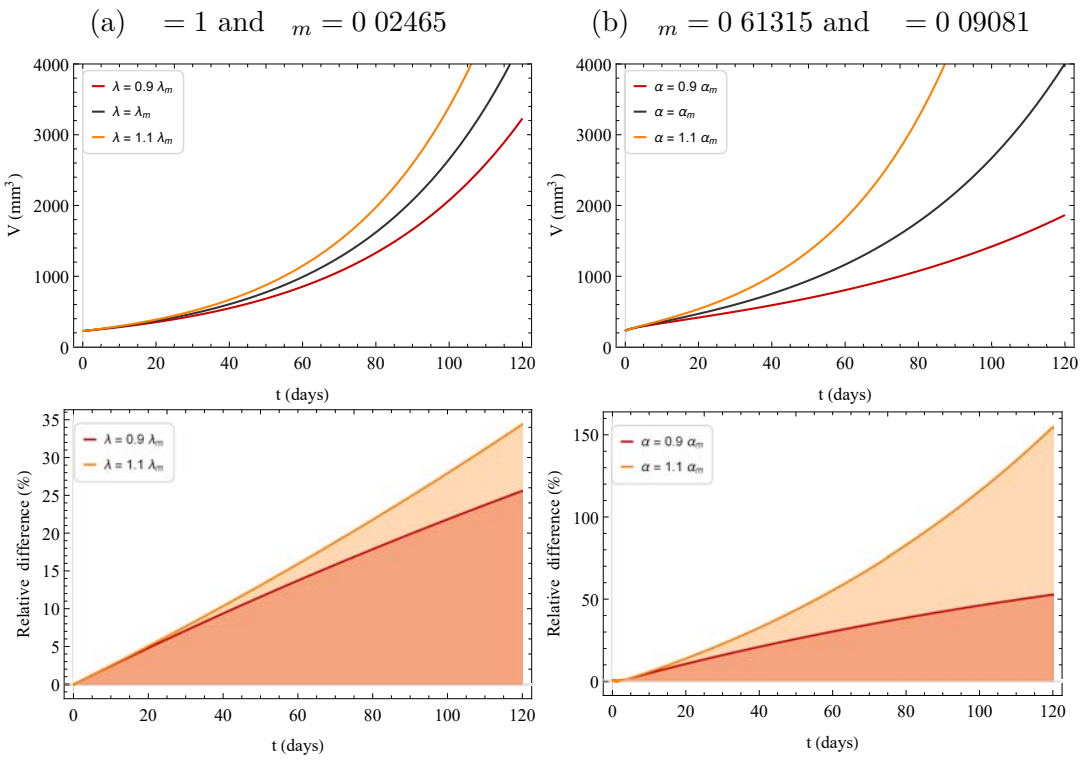

Source: Valentim et al. (2021).

Constraints were chosen to guarantee numerical stability and closeness to characteristics being simulated. Accordingly, growth rate λ was forced to be positive and variable-order $\alpha(t)$ ranged between 0 and 1 regardless of the profile being used. As adjustable parameters distinctly influence $\alpha(t)$, aforesaid conditions impact differently on these model parameters, which must thus be specifically constrained to each profile.

The same evaluation indexes described in subsection 4.2.9 were applied, with the exception of SMAPE. The fitting evaluation herein conducted employed the 14 extant points from the experimental time series in Table 3 to find the parameters yielding the minimum SSR possible. The best-fitted variable-order models for each profile, which can be used to analyze tumor behavior, are presented in section 5.3. A visual description of the optimization in the algorithm employed in this section is included in appendix 5.5.2.

5.3 Results and discussion

This section explores the results from applying the algorithm described in subsection 5.2.4 to the extant $n = 14$ points of clinical data listed in Table 3. Firstly (before dealing with variable-order model $\mathcal{M}_2$), integer and fractional constant-order exponential models $\mathcal{M}_1$ were best-fitted using Eq. (5.2). Evaluation indicators for optimal configurations are shown in Table 6 and they can be used as benchmark performances that

Figure 15 – Algorithm to obtain the best-fitted model parameters.

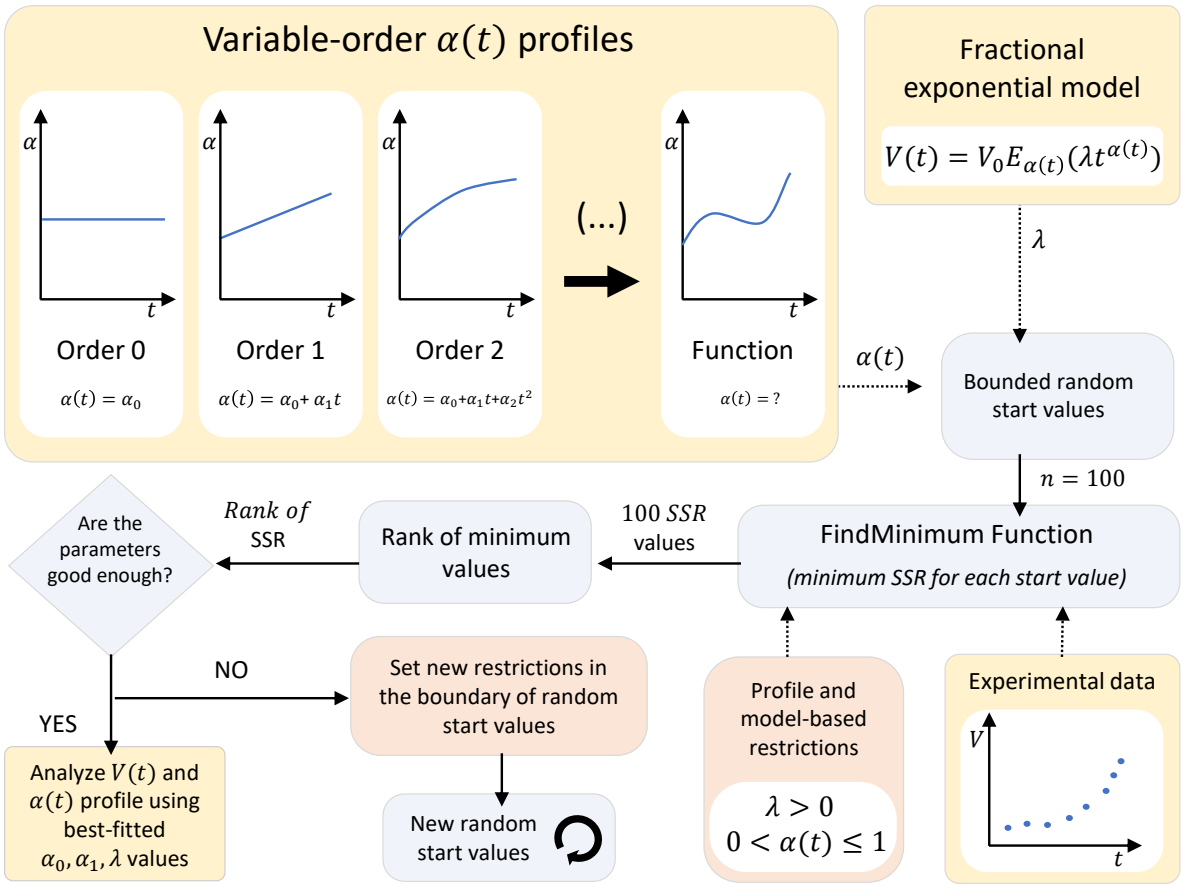

Source: Valentim et al. (2021).

variable-order models should excel to be useful.

Table 6 – Results and evaluation indicators concerning classical and fractional exponential models, given by Eq. (5.2), best-fitted against clinical data.

	Best-fitted parameters		Evaluation indicators		
Model	α	λ	SSR	RMSD	R^2
Classical	1	0 024648	4 391 10^5	177 1	0 9703
Fractional	0 61315	0 090810	2 029 10^5	120 4	0 9863

Source: Valentim et al. (2021).

Best-fitted profiles for variable-order exponential model $\mathcal{M}_2$ given by Eq. (5.6) are listed in Table 7. Being a fractional constant-order parameter, the zeroth order $\alpha(t)$ naturally yields the same results as those from the fractional model reported in Table 6. Referring to growth rate, in those fittings parameter λ is kept at $\lambda = 0\ 090810$, which is the value obtained when fitting the fractional constant-order model $\mathcal{M}_1$ (as shown in Table 6). Variable-order models perform better than either integer or constant fractional order formulations with SSR error decreasing inversely with the order of polynomial profile $\alpha(t)$.

Such trend indicates that $\alpha(t)$ may be successfully described by a high-order polynomial or eventually by a specific function (e.g. trigonometric).

Table 7 – Results and quality indicators concerning the variable-order exponential models given by Eq. (5.6) best-fitted against all points from available clinical data.

	Best-fitted parameters ($\lambda = 0\ 090810$)							Evaluation indicators			
$\alpha(t)$ profile	α_0	α_1		α_2		α_3		SSR		RMSD	R^2
Zeroth order	0 61315	-		-		-		2 029	10^5	120 4	0 9863
First order	0 61832	5 0525	10^{-5}	-		-		2 001	10^5	119 5	0 9865
Second order	0 50484	2 4386	10^{-3}	1 3280	10^{-5}	-		1 365	10^5	98 76	0 9908
Third order	0 63924	2 6285	10^{-3}	4 7636	10^{-5}	2 3570	10^{-7}	1 257	10^5	94 76	0 9915

Source: Valentim et al. (2021).

As an illustration of how SSR index behaves for the variable-order model $\mathcal{M}_2$, Figure 16 presents the error curves around the best-fit model parameters with $\alpha(t)$ approximated by a third order polynomial. In those figures, the red dot indicates the lowest SSR and, accordingly, the best-fitted parameters for each profile. In these plots, only two calibrating parameters are varied at each time while remaining parameters are kept constant for visualization purposes.

Behavior of $\alpha(t)$ on best-fitted variable-order is better captured when the corresponding models $\mathcal{M}_2$ are plotted against the fitted clinical data, as shown in Figure 17. Table 7 shows that SSR indicator is considerably smaller when $\alpha(t)$ is approximated by second and third order polynomials. In fact, as the order of the polynomial approximating $\alpha(t)$ increases, its behavior suggests that it may be satisfactorily modeled by some type of periodic function (i.e. profile). While higher order polynomials might still be adopted (probably yielding sequentially better results as the polynomial order increases), fitting of these long expressions requires much more computational effort. Instead, a periodic profile is proposed as $\alpha(t) = \alpha_0 + \alpha_1 \sin(\alpha_2 t + \alpha_3)$, which may potentially capture the variable-order capable of better describing the tumor growth given by the fitted clinical data.

Two different propositions were envisioned for the periodic profile, whose fitting results are presented in Table 8. The first one considers only α_0, α_1, α_2 and α_3 as adjustable parameters, maintaining $\lambda = 0\ 090809$ constant, as in profiles approximated by polynomials. The second proposition considers λ as an additional adjustable parameter. Both periodic time profiles $\alpha(t)$ outperform the previous ones, achieving less than half of SSR error. Figure 18 presents the best-fitted periodic variable-order models $\mathcal{M}_2$ against tumor clinical data. Figure 19 shows SSR error curves for optimal parameters.

If $\alpha(t)$ is interpreted as memory index, then it may partially translate the so-called hallmarks of cancer (HANAHAN; WEINBERG, 2011) (which are capabilities acquired in most types of human tumor cells, heavily impacting cancer formation) into mechanistic characteristics a mathematical model can grasp. In other words, variation of $\alpha(t)$ may be

Figure 16 – SSR log-scaled plots: lowest error regions around the best-fitted parameters (indicated by the red dot) for variable-order $\alpha(t)$ approximated by a third order polynomial.

(a) Variation of $_0$ and $_1$ while , $_2$, and $_3$ are kept constant.

(b) Variation of $_1$ and $_2$ while , $_0$, and $_2$ are kept constant.

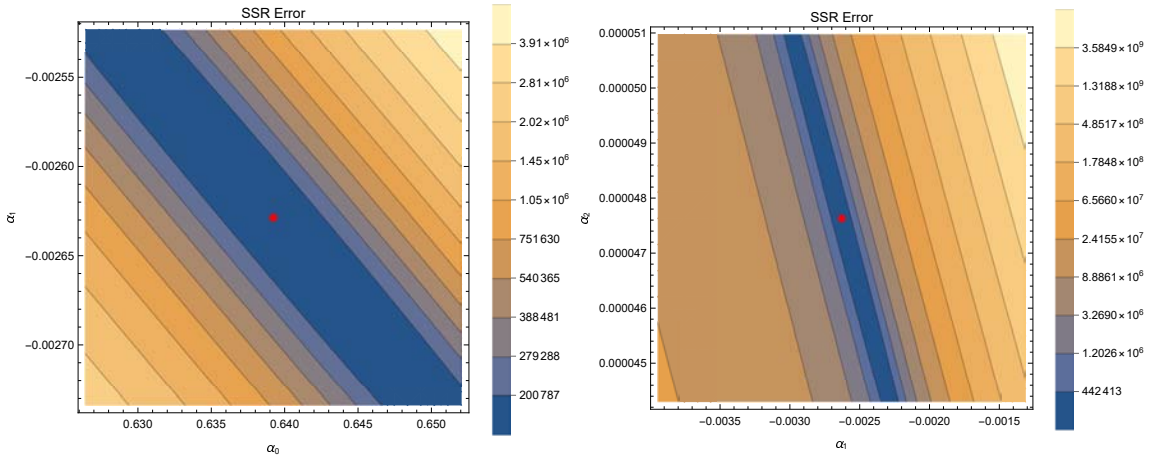

(c) Variation of $_2$ and $_3$ while , $_0$, and $_1$ are kept constant.

(d) Variation of $_3$ and $_0$ while , $_1$, and $_2$ are kept constant.

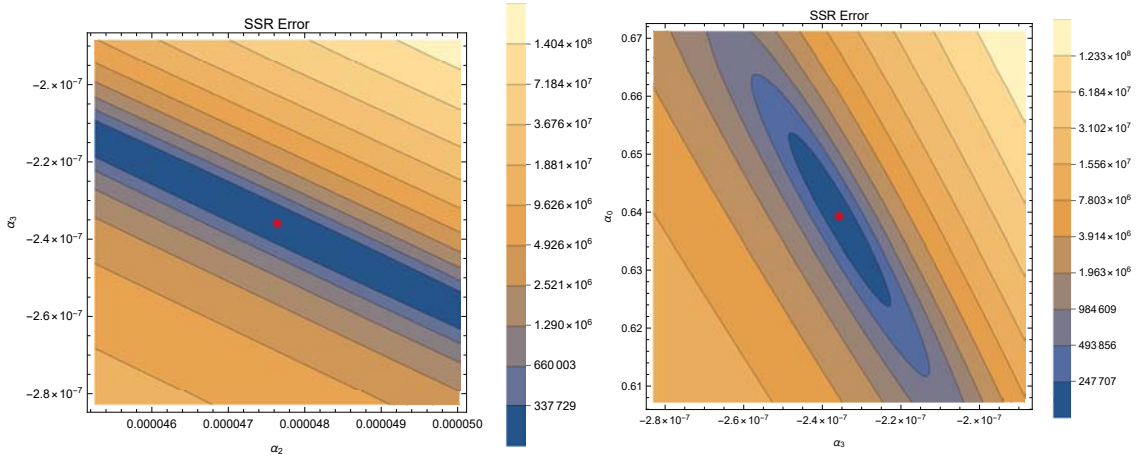

Source: Valentim et al. (2021).

related to activation or even development of specific hallmarks during tumor evolution. When α 1 tumors have full memory and follow an exponential increase programmed in their original cells (activating hallmarks related to the evasion of growth suppressors and sustainability of proliferative signaling). On the other hand, when α is lower, tumors evolve at a slower growth rate, potentially due to challenges from the micro-environment (e.g. shortage of nutrients, extracellular matrix resistance). In this case, they forget (or inactivate) part of their original programming, developing traits suitable to their current evolution stage (hallmarks related to angiogenesis and invasion).

Figure 17 – Tumor growth: comparison between clinical data (dots) and best-fitted variable-order models (solid line) given by Eq. (5.6) with $\alpha(t)$ approximated by polynomials.

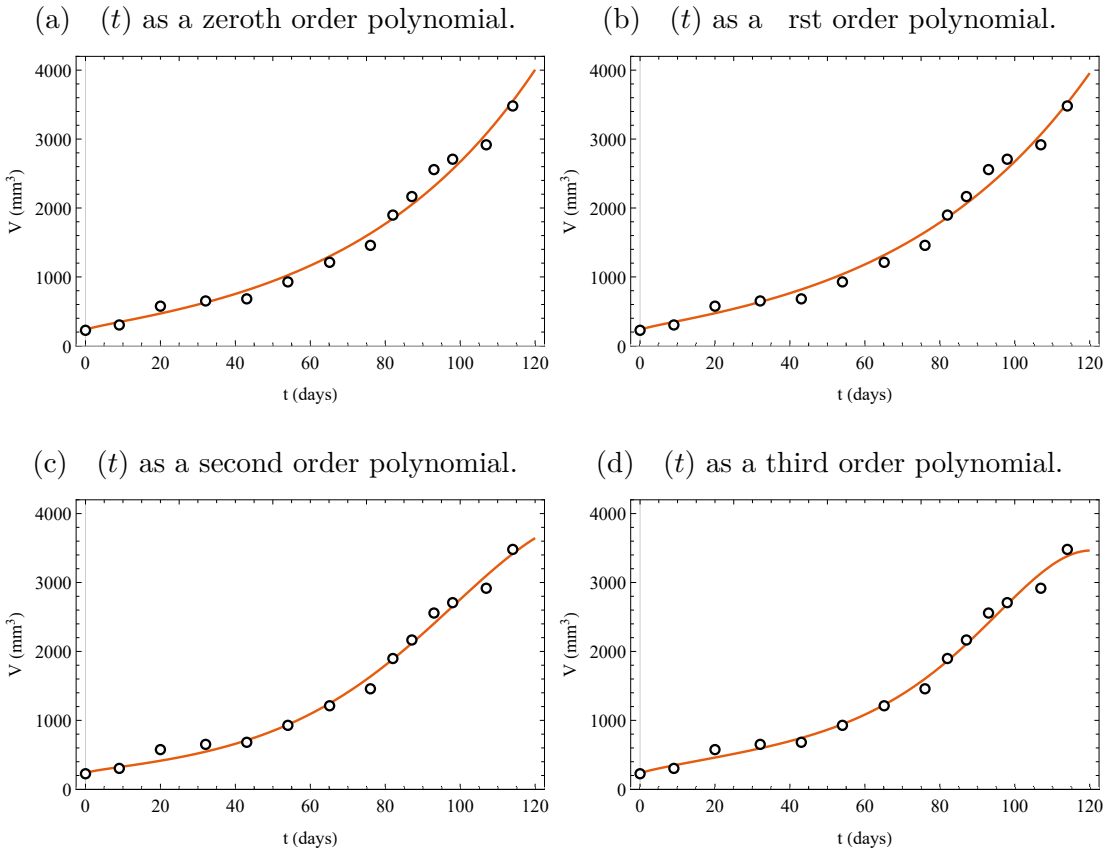

Source: Valentim et al. (2021).

Figure 18 – Tumor growth: comparison between clinical data (dots) and the best-fitted variable-order model (solid line) given by Eq. (5.6) with $\alpha(t)$ approximated by the periodic profile $\alpha(t) = \alpha_0 + \alpha_1 \sin(\alpha_2 t + \alpha_3)$.

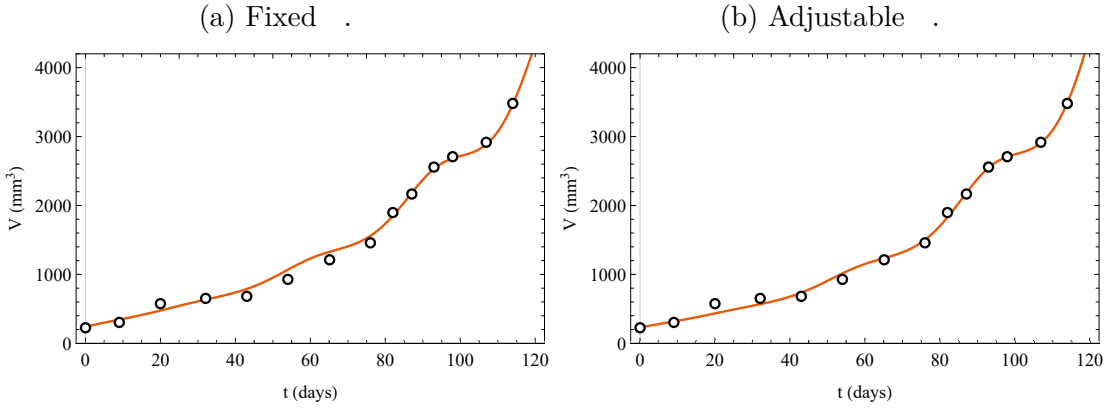

Source: Valentim et al. (2021).

The variable-order $\alpha(t)$ is better approximated by a periodic profile. In this case, when fitted clinical time series begins, one might argue that tumors no longer have a sharp

Table 8 – Results and quality indicators concerning the variable-order exponential models given by Eq. (5.6) with periodic profiles best-fitted against available clinical data.

	Best-fitted parameters						Evaluation indicators			
$\alpha(t)$ profile	λ	α_0	α_1		α_2	α_3	SSR		RMSD	R^2
Periodic (fixed λ)	0 090808	0 61476	7 0478	10^{-3}	0 18681	3 3215	7 169	10^4	71 56	0 9951
Periodic (adjusted λ)	0 057568	0 74934	9 5074	10^{-3}	0 17506	1 3265	4 567	10^4	57 11	0 9969

Source: Valentim et al. (2021).

memory of perfect exponential growth but a partial index given by α_0. Therefore, such non-integer order does not provide a pure exponential growth, but a slower one. Furthermore, tumor memories are not immutable and their variation potentially characterizes dormancy periods and/or which programmed cancer hallmark prevails at a different evolution stage. This is modeled as an oscillatory behavior for $\alpha(t)$ that alternates between faster and slower growth rates.

Future investigation might relate variable-order profiles to the type of tumor being modeled. In view of their particular properties, different cancers are prone to be modeled by distinct profiles. As results in this work suggest, periodic profiles (of variable non-integer order) seem to better model breast cancer while linear, parabolic, and other functions may be suitable to other tumors. This issue might be prospectively explored by relying on different clinical data sets.

5.4 Conclusions

This chapter proposed variable-order $\alpha(t)$ profiles in the model description of multistep tumor dynamics. Time-dependent $\alpha(t)$ may be interpreted as a variable memory index, exercising a different behavior compared to traditional growth parameters in exponential models.

The variable-order $\alpha(t)$ profiles herein investigated performed very well when describing multi-step tumor growth (i.e. best-fitted scenarios). When employing a variable-order approximated by a periodic function, the model seamlessly followed almost all clinical data points, offering interesting interpretations relating memory index and multistage characteristics acquisition.

The literature seemingly lacks studies on modeling multistep tumor growth under a variable-order fractional approach. This study presents encouraging and opening results for further discussion. Power and flexibility of variable orders may favor the adoption of fractional ordinary differential equations for describing tumor growth, potentially contributing to decision making in clinical applications.

Further exploration of this work is thus required upon more available datasets. In future studies, the periodic variable-order herein examined should be compared with different clinical data. Possible relations between variable-order profiles and specific types of

Figure 19 – SSR log-scaled plots: lowest error regions around the best-fitted parameters (indicated by the red dot) for variable-order $\alpha(t)$ approximated by $\alpha(t) = \alpha_0 + \alpha_1 \sin(\alpha_2 t + \alpha_3)$ and an adjustable λ.

(a) Variation of $_0$ and $_1$ while , $_2$ and $_3$ are kept constant.

(b) Variation of $_1$ and $_2$ while , $_1$ and $_3$ are kept constant.

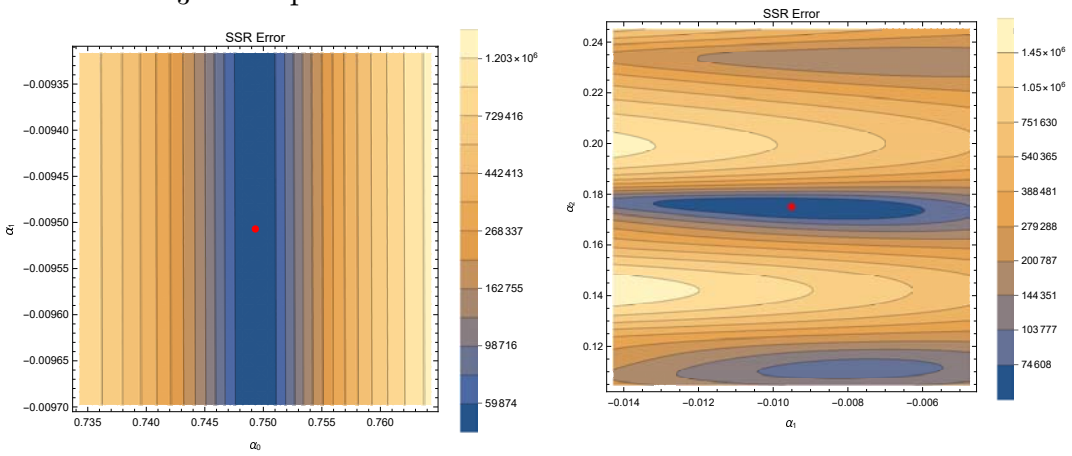

(c) Variation of $_2$ and while $_0$, $_1$ and $_3$ are kept constant.

(d) Variation of $_3$ and while $_0$, $_1$ and $_2$ are kept constant.

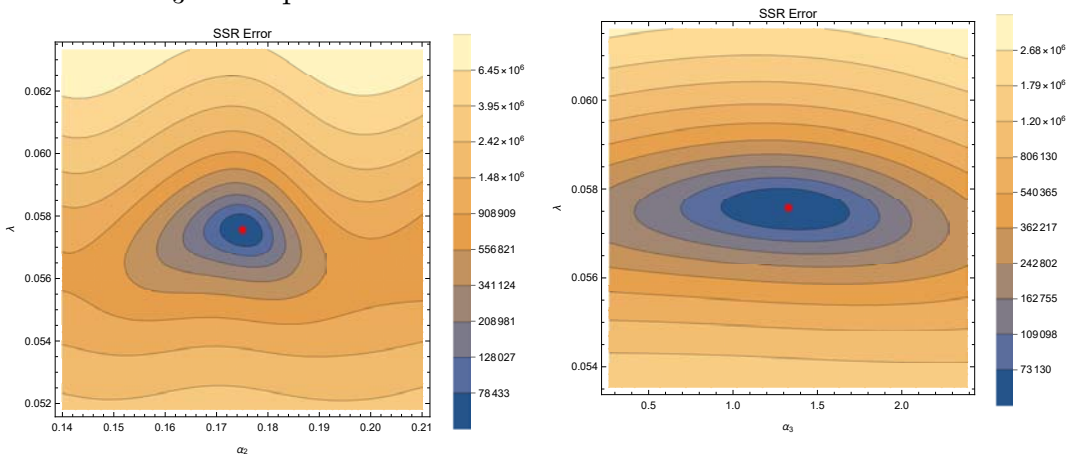

Source: Valentim et al. (2021).

cancer should be investigated. Other fractional ODE models (e.g., logistic and Gompertz) could also be analyzed under the optics of variable-order profiles. Furthermore, the possibility for new profiles is vast, including combinations of those herein studied and others.

5.5 APPENDIX: Variable-order models veri cation

5.5.1 Numerical comparison

The validity of the approximate analytical solution given by Eq. (5.6) was verified against a numerical solution for $0 < \alpha(t) \leq 1$ and $0 < t \leq T$, with $T = 120$ days. It should

be highlighted that such limit does not imply that solutions are necessarily invalid for $t > T$, but care must be exercised when using $\alpha(t)$ for an overly long t (e.g., linear and parabolic profiles can make Eq. (5.6) invalid if $\alpha_1 < 0$ or $\alpha_2 < 0$ and t is large enough to $\alpha(t)$ reach zero).

For the numerical solution, a modified version of the Adams-type predictor-corrector scheme proposed by Diethelm et al. (DIETHELM; FORD; FREED, 2002; DIETHELM et al., 2005) was implemented (so to accept variable orders) and the approximate analytical solutions given by Eq. (5.6) were compared for each best-fitted $\alpha(t)$ profile. The modified algorithm solved the fractional ODE given by Eq. (5.3) for N sub-divided time periods. Each period considered a constant α_{t_n} given by the profile $\alpha(t)$ for the instant t_n at the beginning of each time step. If we consider the fractional ODE as

$$D_t^{\alpha} V(t) = \lambda V(t) = f(t, V(t)), \tag{5.8}$$

for each sub-divided time period N with constant α_{t_n}, the predictor is defined as

$$V_h^P(t_{n+1}) = V_0 + \frac{1}{(\alpha_{t_n})} \sum_{j=0}^{n} \frac{h^{\alpha_{t_n}}}{\alpha_{t_n}} ((n+1 \quad j)^{\alpha_{t_n}} \quad (n \quad j)^{\alpha_{t_n}}) f(t_j, V_h(t_j)), \tag{5.9}$$

where $h = T \ N$ is the sampling time period, or time step, and the corrector is defined as

$$V_h(t_{n+1}) = V_0 + \frac{h^{\alpha_{t_n}}}{(\alpha_{t_n}+2)} f(t_{n+1}, V_h^P(t_{n+1})) + \frac{h^{\alpha_{t_n}}}{(\alpha_{t_n}+2)} \sum_{j=0}^{n} a_{j\,n+1} f(t_j, V_h(t_j)), \tag{5.10}$$

and

$$a_{j\,n+1} = n^{\alpha_{t_n}+1} \quad (n \quad \alpha_{t_n})(n+1)^{\alpha_{t_n}} + (n \quad j+2)^{\alpha_{t_n}+1} + (n \quad j)^{\alpha_{t_n}+1} \quad 2(n \quad j+1)^{\alpha_{t_n}+1}$$

In order to assess how the approximate analytical solutions progress in comparison to numerical counterparts, Eq. (5.6) was simulated with some of the best-fitted $\alpha(t)$ profiles adopted in the thesis along with corresponding numerical solutions using $N = 100$ time steps. The simulated profiles were polynomials of first ($\alpha(t) = \alpha_0 + \alpha_1 t$), second ($\alpha(t) = \alpha_0 + \alpha_1 t + \alpha_2 t^2$) and third order ($\alpha(t) = \alpha_0 + \alpha_1 t + \alpha_2 t^2 + \alpha_3 t^3$) and a periodic profile ($\alpha(t) = \alpha_0 + \alpha_1 sin(\alpha_2 t + \alpha_3)$).

The results indicated an agreement between approximate analytical and numerical solutions, as presented in Figure 20, where the left side shows tumor evolution and the right side presents the relative error between them, given in percentage form and calculated as

$$\text{Relative error}(\%) = \frac{\text{Analytical solution} \quad \text{Numeric solution}}{\text{Analytic solution}} \quad 100\%$$

Even with a small number of time steps, the maximum relative error obtained in all cases was only 0 4%. Such result not only corroborates the notion that the variable-order model given by Eq. (5.6) is valid for the studied profiles, but also suggests that it may be extended for other $\alpha(t)$ profiles.

5.5.2 SSR index trajectory for a given start value

In the numerical routine presented in subsection 5.2.4, one finds the best-fitted model parameters based on the minimal SSR values yielded. For each starting value, an iterative process tries to numerically approach the local minimum and identify corresponding free parameters.

As an illustration of this process Figure 21, represents the trajectory of minimal SSR indexes for some variable-order profiles. In these plots, the blue point represents the start value, the yellow points refer to iterative steps (i.e. intermediate values), and the red point is the lowest SSR error (i.e. it refers to best-fitted parameters). One must note that these trajectories are *sui generis*, presented here to illustrate part of the algorithm in Figure 15. For that reason, they were generated after the fitting process, with convenient start values.

Figure 20 – Comparison and relative error between approximate analytical (Eq. (5.6)) and numerical solutions for best-fitted variable-order $\alpha(t)$ approximated by first (a), second (b), third (c) order polynomials, and a periodic profile (d).

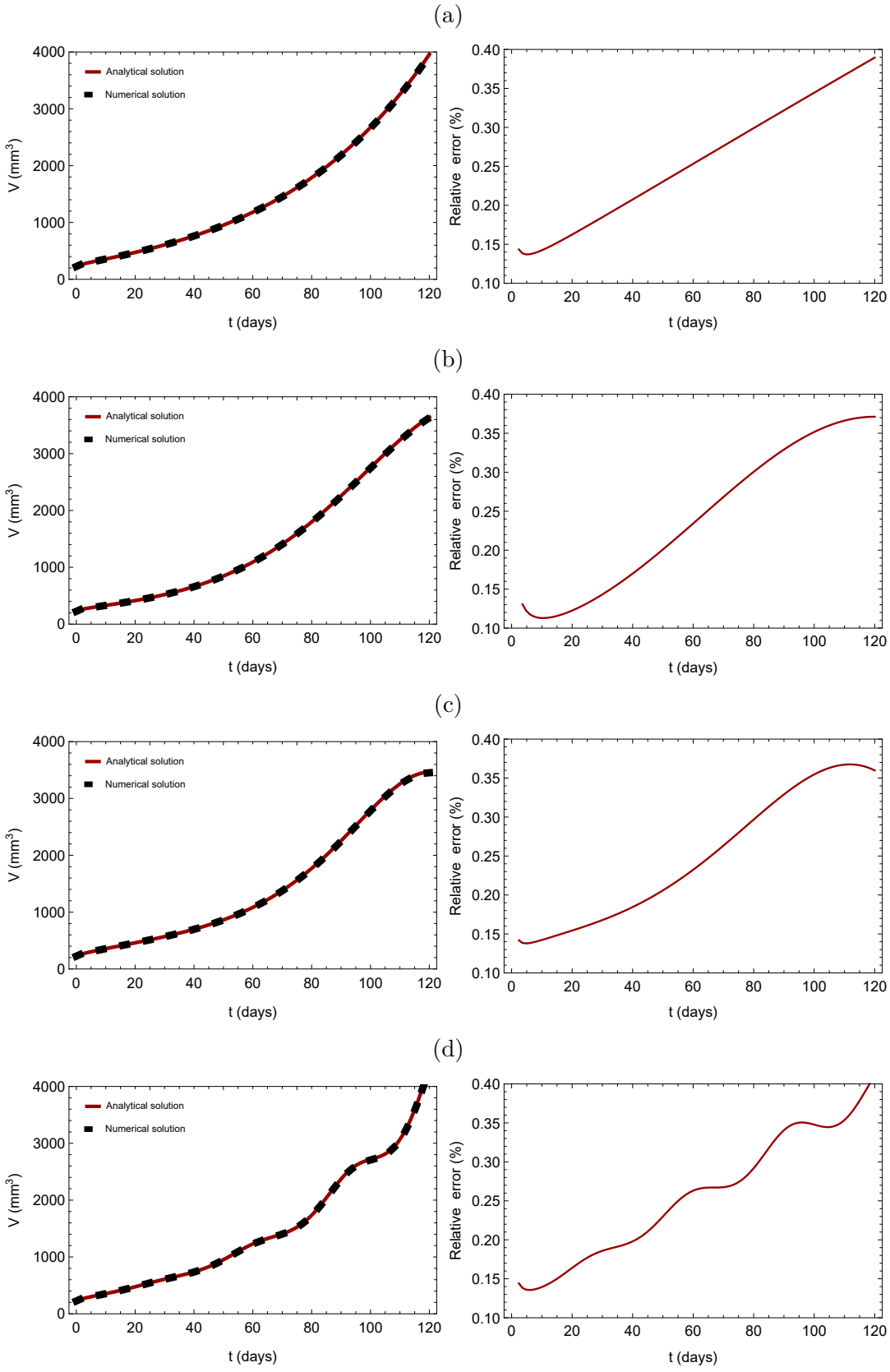

Source: Valentim et al. (2021).

Figure 21 – Illustration of the log-scaled SSR trajectory during the optimization routine.

(a) (t) as a zeroth order polynomial.

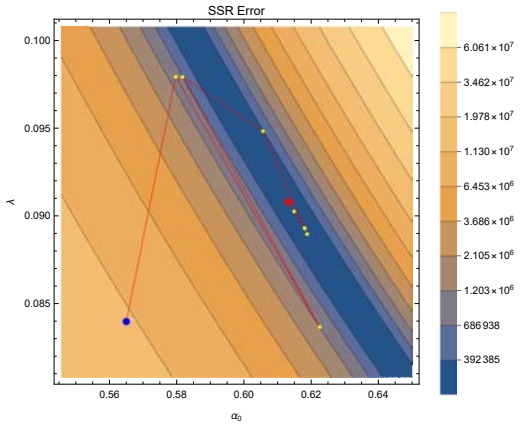

(b) (t) as a rst order polynomial.

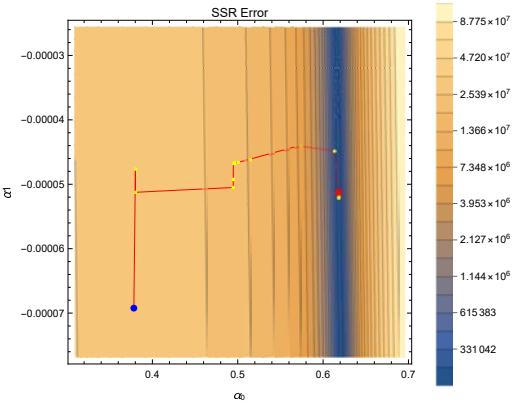

(c) (t) as a periodic pro le.

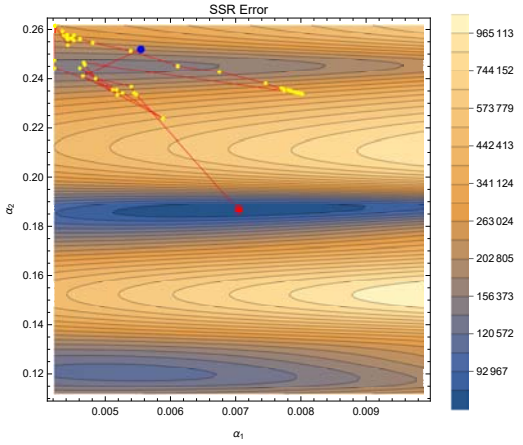

(d) (t) as a periodic pro le with an adjustable .

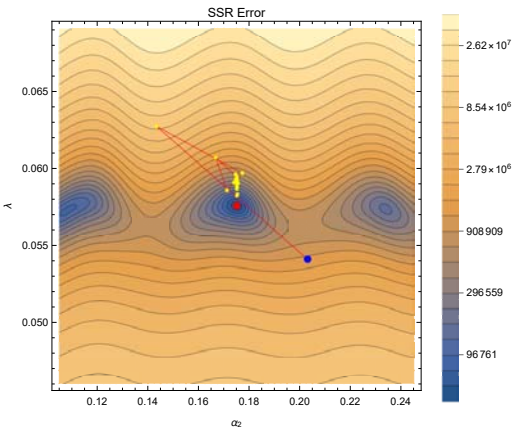

Source: Valentim et al. (2021).

6 CELLULAR-AUTOMATON MODEL FOR TUMOR GROWTH DYNAMICS: VIRTUALIZATION OF DIFFERENT SCENARIOS

This chapter reproduces and adapts the paper entitled "Cellular-automaton model for tumor growth dynamics: virtualization of different scenarios", which is part of the study conducted over the doctorate and was published in the journal Computers in Biology and Medicine (Elsevier) (VALENTIM; RABI; DAVID, 2023). Until this point in the thesis, investigation has only addressed dynamic (i.e. time dependent) population models, with no consideration of spatial variability.

In this context, cell-based models allow monitoring independent single parameters, which might vary in both time and space. By relying on extant tumor growth models in the literature, this chapter introduces cellular-automata simulation strategies that admit heterogeneous cell population while capturing both single-cell and cluster-cell behaviors. In this agent-based computational model, tumor cells are limited to follow four possible courses of action, namely: proliferation, migration, apoptosis or quiescence.

Despite the apparent simplicity of those actions, the model can represent different complex tumor features depending on parameter settings. This study virtualizes five different scenarios, showcasing model capabilities of representing tumor dynamics including alternate dormancy periods, cell death instability and cluster formation. Implementation techniques are also explored together with prospective model expansion towards deterministic features.

The proposed stochastic cellular automaton model is able to effectively simulate different scenarios regarding tumor growth effectively, figuring as an interesting tool for in silico modeling, with promising capabilities of expansion to support research in mathematical oncology, thus improving diagnosis tools and/or personalized treatment.

In this context, section 6.1 introduces the study while the chosen methodology is divided into three parts: section 6.2.1 presents the mathematical background and definitions, 6.2.2 describes biological constructs and model assumptions, and section 6.2.3 reports programming aspects and computational implementation. Next, the virtualization of several case scenarios is conducted and discussed in 6.3. In 6.4, we explore potential shortcomings of this cellular automaton and how it is being developed as a grounding framework for a later-to-be-implemented hybrid model. In 6.5 we state final remarks.

6.1 Introduction

In the last decades, mathematical concepts have been increasingly applied to oncological phenomena not only to better understand the progression of related diseases but also to develop new methods of diagnosis and treatment, contributing to the emergence of a new research area (ROCKNE; SCOTT, 2019; HAMIS; POWATHIL; CHAPLAIN, 2019;

BYRNE, 2010). Mathematical oncology comprehends the development and application of models to phenomena ranging from neoplastic growth to personalized treatment (JACKSON; KOMAROVA; SWANSON, 2014). As a strategic advantage, mathematical models can test and reproduce several scenarios either unfeasible or impossible through either in vivo or in vitro experiments, which turns it into an important analysis tool as clinical tests in lab animals or humans are time and resource consuming (KASHKOOLI et al., 2021).

Mathematical models in oncology may be categorized into two large groups: data-driven and physics-based models. Considering the prevailing scenario of elevated difficulty (in terms of resources and feasibility) in obtaining consistent data from oncologic patients, the later category, also called phenomenological or mechanistic approach, has advanced in modeling related phenomena. Examples including ordinary and partial differential equations (ODEs and PDEs, respectively) illustrate the success of those approaches, such as strategies based on ecological models and the underlying of general avascular tumor growth (SAVAGEAU, 1980; SACHS; HLATKY; HAHNFELDT, 2001; SARAPATA; DE PILLIS, 2014). With their relative simplicity, ODE-based approaches enable analytical solutions and have conveniences that motivate their use until today (WODARZ; KOMAROVA, 2014; BENZEKRY et al., 2014; HARTUNG et al., 2014). On the other hand, PDEs can model tumor growth into surrounding tissue (POLOVINKINA et al., 2021). Some models describe tumors as a fluid or mixture via transport equations (BYRNE; PREZIOSI, 2003), while others employ transport phenomena to model metastatic processes and beyond (HARTUNG et al., 2014; XU; VILANOVA; GOMEZ, 2016).

When a model requires specific cellular structure and probabilistic nature involving cell proliferation, equation-based approaches may not suffice. In that context, Anderson et al. (2007) claim that while continuum mathematical models have been successfully employed to describe several portions of matter, these portions in nature are actually particles and cells, thus discrete. In the wake of the impressive progress of biochemistry and biology concepts on genetics, sub-cellular levels and inner works, computational-enhanced mathematical oncology faces the difficult task of transforming specific portion-sized data into complex information describing emergent higher-level multi-scale cellular phenomena.

In recent years, many cell-based models have been proposed to face such challenge (DEUTSCH et al., 2021; WEERASINGHE et al., 2019). Cell-based or discrete models are organized frameworks that keep track of fully independent individual parameters varying spatially and temporally, reflecting the heterogeneity and complex emergence found in cancer phenomena. Computationally, they can rely on different approaches including Monte-Carlo simulations, energy minimization techniques, volume conservation laws, and motion rules (ANDERSON; CHAPLAIN; REJNIAK, 2007).

If these models follow a structural or grid organization, they are considered lattice-based models, which are categorized according to the number of cells that each lattice cell can hold (METZCAR et al., 2019). Lattice-gas cellular automata (LGCA) models admit

more than one cell per lattice (being suitable for larger systems). On the other hand, if the model admits that a single cell can occupy many spots, it is thus ideal for modeling sub-cellular systems (JAMALI; AZIMI; MOFRAD, 2010). Finally, if each cell can occupy a single lattice, it is a regular cellular automaton (CA) model (METZCAR et al., 2019).

Numerical simulations involving cell-based models are often referred to as in-silico modeling because of their similarity and logical extension of in vitro experimentation (JEANQUARTIER et al., 2016). Concerning regular cellular automaton models, relatively simple implementations can go a long way in providing emergent complex behavior. Enderling et al. (2009) established only a basic set of rules concerning proliferation and migration rates for each type of tumor cell (regular or stem) in a CA and investigated the virtualization of very different emergent scenarios when changing these rules, including cell clustering and tumor dormancy. Later, Poleszczuk and Enderling (2014) improved the model by implementing it with high-performance computational techniques. These two studies arise as the grounding basis of the automaton model herein developed.

6.2 Methodology

6.2.1 Mathematical aspects

Since a cellular automaton is composed of a multitude of equally identifiable cells and for every cell a certain set of neighbors is used to calculate a new state, the resulting network structure of neighborhood relations is a further important characteristic of cellular automata. In order to describe the method adopted in this study, we initially revisit the definition and some concepts related to cellular automata.

6.2.1.1 Basic concepts of cellular automata

In a simplified manner, a cellular automaton can be typically defined as a basic structure considering the quadruple (C, n, S, f) as follows (DEUTSCH; DORMANN, 2005):

- C is a set of cells, not required to be finite.
- $n : C \quad C \qquad 0, 1$ is a neighborhood function that can be seen as a relationship (usually reflexive and symmetric) between cells. This function shows which pairs of cells are neighbors, that is, the geometry of the cell organization. Furthermore, n must satisfy the neighborhood size independence condition $N(c_0) = c \quad C : n(c_0, c) = 1 = N$, which is constant for every $c_0 \quad C$, i.e., the size of the neighborhood is the same for all cells.
- S is a set of states. Each cell will have an associated state, in each moment.
- $f : S\ N \qquad S$ is a transition function. The transition function is a core of the CA dynamics and is commonly expressed through rules that define the state of the cell

in the subsequent time instant from the current state of the cell neighbors. The set of cells C with the neighborhood function n defines the structure of the cell space. The simplest CA model can have binary cells (e.g., two states: tumor or healthy) (HU; RUAN, 2003). More commonly, multiple states are represented by a set of integer values (0, 1, 2, ...), each having an appropriate physical or biological interpretation (see sections 6.2.2.1 and 6.2.2.2 for our model's neighborhood geometry and cell states).

6.2.1.2 Stochastic cellular automata

In some situations, such as when evolution operators are stochastically approximated, the resulting states have stochastic character. Random or stochastic states can be mathematically represented as random variables. Stochastic cellular automata can be defined in the following way, which settles them between Bayesian networks (FRIEDMAN et al., 2000) and multi-parameter stochastic processes (KHOSHNEVISAN, 2002):

- M is a finite set of cells.
- $\mathcal{N}$ is a neighbourhood mapping $\mathcal{N} : M \quad M^k$.
- $\mathbb{S}$ is a separable measurable Hausdorff space ($\mathbb{S}$, $\mathcal{B}$) with random variables $S_{t\,m}$ from a probability space ($,\mathcal{U},\mathcal{P}$) to ($\mathbb{S}$, $\mathcal{B}$).
- $\mathcal{K}$ is a Markov-kernel : $\mathbb{S}^{\mathcal{K}} \quad \mathcal{B} \quad [0,1]$, such that $\mathcal{P}(\mathcal{S}_{t+1\,m} \quad \mathcal{B}\,\mathcal{S}_t, \mathcal{N}_{(m)} = s) = \mathcal{K}(s,\mathcal{B})$.

An equivalent definition of stochastic cellular automata can be formulated through filtrations of -algebras based on the graphical structure of the neighbourhood relations (SCHNECKENREITHER, 2014). Some direct conclusions from stochastic cellular automata include that the global stochastic process, (describing the simultaneous transition of the states of all cells), is a Markov process itself. Furthermore a Chapman-Kolmogorov like equation can be formulated for stochastic cellular automata.

In addition, stochastic processes are intrinsically connected to cellular automata modeled through multi-agent systems (also called agent-based modeling) (CROOKS; HEPPENSTALL, 2012). In those models, micro-scale autonomous agents (cells) follow simple and programmable actions and cascade into different emerging processes, thus creating complex macro-scale systems (tumors) with varied behavior (WANG et al., 2015). In this paper, we explore further our model's behaviors and stochastic characteristics in sections 6.2.2.3 and 6.2.2.4.

6.2.2 Biological constructs and considerations

The agent-based cellular automaton model developed in this study was based on a mix of characteristics in (ENDERLING et al., 2009; POLESZCZUK; ENDERLING,

2014) and follows the mathematical groundings in section 6.2. It is a stochastic framework in which a single cell (agent) originates a tumor that can have several different features depending on model configurations and its parameters.

The model is discrete both in time and space. Regarding the latter, section 6.2.2.1 describes lattice geometry and model neighborhood. Section 6.2.2.2 presents the possible states for each agent or cell in the model. The simulation advances in steps of t days, where every cell in the tumor will obligatorily present one of the behaviors described in section 6.2.2.3, which also describes the main parameters of the model. Finally, as we deal with a stochastic model, the automaton results are discussed in section 6.2.2.4 in terms of averages of simulation batches.

6.2.2.1 Lattice and neighborhood geometry

In this work, a 2D lattice is considered in which each element can hold up to one cell at a time. The length of each lattice element is $10\mu m$, which is comparable to the size of a regular cell. A 2D Moore neighborhood is considered, implying that a tumor cell can move to any adjacent free place during a computational time step, as shown in Fig. 22a. When there are no free lattice positions (i.e. empty space) surrounding the cell, it cannot move nor proliferate thus staying quiescent, as depicted in Fig. 22b.

Figure 22 – Representation of the computational lattice, where each space of $100\mu m^2$ can hold up to one cell (2D Moore).

(a) If there are available spaces, the cell can move or proliferate to any of the adjacent positions.

(b) If there are no available spaces, the cell becomes quiescent until an adjacent cell either moves or dies.

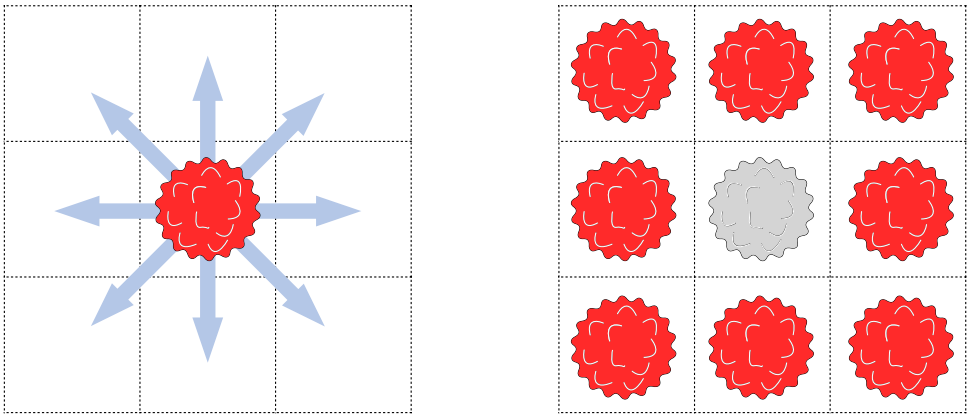

Source: Valentim, Rabi and David (2023).

6.2.2.2 Cell states

The model comprehends a heterogeneous population of tumor cells: they can either be a regular tumor cell (RTC) or a stem tumor cell (STC). Both healthy and dead cells are not accounted in this approach.

There are some crucial differences between those two types of cells. The vast majority of tumor cells will usually be RTCs, which have a maximum proliferation potential p_{max}, thus generating a finite number of offspring cells. They can only give birth to RTCs and eventually may die (either by programmed death, apoptosis, or when they reach their maximum replication potential). In those cases, the tumor cell is removed from the lattice. Also called nonclonogenic cells, RTCs are visually represented in this model in colors ranging from red (maximum proliferation potential) to black (exhausted cell). By relying on this graphical pattern, this mechanism is sketched in Fig. 23.

Figure 23 – A graphical representation regarding the proliferation potential of RTCs.

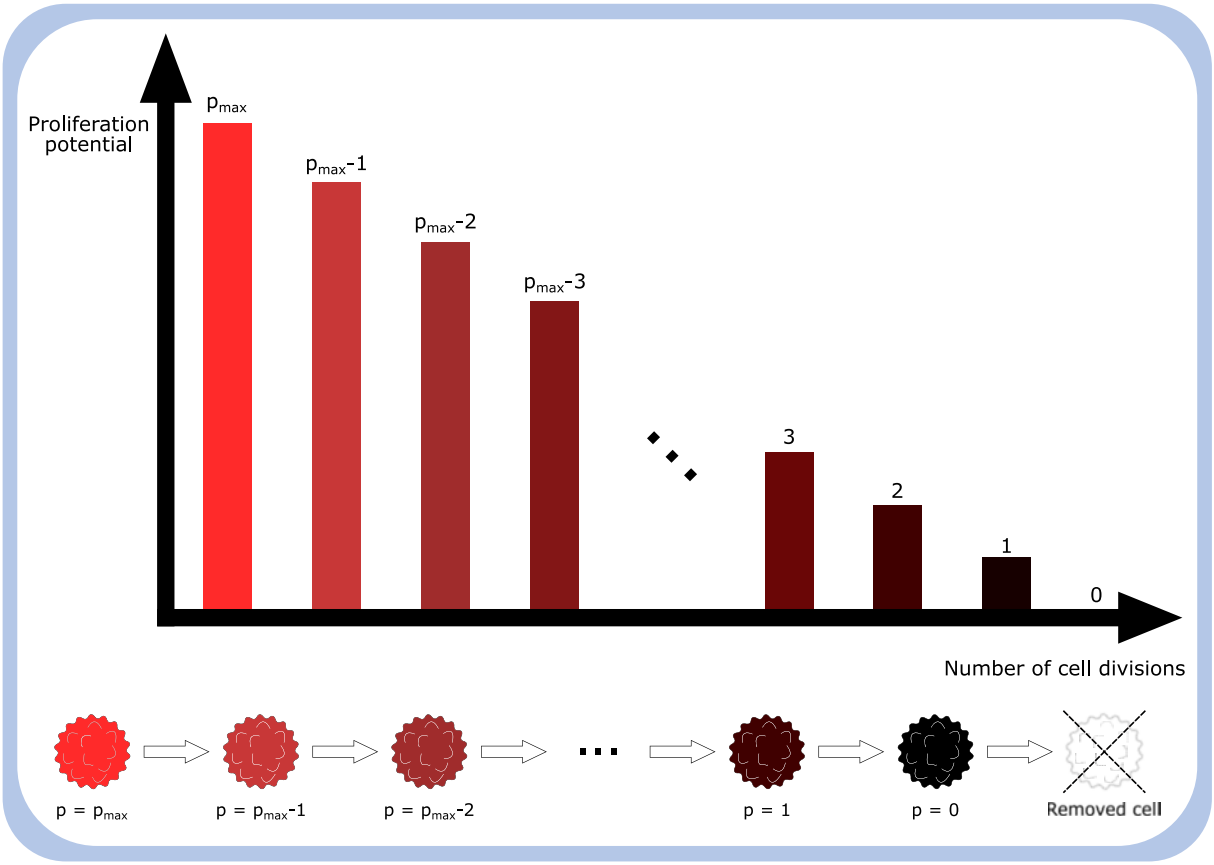

Source: Valentim, Rabi and David (2023).

On the other hand, STCs completely lack internal regulatory mechanisms regarding cell death, thus being permanent. They have an infinite proliferation capacity and will continue replicating independently of how may divisions they have endured. These cells can be categorized in clonogenic or true stem cells. The first group can only give birth to regular (i.e. mortal) cells with limited proliferation potential. The latter can perform an asymmetric division in which the daughter is an RTC, but might also generate an identical true stem cell. The mechanisms regarding the differences between aforementioned cells are depicted in Fig. 24, in which STCs are represented in yellow and the probability of a symmetrical division from a true stem cell is P_S.

Figure 24 – Cell populations included in the model. Outcomes of an evolving tumor will depend on its original progenitor cell and if it is either nonclonogenic, clonogic, or stem.

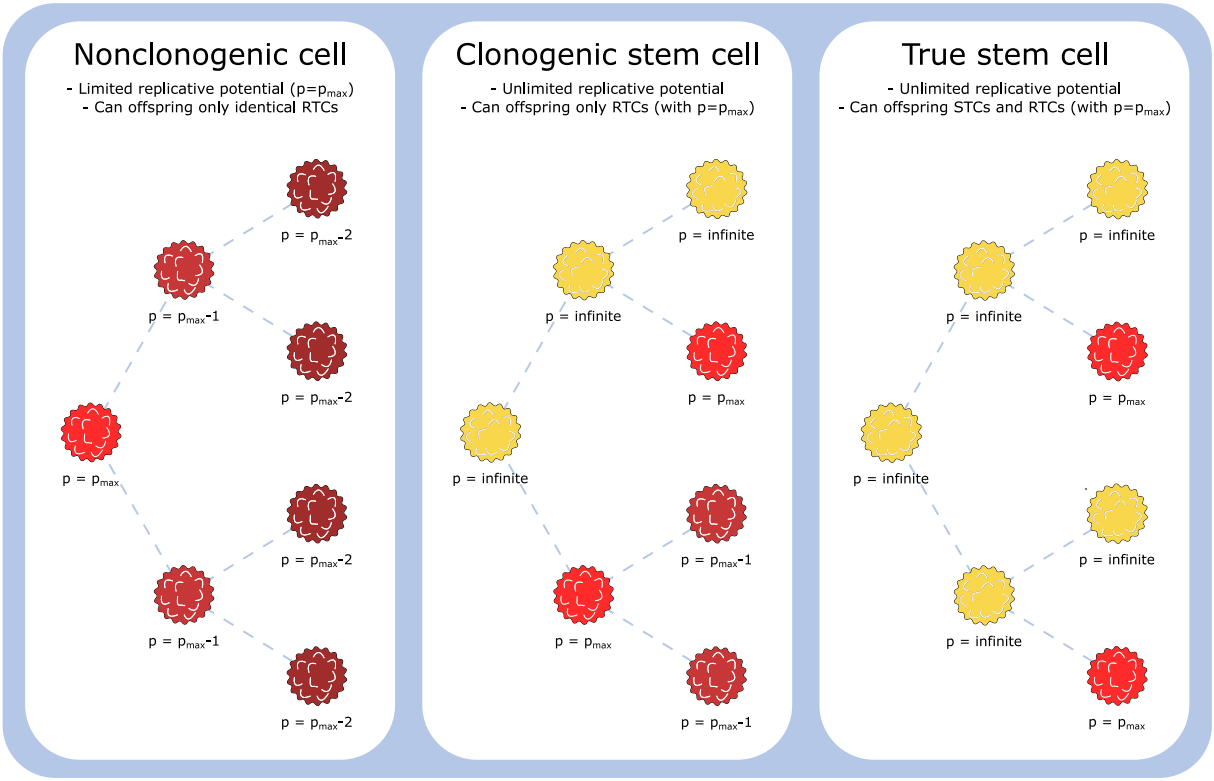

Source: Valentim, Rabi and David (2023).

6.2.2.3 Model mechanics and cell behavior

Every cell in the model will obligatorily present one of the following behaviors during each time step. At first, every cell has a chance P_A of undergoing apoptosis. This is usually a very low rate, since tumor cells can generally activate a number of processes to avoid cell death (HANAHAN; WEINBERG, 2011). Naturally, $P_A = 0$ for every STC since they are allegedly immortal.

If the cell endures, it has a proliferation probability $P_P = CCT \quad t \ 24$, where CCT is cell cycle time. This probability suggests that a cell will replicate more or less according to its natural cycle. If the original cell is a true STC, it will have a low, but essential, chance P_S of generating another identical STC.

If the cell neither dies nor replicates, it has a chance $P \ = \mu \ t$ of migrating according to its displacement capacity μ. In case the cell fails upon all these probabilities within the same time step, it stays quiescent or dormant. This state of dormancy is also achieved if the cell is completely surrounded and lacks free space for either proliferating or moving.

Figure 25 sketches the four possible mechanisms for each cell during any time step, along with their probabilities. By including t, every probability is adjusted to the respective time scale used in the simulation. One exception is the chance for symmetrical

division by stem cells because the time scale has already been considered when calculating its proliferation chance.

Figure 25 – During each time iteration, a tumor cell obligatorily triggers one of four events: apoptosis, proliferation, migration, or quiescence. These events are temporarily exclusive (i.e., a cell will only perform one of them during a single time step).

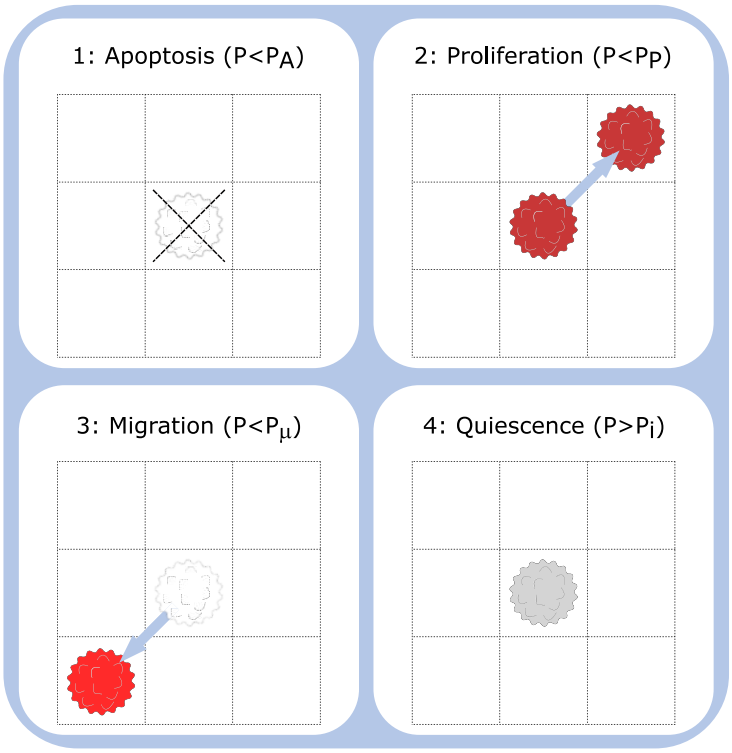

Source: Valentim, Rabi and David (2023).

The flowchart in Fig. 26 summarizes the logic developed for this model and implemented in the algorithm discussed in section 6.2.3. While this figure provides a general overview of how each cell can act during a simulation time step, some specific details are addressed in section 6.2.3, such as the approach regarding domain/lattice extension.

Figure 26 – Logic flowchart for the CA algorithm.

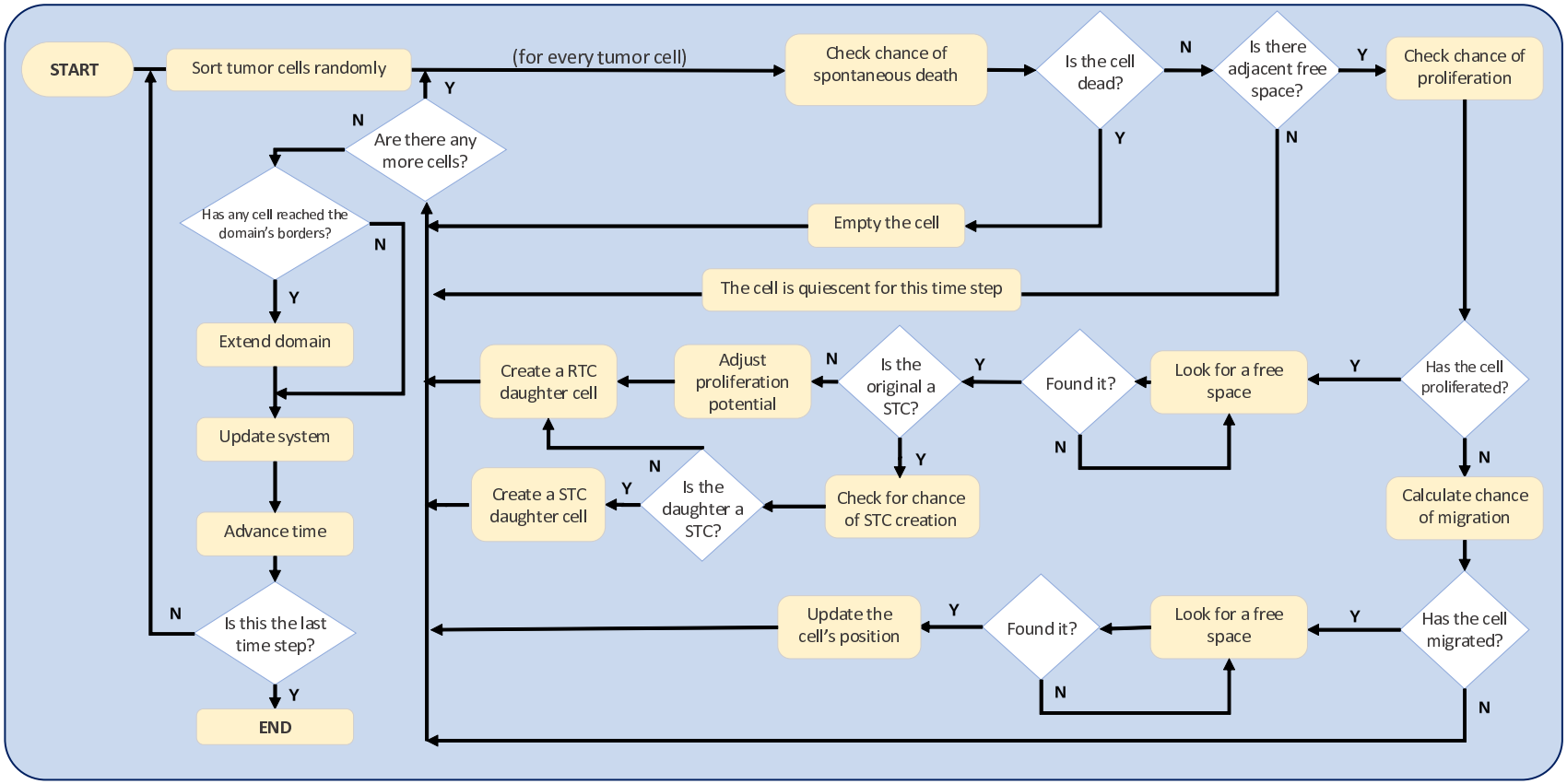

Source: Valentim, Rabi and David (2023).

6.2.2.4 The stochastic process

Cell behavior described in section 6.2.2.3 is modeled through probabilities so that the cellular automaton herein considered is a stochastic process. Therefore, a batch of simulations must be carried out for any investigation (study) using the model.

Some authors argue that for general trends and ideas a low number of simulations - such as five - is enough (ENDERLING et al., 2009) whereas for more delicate testing (or performance evaluation) a number from 50 to 100 should suffice (POLESZCZUK; ENDERLING, 2014). This necessity for replications casts a light on the importance of developing a simulation code with as low computational effort (in terms of CPU time and memory) as possible, which is a programming goal discussed in section 6.2.3. An alternative to decrease the number of simulations is to implement some deterministic characteristics to the model, thus transforming it into a hybrid approach. For more information on the latter, please refer to section 6.4.

In order to express overall results from the batch of simulations, one can use averages and standard deviations to describe cells population dynamics, with RTC and STC populations being described separately. On the other hand, tumor development in space cannot be mathematically described using averages. Therefore, in order to spatially represent a virtualized tumor one must elect the most representative replicate from the simulation batches (i.e. one whose average diffusivity, RTC and STC counts are closer to average values).

6.2.3 Computational implementation

The cellular automaton herein described was coded in Python, chosen as programming language due to its versatility and accessible learning curve. Even though other languages such as Fortran, C and C++ could be faster to tackle procedures such as array swapping and random events, Python has a number of libraries that greatly improve both code accessibility and readability without jeopardizing its speed.

In (POLESZCZUK; ENDERLING, 2014), some high-performance techniques are presented towards the development of a cellular automaton for tumor growth. According to their tests regarding speed and memory, an improved code containing their suggestions would greatly improve performance in comparison to a naive code. Overall, the authors defend the use of specific libraries of the target language instead of trying to build customized code (e.g. use of C++ Standard Template Library, STL, to tackle random events). Many of their suggestions have been applied in the present automaton, with a few occasional caveats and adaptations since the programming languages are different (e.g., *numpy* was used instead of STL). Those suggestions are briefly discussed in this section along with some details regarding code implementation. The final code used for simulations in section 6.3 has been shared on a public GitHub repository (VALENTIM, 2022).

6.2.3.1 The coded lattice

A squared matrix represents the 2D-lattice in the model described in section 6.2.2.1, Therefore, each tumor starts as an empty matrix with a single cancerous cell at its center. The *numpy* library then provides the data structure for the matrix, namely a 2D array with only integer values.

In the tumor matrix, a zero represents an empty space while a nonzero element is a tumor cell. Although one could simply use a matrix of zeros and ones, Poleszczuk and Enderling (2014) suggest using a so-called coded lattice, in which each element value in the tumor matrix not only indicates the presence of a cell but also provides some additional information without relying on extra memory. In this case, each element value represents the proliferation potential of the corresponding cell positioned at that site. Following this approach, after each successful replication of a nonclonogenic cell, its current proliferation potential is updated by simply subtracting one. Besides, by looking at each element value in the matrix, one can quickly grasp how many divisions that corresponding cell can still endure.

In the coded lattice, STCs are characterized by the smallest integer value above the maximum proliferation potential for that tumor setting. For instance, if a tumor with $p_{max} = 10$ is simulated, new RTCs will be represented by the value 11 and will decrease this value by one for every successful division (generating a cell with an identical value). Then, in this simulation STCs would be represented by the value 12. In the algorithm, one would have to establish that, if an element of the tumor matrix is higher than 11, then it is a stem cell and normal rules do not apply to it (such as apoptosis). Figure 27 illustrates that process.

Figure 27 – An example of a coded lattice. Colors represent the convention adopted in Figs. 23 and 24.

0	0	0	0	9	0
0	12	11	10	9	0
10	11	12	12	12	0
0	10	11	11	10	9
0	9	11	11	9	8
8	0	0	0	0	0

Source: Valentim, Rabi and David (2023).

6.2.3.2 Loops and array operations

When using a numerical matrix as lattice, one needs to sweep every row and column in order to access every element. One usual way to program such a routine is using nested loops, which is a very slow computational task in Python. An alternative is to use array operations, which perform, for instance, algebraic calculations on entire arrays and matrices.

Nevertheless, these operations do not fit very well with the systematic time-incremental procedure that a cellular automaton generally follows, particularly because the code will need to rely on random events to determine how a cell will act. Therefore, as a middle-ground solution, one can opt for using the matrix-specific *numpy* command *matrix.nonzero*, which will quickly scan the matrix and return row and column indexes related to every tumor cell (i.e., all elements greater than zero).

Next, a single array pertaining the coordinates from all tumor cells in the tissue will be created. This will enable a single iterative loop to check the content in the main tumor matrix according to the coordinates in the array. This approach is generally faster than relying on nested loops to find tumor cells in this matrix.

6.2.3.3 Random ordering and neighbor selection

There are multiple ways of having access to random numbers using Python. One usual way is through the package *random* and drawing a pseudo-random number between 0 and 1 each time the chance of a cell fulfill some action is tested. Another approach is to use the *numpy* library to draw a full array of pseudo-random numbers at once. The latter can be faster than the former when the length of the referred array is sufficiently large.

In our model, one always knows the number of tumor cells at the beginning of each time iteration. Therefore, one can use numpy.random to generate an entire array of random numbers, thus generating random chances for apoptosis, proliferation, and migration for each cell at the beginning of each time iteration. Those chances are stored in three separate arrays and compared to the respective set probabilities when the behavior of each cell is tested and decided.

For a model to describe different tumor geometries, random arrays can also be applied when considering the direction along which the tumor will effectively grow. In this cellular automaton, such direction is considered twice, first when the coordinate array is swept and behavior is attributed to each cell. If any specific direction is arbitrarily chosen, it will interfere in growth orientation (i.e. left to right). Therefore, the coordinates regarding cells can be randomly accessed during each time step by means of *numpy.random.shuffle* command, guaranteeing that no geometric shape will be favored during tumor evolution.

The second time occurs when checking for free adjacent spots (or neighbors) each time a cell might proliferate or move. An array containing the directions for each of the 8 possible neighbors (see Fig. 22a) is shuffled every time a cell behavior is activated. Then,

tumor matrix is checked for each possible location, returning the content when the first free lattice is matched. If all adjacent spots are occupied, cell quiescence command is passed.

It is worth mentioning that although this approach of not checking every neighbor before acting is faster according to Poleszczuk and Enderling (2014), it may be problematic when extending the stochastic cellular automaton model to a hybrid model. In this case one would need to have information on all neighbors surrounding a tumor cell, since it may "prefer" to migrate to a place with a higher nutrient availability.

6.2.3.4 Dynamically growing domain

A frequent problem when modeling tumor growth is that one does not know a priori the final size of the neoplastic mass. One would have to know beforehand properties such as cell density and diffusivity, besides emergent complex dynamics. Therefore, it may be difficult to establish tumor matrix size in the cellular automaton.

Poleszczuk and Enderling (2014) suggest that a dynamically growing domain could be used as a workaround for such problem. Therefore, the present model starts every simulation with a small 11x11 matrix whose center hosts the progenitor tumor cell. After every new proliferation or migration, the model keeps track of how close every tumor cell is from this domain/matrix borders. The automaton is coded to add a few rows and columns to tumor matrix and re-center the old lattice to the new one every time that a tumor cell reaches the penultimate empty spot in every lattice direction. This approach allows the model to effectively deal with different types of tumor configuration by relying on very large matrices only when really necessary.

Such approach has an important caveat. As this automaton was developed aiming at a future expansion to a hybrid model, dealing with expanding matrices lacking border definitions would be a problem when synchronously considering PDEs (whose borders are really important). Nevertheless, we decided to maintain this approach, relying on linear transformations and scaling tools to handle the future expansion.

6.2.3.5 Dense vs. sparse matrices

Even when using dynamically growing domains, the tumor matrix customarily has a high number of zero elements (characterizing free space). Therefore, it is natural to think of employing sparse matrices since those are commonly used in simulations of mathematical problems (such as PDE solving). However, when sparse matrices were implemented in this model, they lagged considerably behind of other approaches during empirical speed tests (check section 6.2.3.6 for more information). Accordingly, in the referenced study (POLESZCZUK; ENDERLING, 2014) there is no mention to using sparse matrices to increase speed performance.

One way to justify such speed disadvantage is that, depending on the input parameters, this model will often describe dense tumors, whose matrices will constitute in its majority nonzero elements. Additionally, this cellular automaton was initially designed with dense matrices in mind and the version using sparse ones was developed later. Therefore, it is here acknowledged that a similar automaton could be conceived using sparse matrices.

In terms of memory saving, sparse matrices are indeed much more efficient. When running several different tests, such as ones in section 6.3, our model stores every snapshot of the lattice for every time step and every replicate of a simulation. This allows revisiting any instance of tumor evolution in order to visualize or post-process any needed detail. Nevertheless, the variables produced are very long lists of large matrices. Converting each matrix to its sparse correspondent is a workaround to save considerable disk space (thus improving speed during variable writing and reading).

6.2.3.6 Speed tests

Over 40 different versions of this cellular automaton have been coded during the development of this model. Some versions were incomplete, some were too slow, and others were not very readable or practical. Since the simulation of in silico models tend to become slower as cell populations increase, runtime speed was a main aspect considered during code development.

In this vein, the most recent version of the code has been continuously improved to become faster and more efficient, mainly in line with implementation approaches previousy discussed. The impact of some of those implementation techniques on average runtime is presented in Fig. 28, which compares performance of five representative versions of the code during development. Main characteristics of each code version are described in Tab. 9. Each test consisted of a batch of 10 simulations using the same parameters and with compatible cell population outcomes. Averages and standard deviations were presented. Code 'E' is the most stable and fastest version of the cellular automaton thus far developed and was used for all subsequent simulations in section 6.3.

Table 9 – Description of each main code version evaluated in the speed performance test.

Code version	Main characteristics (comparatively)
A'	Sparse matrix to represent tumor cells
B'	Use of large lattice with no expanding domain
C'	Coordinate system with an expanding domain; use of Random library
D'	Similar to C', but using Numpy-Random library
E'	Similar to D', but using *shuffle* instead of *choice*

Source: Valentim, Rabi and David (2023).

Figure 28 – Speed performance tests for representative code versions and time steps (N=10 replicates).

(a) T = 500 time steps. (b) T = 2000 time steps. (c) T = 5000 time steps.

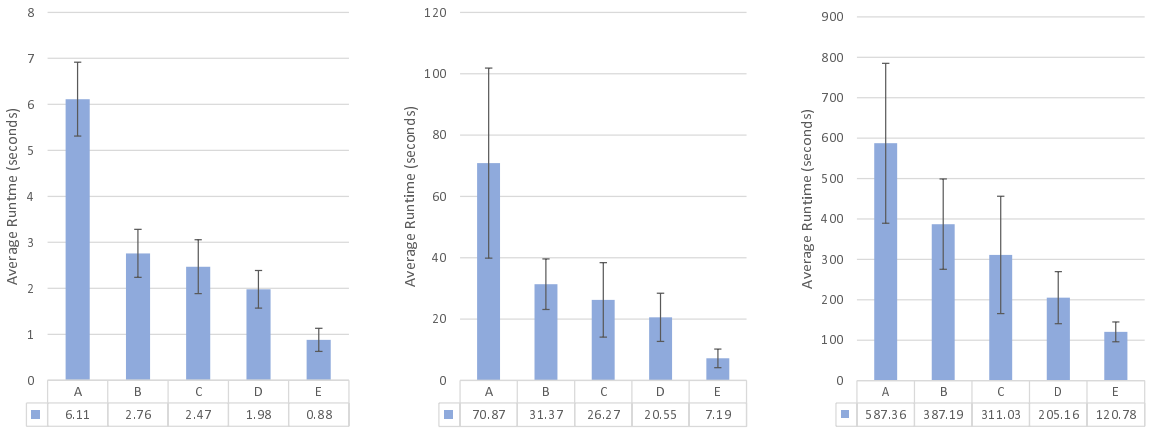

Source: Valentim, Rabi and David (2023).

6.3 Results

In this section, some of the complex scenarios that can be generated from the stochastic cellular automaton are discussed by reproducing the cases studied by Enderling et al. (2009). Firstly, some general parameters and details are presented in section 6.3.1. Different cases pertaining dormancy periods, stem cells, and diffusive/dense tumors are then exposed and commented in subsequent sections.

6.3.1 Parameters and details

Although the scenarios studied in this section were taken from the work by Enderling et al. (2009), it is worth highlighting that this cellular automaton model also presents mixed attributes from the one detailed in a more recent paper (POLESZCZUK; ENDERLING, 2014). Therefore, actual input values used in the simulations were from the latter. Nevertheless, the qualitative behavior and magnitude of results are the same.

In all simulations some parameters were kept constant, namely time step t, cell cycle time CCT proliferation probability P_P, and lattice cell width, whose values are presented in Tab. 10. Other variables, such as migration potential μ, maximum simulation steps T, maximum proliferation potential p_{max}, apoptosis rate P_A, and probability of symmetrical stem division P_S, were set in view of the tested scenario.

All tumors originated from a single progenitor cell. All simulations were replicated five times. The population dynamics in every scenario considered averages and standard deviations of these replicates. The spatial snapshots of evolving tumors considered the one whose number of cells were closer to the calculated average.

Table 10 – Common parameters and probabilities for all studied scenarios.

Parameter	Value	Unit
Time step (t)	1 24	day
Cell cicle time (CCT)	24	hours
Proliferation probability	4 17%	(per time step)
Lattice cell width	10	μm

Source: Valentim, Rabi and David (2023).

6.3.2 First scenario: Tumor growth from a cell without clonogenic potential

The first scenario refers to an original nonclonogenic cell, i.e. a tumor cell with limited replication capacity. In this scenario, migration potential is $\mu = 10$ cell width/day, apoptosis probability is null $P_A = 0$ and tumor cells only die after they expire their maximum proliferation potential, which can be $p_{max} = 10$, $p_{max} = 15$, or $p_{max} = 20$. For each of these cases, the population dynamics is shown in Fig. 29 and a representative spatial snapshot of tumor evolution is pictured in Fig. 30.

Table 11 lists the maximum and final cell count for each modeled proliferation potentials. From these results, it is noticeable that, regardless of how many times cells are able to divide, they can never generate a long-lasting tumor with every cell dying after sufficient time is passed. The tumor size is also limited, with cells still capable of proliferating in inner parts of neoplastic tissue while exhausted/dying ones concentrate at extremities. These results are in accordance with those obtained by Enderling et al. (2009) and indicate that tumors originating from a nonclonogenic cell will eventually perish.

Table 11 – Average results for the first scenario. Tumor growth from a cell without clonogenic potential.

Proliferation potential	Max. RTC count		Final RTC count
$p_{max} = 10$	280	43	0
$p_{max} = 15$	3,191	306	0
$p_{max} = 20$	8,657	574	0

Source: Valentim, Rabi and David (2023).

Figure 29 – First scenario: Population dynamics of a tumor originated by a nonclonogenic cell with different proliferation potentials (average of 5 simulations with $p_{max} = 10$, $p_{max} = 15$, and $p_{max} = 20$).

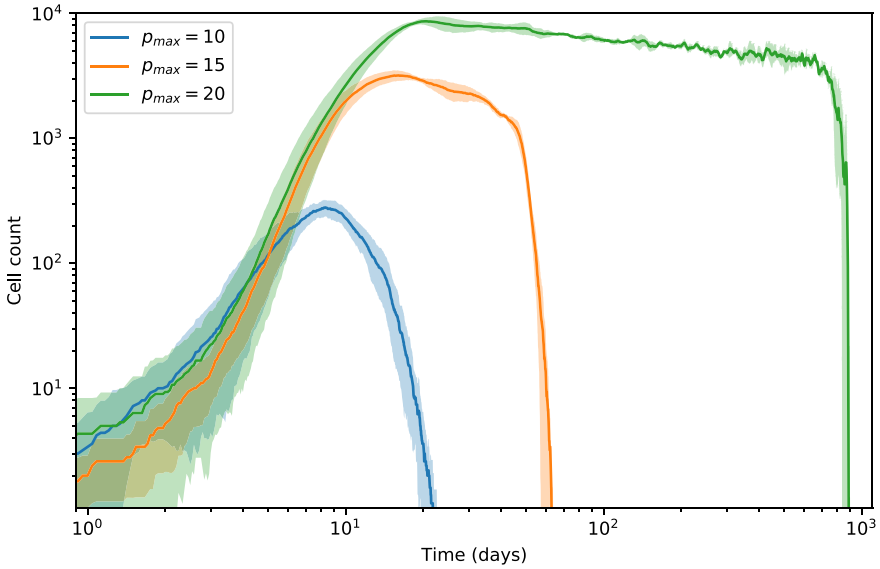

Source: Valentim, Rabi and David (2023).

Figure 30 – First scenario: Spatial evolution of a representative tumor originated by a nonclonogenic cell with different proliferation potentials.

(a) $p_{max} = 10$

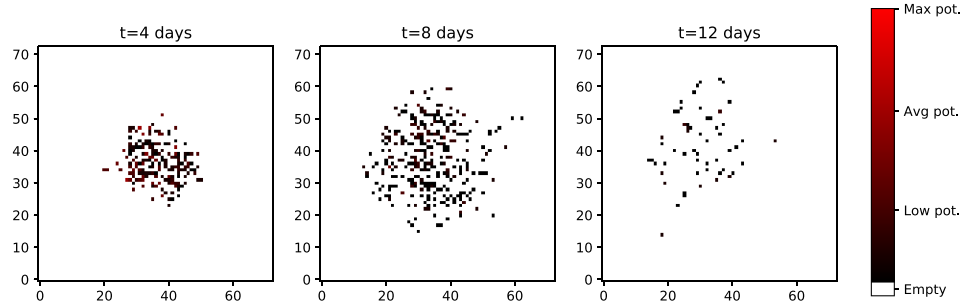

(b) $p_{max} = 15$

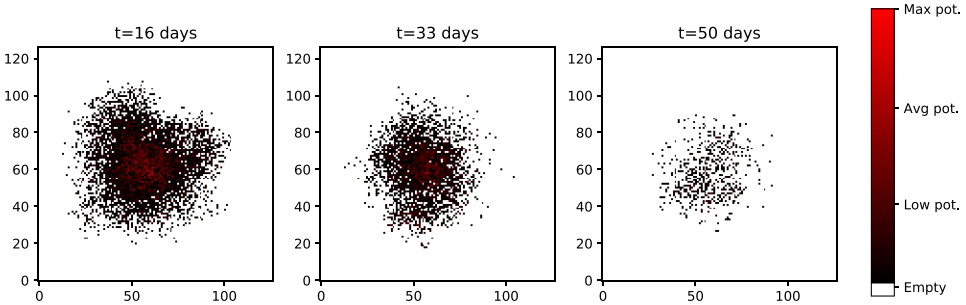

(c) $p_{max} = 20$

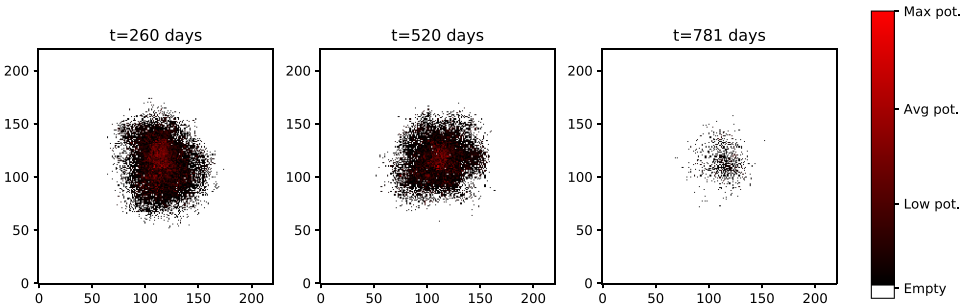

Source: Valentim, Rabi and David (2023).

6.3.3 Second scenario: Tumor growth from a clonogenic cell

In the second scenario, the modeled tumor is generated from a clonogenic cell, i.e. a tumor stem cell that, though permanent can only generate daughter cells with limited capabilities. Migration potential, apoptosis probability and maximum proliferation potential are the same as in the first scenario, i.e., $\mu = 10$ cell width/day, $P_A = 0$, and $p_{max} = 10$, $p_{max} = 15$ or $p_{max} = 20$. The population dynamics is shown in Fig. 31 and a representative spatial snapshot of tumor evolution is presented in Fig. 32. Table 12 lists the maximum and final cell counts for each simulated case.

Differently from the previous scenario, the tumor does not disappear regardless of how many days pass, but reaches a stable size indefinitely maintained. This new feature is due to the clonogenic STC in neoplasm center, which creates a new RTC with full proliferation capacity every time it replicates. Besides, the clonogenic cell never dies, thus replenishing RTC population as those cells become exhausted. The maximum possible tumor size is indicated by cells migration and proliferation potentials, with higher values generating larger masses.

It is noticeable from spatial projections in Fig. 32 that, regardless of p_{max}, tumor shape is always circular (spherical if extended to three dimensions), with new cells in the inside and exhausted cells on the outside. Results from this scenario also match those obtained by Enderling et al. (2009), where authors claim this outcome can likely be used to describe some types of benign tumors, which live in patients for up to decades and never reach a dangerous size nor become malignant.

Table 12 – Average results for the second scenario. Tumor growth from a clonogenic cell.

Proliferation potential	Max. RTC count		Final RTC count	
$p_{max} = 10$	$2,049$	241	$1,699$	522
$p_{max} = 15$	$6,676$	$1,070$	$4,442$	872
$p_{max} = 20$	$13,012$	$1,525$	$8,912$	$1,643$

Source: Valentim, Rabi and David (2023).

Figure 31 – Second scenario: Population dynamics of a tumor originated by a clonogenic STC for different proliferation potentials (average of 5 simulations with $p_{max} = 10$, $p_{max} = 15$, and $p_{max} = 20$).

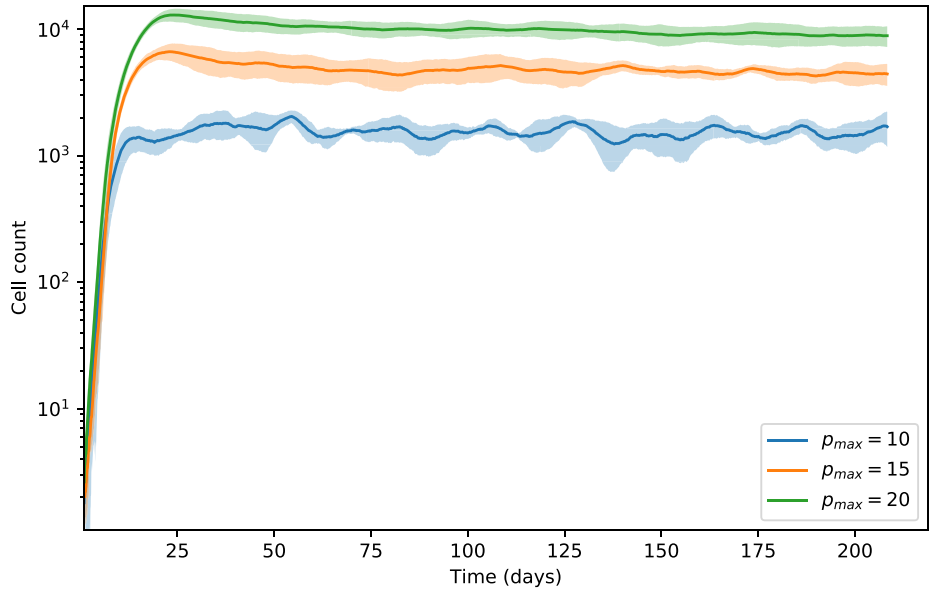

Source: Valentim, Rabi and David (2023).

Figure 32 – Second scenario: Spatial evolution of a representative tumor originated by a clonogenic STC with different proliferation potentials.

(a) $p_{max} = 10$

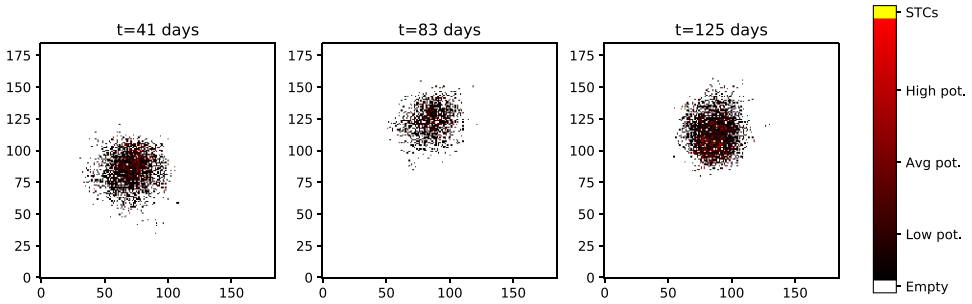

(b) $p_{max} = 15$

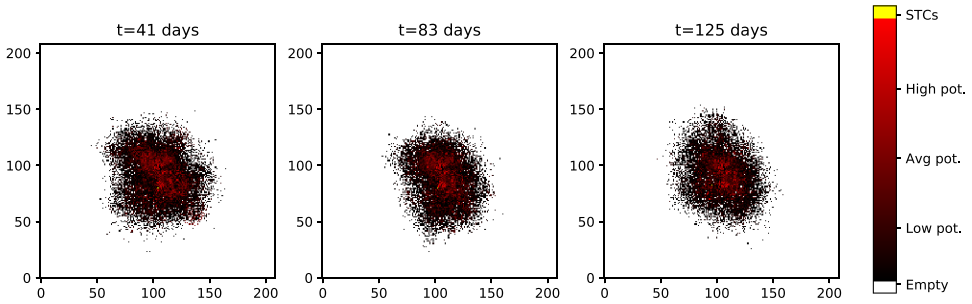

(c) $p_{max} = 20$

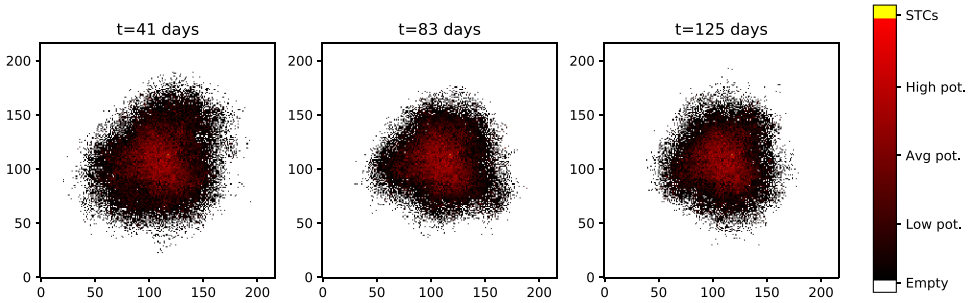

Source: Valentim, Rabi and David (2023).

6.3.4 Third scenario: Tumor growth from a true stem cell

The third scenario presents a tumor originated from a true stem cell, i.e., a permanent tumor cell with probability P_S of generating an identical daughter cell, as indicated in the third frame of Fig. 24. Migration potential is $\mu = 10$ cell width/day and apoptosis probability is null $P_A = 0$ (same as scenarios 1 and 2). Tumor cells only die after they expire their maximum proliferation potential, which can be $p_{max} = 10$, $p_{max} = 15$, or $p_{max} = 20$. The chance for symmetrical STC replication is $P_S = 5\%$. The population dynamics is shown in Fig. 33 and a representative spatial snapshot of tumor evolution is pictured in Fig. 34. Table 13 lists both RTC and STC final counts for each simulated case.

Table 13 – Average results for the third scenario. Tumor growth from a true stem cell.

Proliferation potential	Final RTC count		Final STC count	
$p_{max} = 05$	$85,167$	$25,076$	$1,947$	594
$p_{max} = 10$	$24,386$	$8,479$	32	12
$p_{max} = 15$	$4,731$	746	$1\ 4$	$0\ 5$
$p_{max} = 20$	$8,273$	$1,385$	$1\ 8$	$0\ 7$

Source: Valentim, Rabi and David (2023).

This scenario is the first in the chapter in which tumors can quickly reach large dangerous sizes. As discussed by Enderling et al. (2009), stem cells population apparently dictates tumor size and endurance. This becomes clearer from Tab. 13, suggesting that neoplasms with higher RTC count are those presenting more STCs.

Figures 33 and 34 also highlight a counter-intuitive idea: cells with lower maximum proliferation potential tend to grow much larger tumors. The underlying reason is that as RTCs with low p_{max} die faster they make available space for STCs to replicate, thus rising chances for symmetrical division and consequently increasing STC population. When RTCs can divide many times before exhausting, they make no room for the very small initial STC population to reproduce, drastically reducing the chances for tumor grow over a stability point. This is what happens in the simulations where $p_{max} = 15$ and $p_{max} = 20$, as shown in aforementioned figures.

Figure 33 – Third scenario: Population dynamics of a tumor originated by a true STC with different proliferation potentials (average of 5 simulations with $p_{max} = 5$, $p_{max} = 10$, $p_{max} = 15$, and $p_{max} = 20$).

(a) Evolution of regular tumor cells (RTCs).

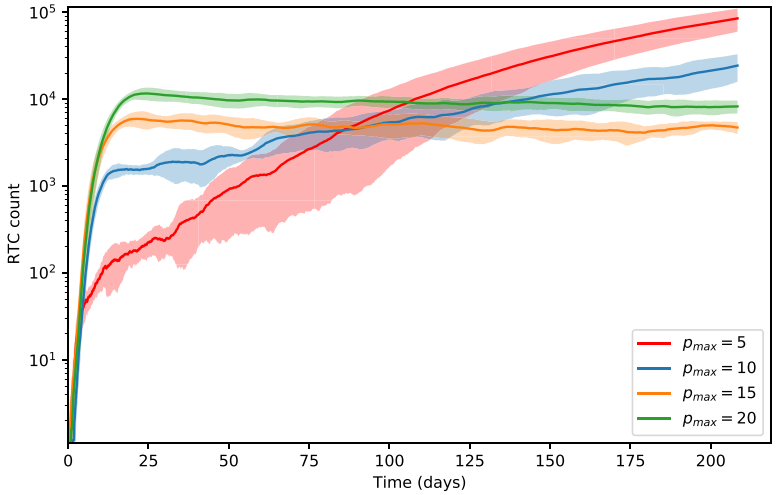

(b) Evolution of stem tumor cells (STCs).

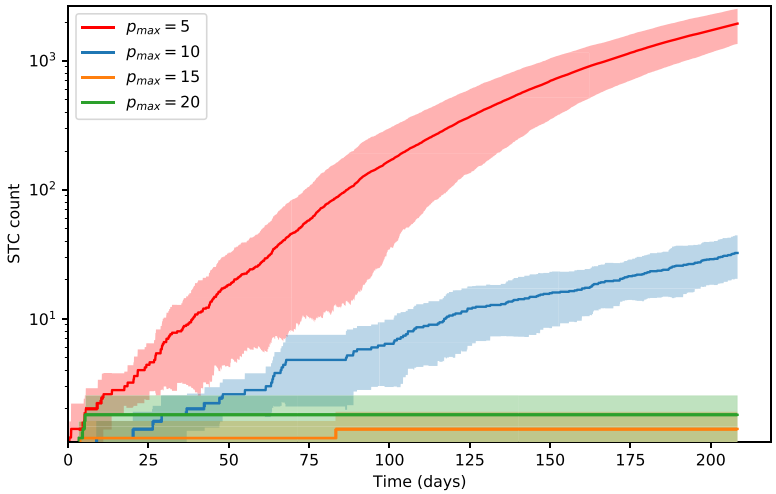

Source: Valentim, Rabi and David (2023).

Figure 34 – Third scenario: Spatial evolution of a representative tumor originated by a true STC with different proliferation potentials.

(a) $p_{max} = 5$

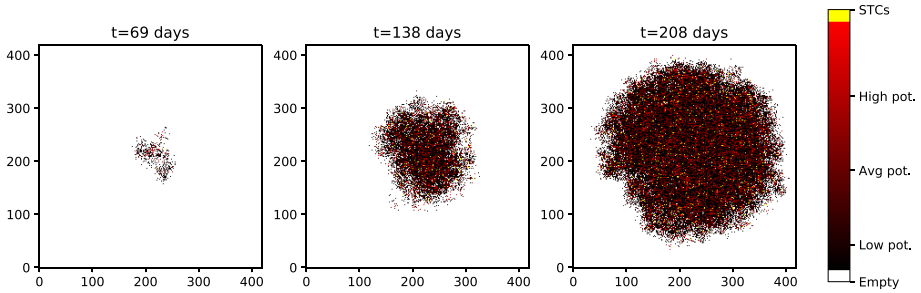

(b) $p_{max} = 10$

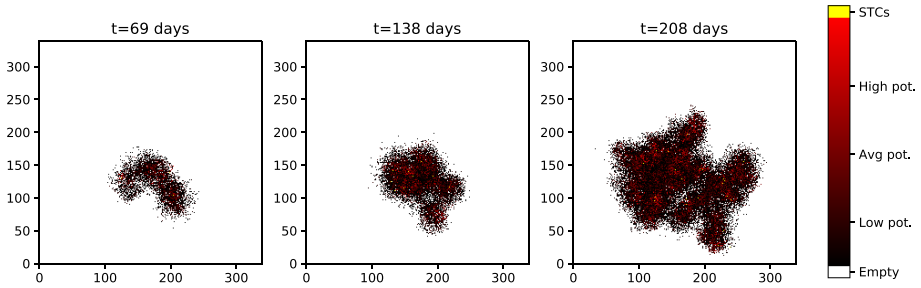

(c) $p_{max} = 15$

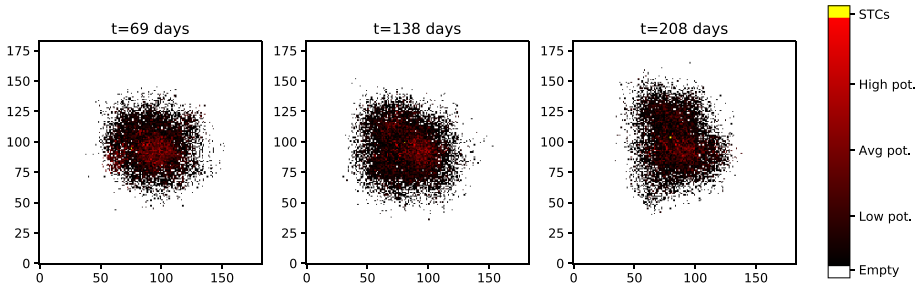

(d) $p_{max} = 20$

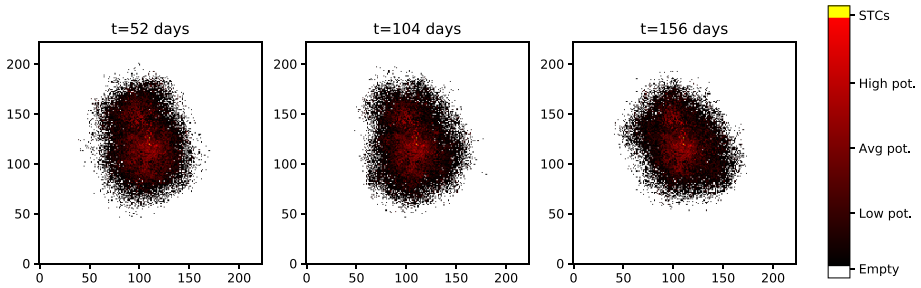

Source: Valentim, Rabi and David (2023).

6.3.5 *Fourth scenario: Tumor growth with different apoptosis rates*

In the fourth scenario, the nonzero apoptosis condition is explored. A tumor originated by a true STC is simulated with $p_{max} = 10$, $\mu = 10$, and $P_S = 1\%$ for four different apoptosis rates. For each outcome, the population dynamics is shown in Fig. 35 and a representative spatial snapshot of tumor evolution is presented in Fig. 36. Table 14 lists the final counts pertaining RTCs and STCs for each simulated case.

Figure 35 – Fourth scenario: Population dynamics of a tumor originated by a true STC with different apoptosis rates (average and standard deviation of 5 simulations with $P_A = 0\%$, $P_A = 1\%$, $P_A = 10\%$, and $P_A = 30\%$ a day).

(a) Evolution of regular tumor cells (RTCs).

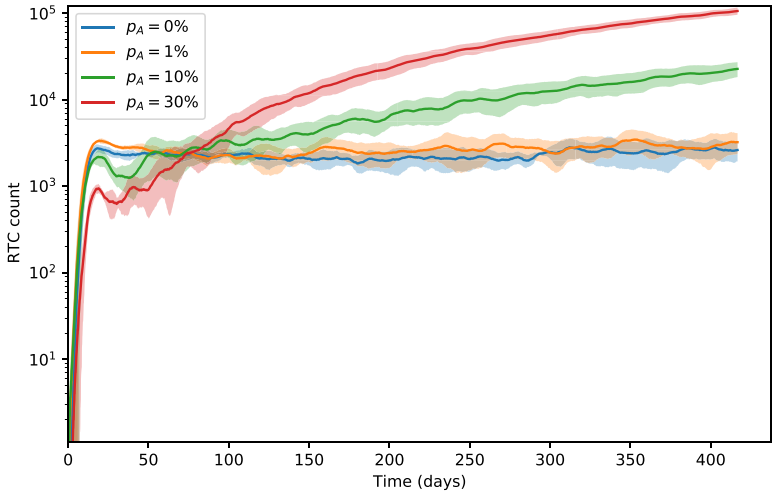

(b) Evolution of stem tumor cells (STCs).

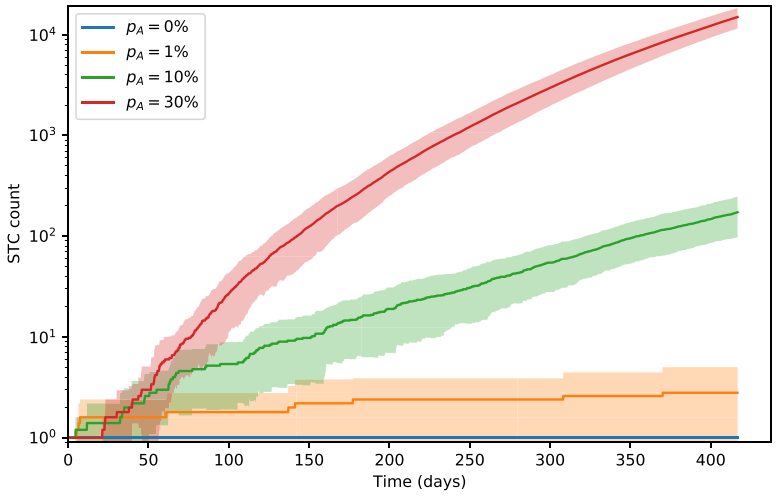

Source: Valentim, Rabi and David (2023).

Figure 36 – Fourth scenario: Spatial evolution of a representative tumor originated by a true STC with different apoptosis rates.

(a) $P_A = 0\%$

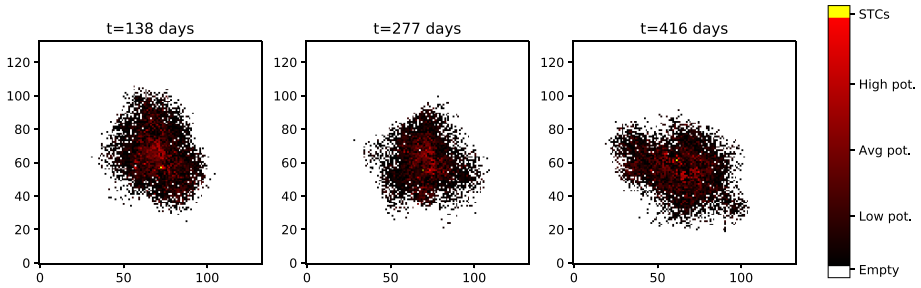

(b) $P_A = 1\%$

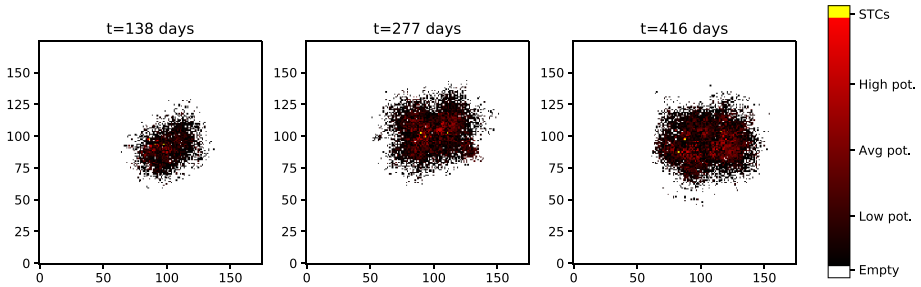

(c) $P_A = 10\%$

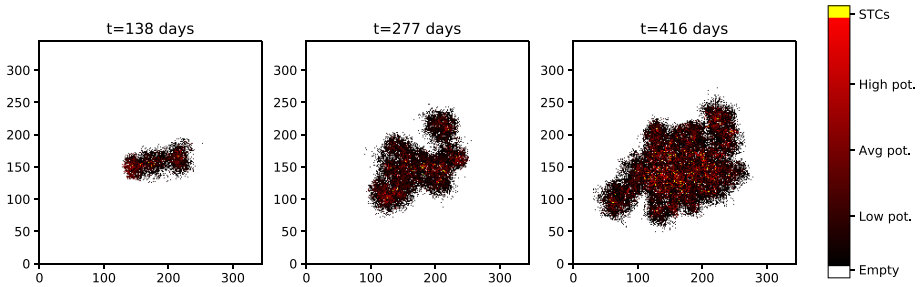

(d) $P_A = 30\%$

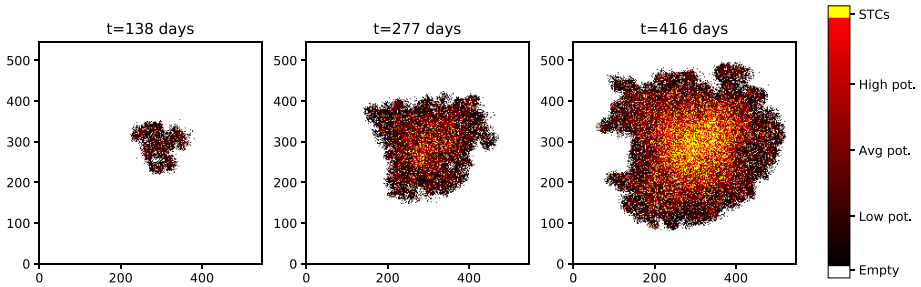

Source: Valentim, Rabi and David (2023).

Table 14 – Average results for the fourth scenario. Tumor growth with different apoptosis rates

Apoptosis chance	Final RTC count		Final STC count	
$P_A = 0$	$2,628$	677	$1\ 0$	$0\ 0$
$P_A = 1\%$ /day	$3,241$	872	$2\ 8$	$2\ 2$
$P_A = 10\%$ /day	$22,771$	$4,443$	173	75
$P_A = 30\%$ /day	$106,296$	$9,969$	$14,958$	$3,400$

Source: Valentim, Rabi and David (2023).

As thoroughly discussed by Enderling et al. (2009), outcomes represented in Figs. 35 and 36 are probably the most interesting and revealing among analyzed scenarios. As the chance of programmed cell death increases, the overall tumor cell populations also dramatically rise. The extreme case of 30% daily chance of apoptosis yields a large neoplastic mass with an average of over 120 thousand cells after 400 days, from which around 12% are stem cells. The elevated number of STCs is actually what justifies such large tumors. In fact, as RTCs can die at an increased rate in this scenario, there is much more free space left for STCs to create identical daughter cells (whose chance of apoptosis is always zero).

Tumor shapes for cases with higher cell death start to present protrusions around their extremities, a morphological sign of malignant advanced tumors (refer to Figs. 36c and 36d). Furthermore, when P_A is low but nonzero, there is still a chance of a tumor with morphology and size as illustrated in Fig. 36b to become similar to the one represented in Fig. 36d. The start of this process is depicted in Figs. 35a and 35b, as the population of stem cells plotted by the orange curve slowly rises. Given enough time, overall population will increase, thus creating potentially large and malignant tumors. This phenomenon of very slow growth with low apoptosis rate can be characterized as some types of dormancy periods seen in many cancers.

6.3.6 *Fifth scenario: influence of migration potential and stem symmetrical proliferation*

The fifth and final simulation accounts for how the migration potential of cells and the chance of STC symmetrical replication affect tumor size and shape. In all cases analyzed in this scenario, $p_{max} = 10$ and $P_A = 1\%$, but μ and P_S vary from 1 to 10 cell width/day and 1% to 10%, respectively. In each case, population dynamics is presented in Fig. 37 and possible spatial forms regarding tumor evolution are represented in Fig. 38. Table 15 lists both RTC and STC final counts for each case combination.

Figure 37 – Fifth scenario: Population dynamics of a tumor originated by a true STC with different migration potentials and probabilities of stem symmetrical division (average and standard deviation of 5 simulations).

(a) RTC dynamics for a low chance of stem symmetric division ($P_S = 1\%$)

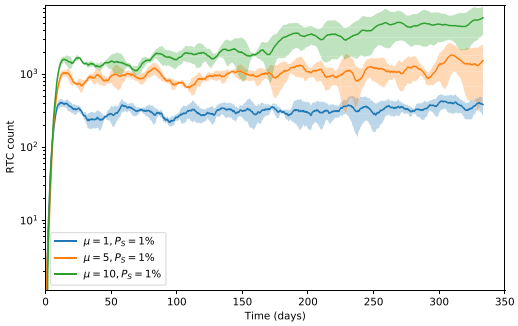

(b) RTC dynamics for a low chance of stem symmetric division ($P_S = 10\%$)

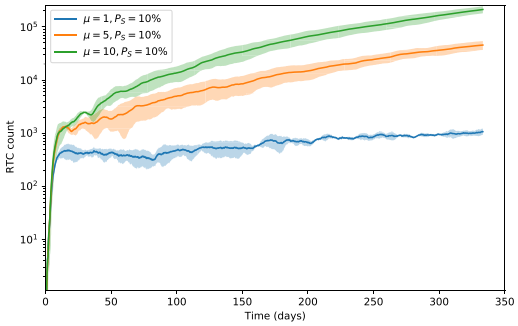

(c) STC dynamics for a low chance of stem symmetric division ($P_S = 1\%$)

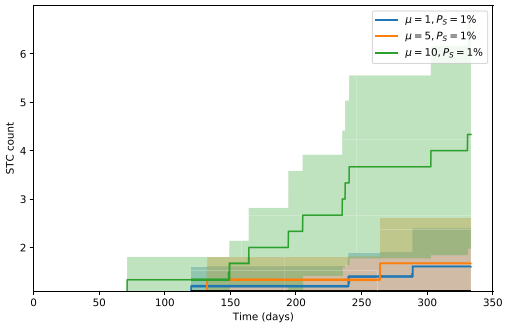

(d) STC dynamics for a low chance of stem symmetric division ($P_S = 10\%$)

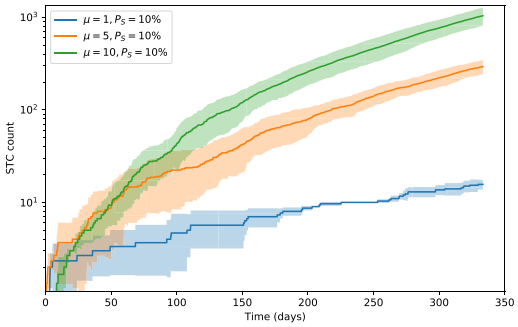

Source: Valentim, Rabi and David (2023).

Figure 38 – Fifth scenario: Spatial evolution of a representative tumor originated by a true stem cell with different migration potentials and stem replication probabilities.

(a) $\mu = 1$ cell width/day and $P_S = 1\%$

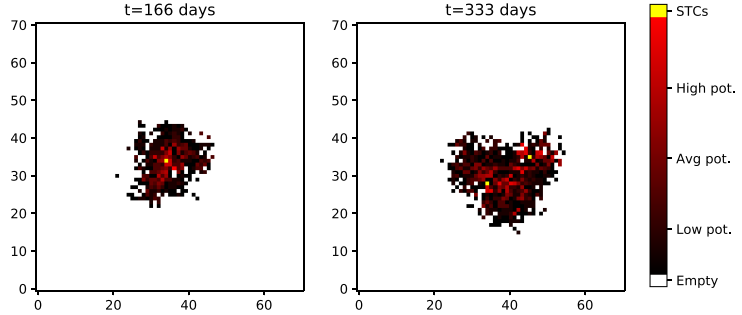

(b) $\mu = 1$ cell width/day and $P_S = 10\%$

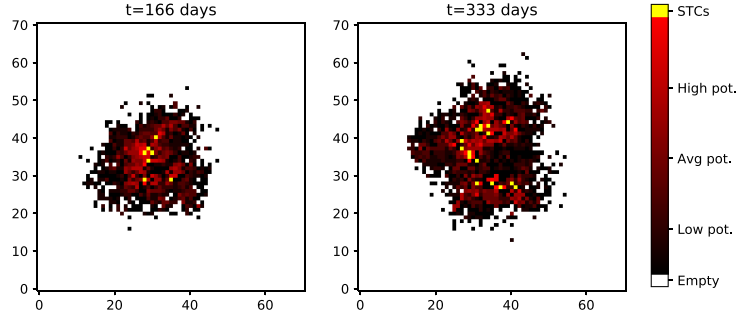

(c) $\mu = 5$ cell width/day and $P_S = 1\%$

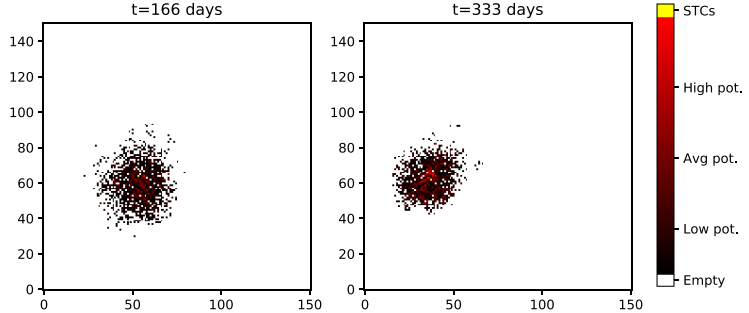

(d) $\mu = 5$ cell width/day and $P_S = 10\%$

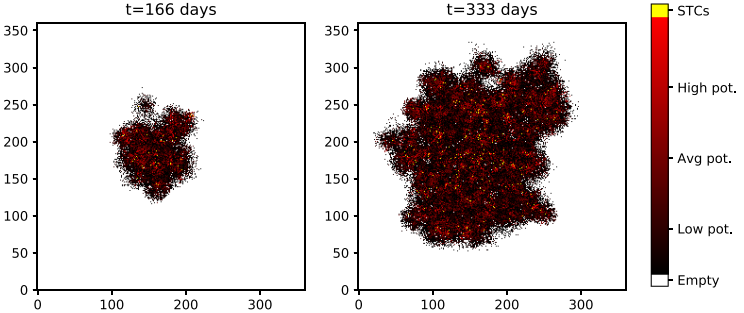

(e) $\mu = 10$ cell width/day and $P_S = 1\%$

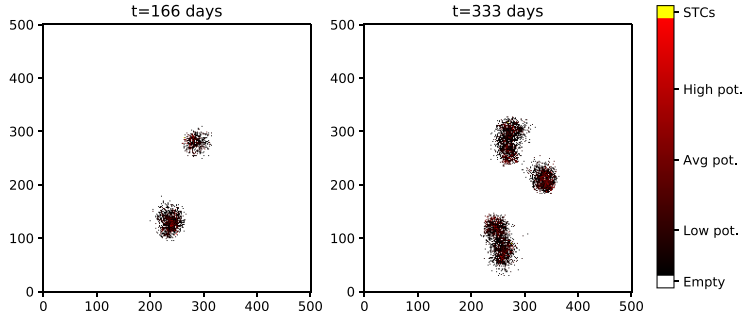

(f) $\mu = 10$ cell width/day and $P_S = 10\%$

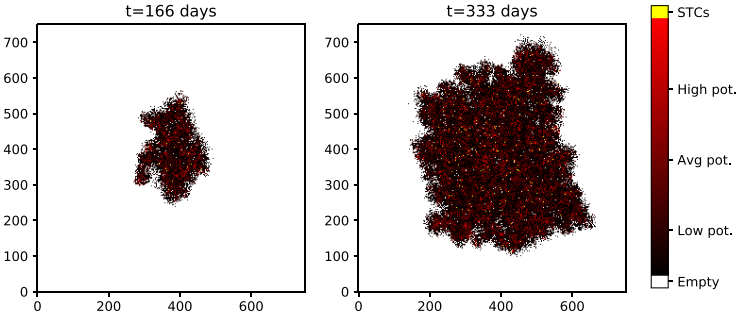

Source: Valentim, Rabi and David (2023).

Table 15 – Average results for the fifth scenario. Influence of migration potential and stem symmetrical proliferation.

	$P_S = 1\%$				$P_S = 10\%$			
Migration pot.	Final RTC count		Final STC count		Final RTC count		Final STC count	
$\mu = 1$	383	110	1 6	0 8	1,063	148	16	2
$\mu = 5$	1,541	1,002	1 7	0 9	45,494	8,729	294	50
$\mu = 10$	5,971	2,483	4 3	2 4	212,795	32,244	1,043	227

Source: Valentim, Rabi and David (2023).

The main interesting aspect of outcomes from fifth scenario is that every combination can lead to potentially large and malignant cancers (Figs. 37c and 37d show growing STC populations in all cases - albeit some much faster than others). Growth speed, on the other hand, seems to be positively connected to μ and P_S values: the higher their values, the more sprawling the resulting neoplasms. As clusters appearance is also identified, some combination of parameters could yield a scenario in which distant metastasis can be virtualized.

In case of highly migrating cells with low potential of STC creation, cell clusters are created (Fig. 38e) and chances of a resulting invasive diffusive tumor are higher. If cells are movable and still generate a high number of STCs, then the resulting neoplasms will be denser but equally prone to invasion and with a much larger overall mass (Fig. 38f).

6.4 Model limitations and future expansion

The automaton model discussed in this chapter is not only capable of describing several different scenarios, as shown in section 6.3, but also is ready to be expanded upon. By coupling PDE systems to the automaton, it is possible to improve the solely stochastic characteristics of the CA, enabling deterministic features to compensate some shortcomings, thus transforming the former into a hybrid model.

Hybrid models are a recent category in which continuum characteristics are incorporated into discrete models. Advantages of such approach are clear for modeling multi-scale phenomena since the discrete part can focus on cell movements scale while the continuum methods can model events on larger scales (REJNIAK; ANDERSON, 2011). This capacity of being able to bridge scale gaps while communicating aspects of different magnitudes across the model makes hybrid approaches very interesting for describing several aspects of cancer phenomena (ANDERSON et al., 2007).

Accordingly, Anderson et al. (2007) proposed a hybrid model constituting of discrete methods to deal with tumor cells while considering continuous methods to model micro-environment factors such as host tissue, matrix-degradative enzymes and oxygens. Their model focused on the micro-scale level to produce simulations of tumor at tissue-scale and could be easily implemented to incorporate other scales range (such as sub-cellular).

Consequently, many other hybrid models emerged, each with their own characteristics and often involving different discrete and continuum tools (IBRAHIM et al., 2015; ALEMANI et al., 2012).

There are some stochastic CA model's main shortcomings that could be directly compensated. Firstly, by disregarding dead cells, the CA model also dismisses the remains of those cells, which could cause toxicity unbalance in tumor micro-environment. Secondly, the CA model does not take into account the nutrient availability in the tissue where the tumor grows. It is known that tumors can react very differently depending on oxygen lack or abundance. For instance, some cells can effectively change the biomechanical characteristics in order to migrate if they are at a oxygen-deprived environment (HORMUTH et al., 2021b). A diffusion PDE coupled to the CA could be used to tackle both these problems.

Therefore, the diffusion equation could be an important tool to model the micro-environment surrounding the tumor. It could correctly describe oxygen (or other nutrient) being diffused throughout the tissue in which the tumor grows as modeled by the CA. Simultaneously, it could also account for the toxicity of cell remains in the environment. Following transport laws, this part of the model would be completely deterministic while also depending on outcomes from the stochastic CA (e.g., if a cell replicates, it will increase the nutrient consumption in that lattice area, interfering with the diffusion equation). On the other hand, the deterministic portion of the model solved at each time step would also interfere with probabilities generated by the CA (e.g., if nutrient availability is very low, the chance of a RTC undergoing apoptosis is higher in that area).

Another problem with the CA model in its current form is that it does not take healthy cells into consideration, not establishing any stress relation between cells and the surrounding extracellular matrix, fact shown to be important in tumor progression (TALONI et al., 2015; WEERASINGHE et al., 2019). As an attempt to improve this characteristic on the hybrid model, a differential equation to model tumor viscoelasticity and its surrounding tissue may well be a very useful strategy.

A hybrid model could potentially contain at least two equations describing tumor micro-environment: one dealing with nutrient diffusivity and the other tackling tissue stresses. In short, the central framework of the model would be the stochastic CA previously described, but it would influence and be influenced by the coupled deterministic models. Governing equations would be simultaneously solved and updated along with the time steps of the CA. Boundary conditions (for the equations) would be correctly selected according to the phenomena being considered.

In this context, fractional calculus can be an interesting tool to model both diffusive and viscoelastic aspects of those systems (WEST, 2021). Fractional models have been applied to vast number of different areas (BALEANU; AGARWAL, 2021), including in health sciences and biomathematics (KUMAR; SINGH, 2020), in which it has provided a singular perspective on mathematical oncology and cancer modeling (WEST, 2022;

VALENTIM; RABI; DAVID, 2021; VALENTIM et al., 2021; VALENTIM et al., 2020). Furthermore, fractional viscoelastic models have been widely explored in the literature, show promising features to describe tissue heterogeneity (GHITA; COPOT; IONESCU, 2021; CARMICHAEL et al., 2015) while non-integer operators are well known for extending the capabilities of diffusive models (DEBBOUCHE et al., 2021; MAGIN et al., 2019).

6.5 Conclusion

In this chapter, we have introduced and discussed the development and implementation of a stochastic cellular automaton model for tumor dynamics. The model has been created based on main characteristics of the frameworks presented by Poleszczuk and Enderling (2014) and Enderling et al. (2009).

Although designed from a relatively simple set of agent-based rules, the stochastic cellular automaton model can simulate several different scenarios regarding tumor growth such as dormancy periods, instability caused by cell-death/competition and invasion – effectively capturing the emergency and complexity inherent to oncological phenomena.

Future expansion is also explored, opening the path to transforming the model into a hybrid framework featuring deterministic characteristics from differential equations capable of potentially mitigate model shortcomings.

The framework herein discussed is an interesting tool for in silico modeling, with promising capabilities and possibilities to support further research in mathematical oncology, thus improving diagnosis tools and/or personalized treatment.

7 TOWARDS A HIGHER INTERDISCIPLINARY COMPLEXITY: HYBRID OR MULTI-PHYSICS MODELS

This chapter addresses the use of either hybrid or multi-physics models in mathematical oncology, both in classical and modern senses, discussing the various interdisciplinary aspects of the theme by recalling to several concepts from previous chapters and combining them into complex frameworks. It also reviews the latest efforts in the literature concerning these models and contextualizes the work produced in the thesis within this frame, paving the prospective way of how this study can be continued and expanded from fundamental to potentially translational research.

It is organized in the following manner: Section 7.1 briefly introduces hybrid models, presenting their main categories. Section 7.2 describes some examples of continuous systems for classical hybrid models, pitching fractional calculus as an additional degree of flexibility and addressing some of the major issues with these models and their most apparent shortcomings. Section 7.3 presents some modern approaches discussed in the literature, using large databases and algorithms combined to physics-based modeling. Finally, section 7.4 wraps up the discussion by defending broad interdisciplinary approaches as the only way viable in mathematical oncology.

7.1 Introduction

Hybrid cellular automata (HCA) models have been used to explore and study cancer and tumor dynamics in recent years. These models can be used to simulate the behavior of cancer cells by incorporating different biological and physical mechanisms that govern tumor growth dynamics. HCA models typically include both continuous and discrete variables, which often characterize phenomena such as cell division and death, cell spatial distribution, and interactions between cells themselves and/or with the surrounding microenvironment (REJNIAK; ANDERSON, 2011; ZANGOOEI; HABIBI, 2017).

Classical HCA models compose a comprehensive category of frameworks in which discrete components can be either on-lattice (Cellular Potts, Hexagonal CA, Square-lattice CA and Multi-compartment CA) or off-lattice (sub-cellular, vertex, ellipsoid, and spherical cell-centered). They show reciprocal relation between the number of cells handled by each modeling technique and the level of included cellular details (e.g., cellular detail vs spatial scale; deformable body vs single points). Continuous components usually address time-dependent intracellular molecular kinetics (via ODEs), cell populations / ecology models (via ODEs), or time- and space-dependent extracellular dynamics (via PDEs), to different extents of complexity (CHAMSEDDINE; REJNIAK, 2019).

HCA models can be used to study the development of different factors on cancer, such as the effects of distinct treatments on tumor growth or the impact of different

microenvironmental conditions on cancer cell behavior. For instance, a finite-state automata model can be used to represent different cell states whereas a continuous dynamics system describes cell behavior according to such state (PHILLIPS et al., 2020). On a different note, those models can also be used to predict the outcome from different medical care strategies or to identify potential targets for cancer treatment - e.g., breast cancer therapy (LAI et al., 2022).

In the last decade, after the recent boost of artificial intelligence and machine learning techniques, the field of data-oriented models has received a lot of attention. In consequence, hybrid models have expanded to additionally combine concepts from continuous and discrete models with approaches from mathematical areas such as machine learning, game theory and data optimization, resulting in a new class of predictive models for cancer analysis and treatment response, being often referred to as multi-physics models. The increasing availability of clinical data in large online repositories (HWANG, 2021) have propelled a rise on data-driven models using statistical correlations and algorithms, particularly the computer vision area. Accordingly, data-driven models can integrate to physics-based models working as calibration and validation resources while the latter can reduce domain dimension and mitigate computational burden (CHAMSEDDINE; REJNIAK, 2019). The integration of physics-based models with data-driven and optimization models can provide a novel systematic search for optimal treatment protocols while considering uncertainties.

7.2 Classical hybrid models: di usion and viscoelastic equations

In classical HCA models, one can consider several different applications or uses for the continuous equation(s). For instance, an ODE can be employed to represent cell density, where the variable represents the number of cells per unit volume in tumor microenvironment. Alternatively, it can be used to model the effects of chemokines on cancer cell behavior, such as the way cancer cells migrate and invade surrounding tissue. Other possible application approaches immune cell density, in which the variable represents the number of immune cells present in the tumor microenvironment. It can also be used to model the effects of the immune system on cancer growth, such as the way immune cells attack and kill cancer cells.

This section will approach two possible applications for continuous equations: (i) The attainability of nutrients (e.g., oxygen), where the variable represents their concentrations in the microenvironment, modeling the effects of their availability on cancer behavior, such as the way cancer cells adapt to hypoxic conditions; (ii) Tissue stiffness, where the variable represents mechanical properties of the tumor microenvironment and their effects on cancer cell behavior, such as how tumor cells can sense, respond, and adapt to tissue changes.

7.2.1 HCA model with a fractional diffusion equation for oxygen concentration

A HCA model for tumor growth that incorporates a continuous variable modeled by a diffusion equation is the hybrid lattice Boltzmann-cellular automaton model. This model combines a continuous-state lattice Boltzmann method (LBM) to simulate the flow of blood and oxygen through tumor microenvironment with a discrete-state cellular automaton to simulate the behavior of cancer cells (ALEMANI et al., 2012; MOHAMAD, 2019). It is important to note that not only mesoscopic LBM can be used, but also other macroscopic discretization methods, such as finite differences or finite volumes, or even purely analytical methods can be employed to describe the continuous part of the model.

In this application, oxygen concentration is a continuous variable governed by a transport equation, describing the way that the nutrient disseminates through the tissue in the tumor microenvironment. By neglecting sink (e.g., consumption) terms, the simplest diffusion equation is of the form

$$\frac{c}{t} = D \quad ^2 c, \tag{7.1}$$

where c is oxygen concentration, t is time, D is the diffusion coefficient, and $\quad ^2$ is the Laplacian operator. In the hybrid model, oxygen concentration can be used as an input to the cellular automaton studied in chapter 6, which can be adapted to simulate the behavior of cancer cells based on the local conditions given by $c(t)$ in Equation 7.1.

Every time the model evaluates their agent-based movement (what each cell can do, i.e., either divide, die, migrate, or remain quiescent), it will consider c value at that point in time and space. For instance, we can program the automaton to increase the likelihood of division and movement towards oxygen-abundant spaces and make the chance of apoptosis higher where the nutrient is deprived. The final action will depend both on chance and also on local oxygen concentration, causing the model to show both stochastic and deterministic characteristics.

Equation 7.1 can also be expanded to integrate a complete fluid system, simulating blood flow around the tumor along with nutrient diffusion. This expansion is particularly useful if the administration of chemotherapeutics and medicine targeted to kill cancer cells should be modeled in view of outcome prediction of different treatment strategies, while identifying potential targets for future cancer therapies. Additional expansions regard different transport geometries, particularly useful to model cancers occurring in specific tissues that can be approximated by a not-so-complex geometry (e.g., in-situ ductal carcinoma). Even though the possibilities are many for hybrid approach (already complex by definition), model complexity must be carefully considered.

In HCA models for tumor dynamics that incorporate diffusion phenomena, domain conditions for the equation can be divided into two main categories: initial and boundary conditions. The former specify system state at time $t = 0$. For example, the initial condition for the oxygen concentration in the tumor microenvironment might be a known value or

it could be derived from experimental measurements. Boundary conditions specify the specifications at the domain limit, such as at tumor surface or at the interface between tumor and surrounding tissue. Traditional boundary conditions (to be) used in HCA models invoking a diffusion equation are the following:

1. Neumann boundary conditions: These conditions specify the normal derivative of the concentration at the boundary. For example, a Neumann boundary condition might specify that the normal derivative of the oxygen concentration is zero at the surface of the tumor, indicating that no oxygen is flowing into or out of the tumor through the surface. It also refers to impermeable boundaries.

2. Dirichlet boundary conditions: These conditions specify the value of the concentration at the boundary. For example, a Dirichlet boundary condition might specify that the oxygen concentration is a known value at the surface of the tumor.

3. Robin boundary conditions: These conditions are a combination of Neumann and Dirichlet boundary conditions, and they specify both the normal derivative and the value of the concentration at the boundary. It also refers to mass/species transfer through convention.

It is important to note that the choice of boundary conditions will depend on the specific cancer being studied and cancer growth mechanisms being modeled. Hence, they should be specified in order to be consistent with specific characteristics or geometries of the tissue approached and will potentially need to be adjusted depending on the tumor location being modeled.

As an additional possibility to expand the capabilities of the diffusion model coupled to the HCA framework, we can employ a fractional order operator on the time-dependent derivative rewriting Eq. (7.1) as

$$\frac{^{\alpha}c}{t^{\alpha}} = D \quad ^{2}c, \tag{7.2}$$

where $0 < \alpha \leq 1$ is the arbitrary order of the model that admits a non-integer order and may change the model behavior through what is known as the memory effect. This additional resource appears because fractional operators are mathematically non-local, defined as a function in which the current state of the system depends on its past history. This is particularly useful to model the transport of dissolved substances in porous media, which is coherent to the context of oxygen diffusing through tissue (IYIOLA; ZAMAN, 2014).

Accordingly, there is considerable amount of research dedicated to exploring the fractional diffusion equation and its many variations (and, in some cases, its generalization to the fundamentally-different wave equation when $1 < \alpha \leq 2$) (WU et al., 2015; COSTA; CAPELAS DE OLIVEIRA, 2012; MAGIN et al., 2008; GORENFLO; MAINARDI, 2003). Besides the aforementioned memory effect, the main aspect researched is anomalous diffusion, in which the mean squared displacement of particles deviates from the linear relationship predicted by the classical diffusion equation. Once again, this effect is in-

teresting for modeling the transport of dissolved substances in porous media. Another important aspect of the generalized model is scale-invariance, which means that the same equation can describe the diffusion process at different length scales, enabling the model to deal with different magnitudes and tissue sizes (and in the context of the hybrid model, different grid sizes for the automaton domain).

One can note in Eq. (7.2) that the spatial derivative is unaltered from the classical diffusion equation – there are other versions in which this derivative is also generalized (VALENTIM, 2018). In addition, it is important to note that the choice of fractional order operator and the order parameter value will depend on the specific tumor / system characteristics. It is also important to use values based on models validated with experimental data, ensuring that the model is well-posed and the parameters are well-calibrated.

7.2.2 Hybrid models with fractional viscoelasticity equations

Even though tissue plasticity and mechanical properties have been studied as important characteristics in cancer progression (TALONI et al., 2015), an HCA model for tumor growth that incorporates a continuous variable modeled by tissue viscoelasticity is not a very common approach. Tissue viscoelasticity is a complex mechanical property that describes the way that tissue responds to applied loads, and it is not totally understood in the context of tumor growth (KUMAR; WEAVER, 2009).

However, some recent papers have proposed the use of HCA models to simulate the mechanical interactions between cancer cells and the surrounding tissue in order to understand the mechanisms of cancer cell migration and invasion. These models are based on the hypothesis that cancer cells can sense and respond to changes in tissue mechanical properties and this behavior is important for the progression of cancer (RICE; DEL RIO HERNANDEZ, 2020).

In the models, the continuous variable is modeled by a constitutive equation that describes the relationship between tissue stress and strain. The equation is based on the concept of viscoelasticity, which describes the way that the tissue behaves as a combination of elastic and viscous materials.

Analogous to the procedure described in the previous section, the discrete-state cellular automaton in chapter 6 is adapted to simulate the behavior of cancer cells and their actions based on the mechanical properties of the tissue and other variables in the model. In this framework, the viscoelasticity model can represent the capacity of a healthy tissue to physically push back the increase in tumor size, potentially hindering its growth, access to nutrients, and consequent general progression towards malignancy.

Viscoelasticity can be modeled using the generalized versions of Kelvin-Voigt or Maxwell model. One can obtain the canonical version of these fractional order models by replacing the integer order derivatives in their respective constitutive equations with fractional order derivatives, which in turn are defined using different fractional order

operators, such as the Riemann-Liouville, Caputo, and Riesz derivatives.

The generalized Kelvin-Voigt model is defined as

$$ (t) = GD^{\alpha} \ (t) + \quad D^{(1-\alpha)} \ (t), \tag{7.3} $$

where $\ (t)$ is the stress, $\ (t)$ is the strain, G is the elastic modulus, D^{α} is the fractional derivative of order α, $\quad$ is the viscosity coefficient, and α is a parameter that can be adjusted to control viscoelasticity degree. The generalized Maxwell model is defined as

$$ (t) = GD^{\alpha} \ (t) + \quad D^{(1-\alpha)} \frac{d \ (t)}{dt}, \tag{7.4} $$

where $\ (t)$ is the strain, G is the elastic modulus, D^{α} is the fractional derivative of order α, $\quad$ is the viscosity coefficient, and α is a parameter that can be adjusted to control viscoelasticity degree. It is important to note that although fractional viscoelasticity models have been increasingly used to characterize tissue materials (COUSSOT et al., 2009; MAGIN et al., 2008) and generally study biological tissue dynamics (MERAL; ROYSTON; MAGIN, 2010; MAGIN, 2010; MAGIN, 2012; GONZALEZ-RODRIGUEZ et al., 2012; MAINARDI, 2012; QIU et al., 2018; CARMICHAEL et al., 2015; JAMALI; AZIMI; MOFRAD, 2010); these are relatively new models and their behavior can be hard to predict. Therefore, the development of fractional order viscoelastic models is an active area of research in mechanics and material science.

7.2.3 Limitations and implementation di culties

Although fractional models can extend model capabilities, this flexibility does not come without some drawbacks. Fractional order models can be more complex than integer order models, and their behavior can be difficult to predict. This can make it challenging to interpret the results from models and to use them to make predictions. In addition, these models can be difficult to solve numerically, making it challenging to obtain accurate numerical solutions (DIETHELM; GARRAPPA; STYNES, 2020).

In terms of parameter identification, some fractional order models may not preserve system initial and boundary conditions, which can make it difficult to apply them to certain types of initial and boundary value problem as well as to identify and estimate model parameters from experimental data. In addition, there is a broad debate on physical interpretations of a fractional derivative and its lack of intuitive meaning, with multiple interpretations depending on author and application context, adding an extra layer of complexity in relating them to physical systems (SABATIER; FARGES; TARTAGLIONE, 2022).

Despite these limitations, fractional order models have been successfully applied in a wide range of fields such as physics, engineering, chemistry, and biology, while showing to be useful in modeling complex systems. However, it is important to be aware of these limitations and to consider if the increased potential entailed by fractional calculus compensates its implementation into an already complex framework such as HCA model.

7.3 A step beyond: combining large data pools and machine learning algorithms

In recent years, the field of hybrid models in mathematical oncology have expanded to include the combination of phenomenological frameworks (such as physics-based equations or cellular automata) with machine learning and data-oriented algorithms, combining the strengths of both categories. Also known as multi-physics modeling, one example of this approach is to use deep learning algorithms to extract features from medical images, such as CT scans and MRI images, and then use these features to fine-tune input parameters to a continuous physical model, such as the aforementioned diffusion equation to simulate the transport of nutrients.

Another example is to use computer-vision algorithms to predict the most appropriate treatment for a patient with cancer and then use continuous physical models to simulate tumor response to treatment. Additionally, it is also possible to use deep learning algorithms to learn the relationship between continuous physical equations and cancer growth, then use this learned relationship to make predictions of different growth scenarios and treatment response. It is important to note that this approach requires a large amount of data and computational resources, being relatively new and active area of research. However, there are major developments and breakthroughs in the area occurring at a remarkable pace (DJURIC et al., 2017; BEJNORDI et al., 2017; YALA et al., 2019; ARDILA et al., 2019).

The lack of quality datasets undergoes slow mitigation by the development of public medical images collections, enabled mainly by universities and medical research centers (KHOURY; IOANNIDIS, 2014; MEYER et al., 2014). The Cancer Imaging Archive (TCIA) repository is probably the most relevant example of joint effort in this aspect, with several terabytes of content made public, duly categorized and identified (CLARK et al., 2013). Therefore, the latent need of developing tools that can harness such information has propelled the scientific community to explore data science (HEY, 2009), recovering and perfecting concepts long ago left aside (FRADKOV, 2020) and profoundly impacting all fields of research, particularly in health (ELAZIZ et al., 2020; WU et al., 2021; ZHENG et al., 2020; CRAIK; HE; CONTRERAS-VIDAL, 2019) and clinical oncology (DE ANDA-JÁUREGUI; HERNÁNDEZ-LEMUS, 2020; HUYNH et al., 2020).

Accordingly, in recent years researchers have proposed supervised machine learning, especially deep learning algorithms, as tools capable of utilizing the increasing computational power available to extract previously inaccessible information from oncologic diagnostic images (BEJNORDI et al., 2017), promising to revolutionize various segments within personalized medicine (DJURIC et al., 2017) and changing the clinical scenario (ARDILA et al., 2019). Specifically with regard to breast cancer, recent studies demonstrate that such algorithms can assist imaging diagnoses, mainly in screening benign cases (patient dispensing) and possibly malignant cases (for subsequent manual confirmation by radiologists) (YALA et al., 2019; YI et al., 2021). Moreover, approaches in this sense seem

to point a direction to the elaboration of low-cost strategies for real-time implementation of decision-making clinical support systems (GANGGAYAH et al., 2019).

In the specific context of a prospective HCA model entailing data-based tools, there seems to exist at least two specific databases in TCIA capable of feeding the proposed model, depending on the desired image exam type. The first option is the Breast Cancer Screening – Digital Breast Tomosynthesis (BSC-DBT) database provided by Duke University (BUDA et al., 2020), with images from 5060 patients and clinical support data (BUDA et al., 2021). The second is the Curated Breast Imaging Subset – Digital Database for Screening Mammography (CBIS-DDSM), provided by Stanford University (SAWYER-LEE et al., 2016), including 1566 patients (LEE et al., 2017). A priori, the first option should probably be preferred because tomosynthesis exams have an extra dimension of information and greater detection capacity compared to traditional digital mammograms. Data from TCIA is already organized and treated, which reduces the need for in-depth data conditioning. Nevertheless, activities such as contrast improvement and segmentation may be necessary. Equally important, the images have already been labeled by professionals, which is essential for training a machine learning model.

Figure 39 outlines a concept framework for creating a modern hybrid model (or multi-physics hybrid model) employing several concepts studied in this thesis, such as multiscale modeling, cellular automata and fractional calculus, along with data-oriented approaches, such as machine learning. The framework depicts the proposal of a model that leverages terabytes of labeled diagnostic cancer images (in this case, breast cancers such as invasive ductal carcinoma or ductal carcinoma in situ) to enable a two-fold contribution: it guides parameter fine-tuning in the multiscale modeling represented by differential equation models and the cellular automata while still being used as a validation baseline for the accuracy of the final model. Results achieved by the framework can be potentially approached both in an exploratory way (elucidating mechanisms, exploring the emergence factors and creating surrogate models) and as a tool to guide and improve decision-making in detection processes (as an enhanced binary classifier in screening trials).

Good practices for data-based computer science algorithms (GÉRON, 2019) enable the aforementioned two-fold data use, where input data is randomly divided into two non-intersecting groups: the training set, composed of 80 to 85% of the input data, and the test set, composed of the remaining 15 to 20% of the data. This compartmentalization is essential for future evaluation of the developed classifier model and, as the name suggests, the two data sets should be used at different stages of the project. Then, the process known as feature extraction takes place, in which significant attribute calculations for the application (such as size, shape, and texture of masses) are derived from the segmented objects in the images. It is important that the features represent tissue attributes and are stable (i.e., insensitive to spatial translations and rotations) (RANGAYYAN et al., 2010), as they are relevant to guide multiscale models. In the literature, there is a collection of

approaches that propose algorithms for feature extraction, whether designed or automatic, each with different success rates depending on the application (XIE et al., 2020). Extracted features are essential in the suggested framework, as they serve as guiding parameters and one of the bridges between machine learning and multiscale models.

Figure 39 – Concept scheme for a complex multi-physics hybrid model.

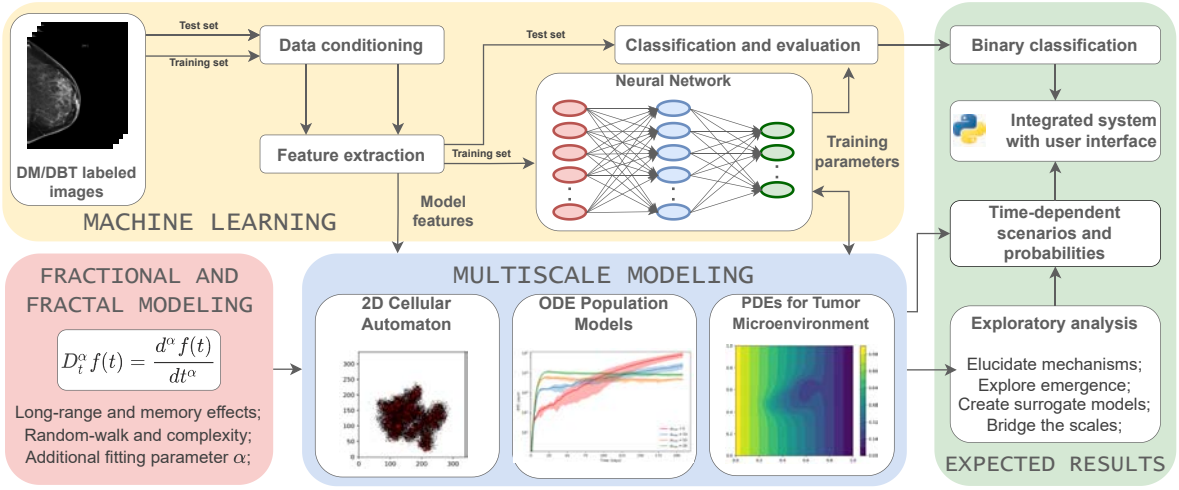

Source: Own authorship.

A deep learning algorithm is the core of the machine learning portion of the framework, where it powers a classifier model that should be able to assess the data as possibly benign or malignant scenarios. Although other machine learning algorithms have been used in the literature to address oncological phenomena, deep learning has been shown to be superior in classifying and organizing data from diagnostic and health-related images (BUDA et al., 2021; DJURIC et al., 2017; YALA et al., 2019; YI et al., 2021; GANGGAYAH et al., 2019; ASRI et al., 2016). These algorithms can vary widely in their characteristics, which involve combinations and depth of neural networks, activation functions, and optimization methods. In fact, fractional calculus has recently been envisioned as a tool in the intrinsic implementation of machine learning algorithms (NIU; CHEN; WEST, 2021).

The implementation of the deep learning model can use the powerful apparatus of TensorFlow 2 (DEVELOPERS, 2021), a wide and robust open source end-to-end platform created by Google, and the high-level Keras API in Python (CHOLLET; SAFARI, 2021). These tools are frequently used in cutting-edge applications, including academic research in various fields, and constitute a broad and flexible ecosystem compatible with the framework devised here (PANG; NIJKAMP; WU, 2020). Although TensorFlow already offers a high number of powerful tools for building and implementing machine learning models, there is also the possibility of modifying and shaping the architecture of its code, if prospectively needed throughout the project. It should be noted that training a deep

learning model requires a high computational power due to the high number of data in source images (in digital mammography and even more in digital breast tomosynthesis). The implementation infrastructure through TensorFlow is facilitated by the optimized use of such computational package and the ability to utilize graphical processing units to handle the millions of algebraic operations required during model training.

The next step after training the model is the evaluation stage, in which adjusted parameters of the model will be used to classify unseen images in the process (those from the test set). The evaluation metrics of the developed classifier should take into account parameters involving the sensitivity and false positive / negative rates of the model, depending on the desired end use. Tools and standards such as BIRADS (Breast Imaging Reporting and Data System) and ROC (Receiver Operating Characteristic) curves can also be incorporated. The classifier should be optimized until its results over the test set are satisfactory (for example, until the model reaches a certain limit of false negatives or a desired point on ROC curve).

After a satisfactory development of the classifier, parameters trained by the deep learning model and identified features are fed to multi-scale models of the framework. It is important to emphasize that more than one model can be used and they function complementarily to each other, in order to leverage and explore information from provided data. Ordinary differential equations (ODEs) of non-integer order can be used to provide an overview of how a particular tumor growth frame can progress over time.

The literature shows that there are several models like these (BENZEKRY et al., 2014), including those that can be used as assistants in medical clinics, and fractional calculus can be used as an additional tool to calibrate such models and explore the so-called memory effects in the tumor (VALENTIM et al., 2020). Some studies explore the relationship between fractional order α and the memory of a particular system (DU; WANG; HU, 2013). In this sense, as investigated in (VALENTIM et al., 2021), non-integer order models can offer ways to explore multi-step models that evoke emerging features of tumors, such as those related to cancer hallmarks (HANAHAN; WEINBERG, 2000; HANAHAN; WEINBERG, 2011).

Furthermore, the multiscale portion of the suggested framework is centered around a cellular automaton, like the one discussed in chapter 6 (VALENTIM; RABI; DAVID, 2023), which tracks entirely individual elements evolving in time and space, therefore capable of reflecting heterogeneity and complexity of tumor growth (DEUTSCH et al., 2021). Although it functions as an in silico virtualization model, such CA model does not have specific characteristics that allow it to virtualize a breast cancer, or clinical data to support its dimensions, shapes, and growth rate. This is where value parameters and features generated by the machine learning model in the framework can be incorporated, adjusting the parameters of the CA model and making it much more specific to the targeted cancer application.

In addition, in the multiscale context, there is the possibility of coupling PDEs, such as the reaction-diffusion equation discussed in section 7.2.1, or the viscoelasticity ODEs in section 7.2.2. By functioning as microenvironmental devices, they could extend the simulation scale and be employed, for instance, to determine whether a tumor virtualized by the automaton could cross the basal membrane, which is crucial to transform from *in situ* carcinoma to invasive ductal carcinoma.

7.4 Final remarks: An interdisciplinary research for transdisciplinary teams

This chapter introduced and explored the composition of different types of hybrid models, both traditional and innovative, by combining concepts introduced in previous chapters while reflecting on approaches in the literature. A potential framework for a complex hybrid model was also outlined.

The hybrid models (described in this chapter) figure as an absolute representation of cancer modeling as an interdisciplinary research subject. They involve biological interpretation in multiple scales, from molecular and cellular level to the tissue and organ level, requiring the integration of different concepts to provide a more complete understanding of the disease. They demand large amounts of data and computational power in order to harness the information in data from different sources such as clinical assets and diagnostic images. They also depend upon a reasonable level of mathematics and physics knowledge, particularly if advanced tools such as fractional calculus are employed.

Hence, hybrid models are perfect examples of how mathematical oncology claims for the collaboration from different disciplines (and researchers) to effectively employ and combine resources and methods into novel frameworks, concepts and treatment strategies. Moreover, multidisciplinary teams can be more capable of coordinating interdisciplinary and transdisciplinary concepts, thus transforming fundamental research findings into clinical applications and narrowing the distance between blackboard research and breakthrough clinical application.

8 CONCLUSION, CONTRIBUTIONS AND FUTURE WORK

This doctorate thesis addresses Mathematical Oncology as a multi-faceted and complex subject, which it is indeed. By all means, the conducted study did not intend to be a thorough analysis of the subject (a widely comprehensive one) but a viewpoint that highlights its interdisciplinary aspects, particularly focusing on fractional calculus applications, phenomenological approaches and hybrid models. It is expected that this work contributes to Mathematical Oncology at least in three distinct ways.

Firstly, it reviews and highlights fractional calculus as an important tool in cancer modeling by publishing the first review paper in the area, coining the term Fractional Mathematical Oncology and underlying the mathematical tool as a powerful and strategic approach in view of prospective challenges and opportunities in tumor dynamics modeling. This work also discusses several particularities of fractional-order models to describe tumor dynamics, assessing their prediction and description capabilities in light of the memory effect phenomenon. Moreover, this thesis proposes a novel variable-order model to describe multi-step tumor growth and shows how a simple periodic function can fit it to extant clinical data seamlessly, thus encouraging and opening results for further discussion on how flexible variable orders may favor the adoption of fractional ordinary differential equations to describe tumor growth

Secondly, this work develops and makes available an open-source code (based on an existing approach in the literature) that models an agent-based stochastic cellular automaton capable of simulating several different scenarios regarding tumor growth such as dormancy periods, instability caused by cell-death/competition and invasion. By effectively capturing the emergency and complexity inherent to oncological phenomena, aforementioned approach figures as an interesting tool for in silico modeling, with promising capabilities and possibilities to support further research in mathematical oncology.

Thirdly, this work contextualizes and summarizes concepts approached across its chapters into hybrid models, which can be interpreted as absolute representations of cancer modeling as an interdisciplinary research subject. The thesis outlines and paves the way to the development of a complex multi-physics framework that encompass deterministic, stochastic, phenomenological, and data-driven characteristics, effectively coordinating approaches of different areas into a combined effort in fundamental and translational research.

Finally, even though Mathematical Oncology often entails the use of complex tools to analyze complex phenomena, respected researchers such as Byrne (2010) and West (2022) seem to suggest that the best approach might actually be a holistic balance achieved only when simple and reducionist concepts of several different areas are coordinated together. In this context, a natural path of evolution for the research conducted in this doctorate

is to expand it in collaboration with multidisciplinary teams capable of translating its fundamental research aspects into clinical applications, thus helping to elevate what is now research at a blackboard stage into devices either to aid decision making in oncology or to increase understanding on the progression of specific cancers.

REFERENCES

ABERNATHY, K. et al. Global Dynamics of a Breast Cancer Competition Model. **Differential Equations and Dynamical Systems**, Springer India, 2017. ISSN 1259101703.

ADAM, J. A.; MAGGELAKIS, S. Diffusion Regulated Growth Characteristics of a Spherical Prevascular Carcinoma. **Bulletin of mathematical biology**, v. 52, n. 4, p. 549–582, 1990.

AGRAWAL, O. P. Solution for a fractional diffusion-wave equation defined in a bounded domain. **Nonlinear Dynamics**, v. 29, n. 1-4, p. 145–155, 2002.

ALEMANI, D. et al. Combining cellular automata and lattice Boltzmann method to model multiscale avascular tumor growth coupled with nutrient diffusion and immune competition. **Journal of Immunological Methods**, Elsevier B.V., v. 376, n. 1-2, p. 55–68, 2012.

ALMEIDA, R.; TAVARES, D.; TORRES, D. F. M. **The Variable-Order Fractional Calculus of Variations**. [S.l.: s.n.], 2018. ISBN 978-3-319-94005-2.

AMBROSI, D. et al. Solid Tumors Are Poroelastic Solids with a Chemo-mechanical Feedback on Growth. **Journal of Elasticity**, Springer Science+Business Media Dordrecht, v. 129, n. 1-2, p. 107–124, 2017.

ANDERSON, A. R. et al. Modelling of cancer growth, evolution and invasion: Bridging scales and models. **Mathematical Modelling of Natural Phenomena**, v. 2, n. 3, p. 1–29, 2007.

ANDERSON, A. R. A.; CHAPLAIN, M. A.; REJNIAK, K. A. **Single-Cell-Based Models in Biology and Medicine**. First. Basel, Switzerland: Birkhäuser, 2007. 400 p. ISBN 978-3-7643-8123-3.

ANDERSON, A. R. A.; QUARANTA, V. Integrative mathematical oncology. **Nature Reviews Cancer**, v. 8, n. 3, p. 227–234, mar. 2008. ISSN 1474-1768 (Electronic)\r1474-175X (Linking).

ARDILA, D. et al. End-to-end lung cancer screening with three-dimensional deep learning on low-dose chest computed tomography. **Nature Medicine**, v. 25, n. 6, p. 954–961, jun. 2019. ISSN 1078-8956, 1546-170X.

AREA, I.; LOSADA, J.; NIETO, J. J. A note on the fractional logistic equation. **Physica A: Statistical Mechanics and its Applications**, Elsevier B.V., v. 444, p. 182–187, 2016.

ASRI, H. et al. Using Machine Learning Algorithms for Breast Cancer Risk Prediction and Diagnosis. **Procedia Computer Science**, v. 83, p. 1064–1069, 2016. ISSN 18770509.

ATICI, F. M. et al. Modeling Tumor Volume with Basic Functions of Fractional Calculus. **Progress in Fractional Differentiation and Applications**, v. 1, n. 4, p. 229–241, 2015.

BALEANU, D.; AGARWAL, R. P. Fractional calculus in the sky. **Advances in Difference Equations**, v. 2021, n. 1, p. 117, dez. 2021. ISSN 1687-1847.

BARRETO, J. O. M. et al. Translational research in public health: Challenges of an evolving field. **Saúde em Debate**, v. 43, n. spe2, p. 4–9, 2019.

BEJNORDI, B. E. et al. Diagnostic Assessment of Deep Learning Algorithms for Detection of Lymph Node Metastases in Women With Breast Cancer. **JAMA**, v. 318, n. 22, p. 2199, dez. 2017. ISSN 0098-7484.

BENZEKRY, S. et al. Classical Mathematical Models for Description and Prediction of Experimental Tumor Growth. **PLoS Computational Biology**, v. 10, n. 8, 2014.

BOLTON, L. et al. A proposed fractional-order Gompertz model and its application to tumour growth data. **Mathematical Medicine and Biology**, v. 32, n. 2, p. 187–207, 2015.

BOVERI, T. Multistage Carcinogenesis Models. **Cell Cycle**, p. 1–10, 2014.

BUDA, M. et al. **Breast Cancer Screening – Digital Breast Tomosynthesis (BCS-DBT)**. [S.l.]: The Cancer Imaging Archive, 2020.

BUDA, M. et al. A Data Set and Deep Learning Algorithm for the Detection of Masses and Architectural Distortions in Digital Breast Tomosynthesis Images. **JAMA Network Open**, v. 4, n. 8, p. e2119100, ago. 2021. ISSN 2574-3805.

BYRNE, H.; PREZIOSI, L. Modelling solid tumour growth using the theory of mixtures. **Mathematical Medicine and Biology**, v. 20, n. 4, p. 341–366, dez. 2003.

BYRNE, H. M. Dissecting cancer through mathematics: From the cell to the animal model. **Nature Reviews Cancer**, Nature Publishing Group, v. 10, n. 3, p. 221–230, 2010.

CAMARGO, R. d. F. **Cálculo Fracionário e Aplicações**. 2009. 135 p. Tese (Doutorado), 2009.

CAPELAS DE OLIVEIRA, E.; TENREIRO MACHADO, J. A. A review of definitions for fractional derivatives and integral. **Mathematical Problems in Engineering**, v. 2014, n. 1940, 2014.

CAPUTO, M. Linear Model of Dissipation whose Q is almost Frequency Independent–II. **Geophysical Journal International**, v. 13, n. 5, p. 529–539, nov. 1967.

CARMICHAEL, B. et al. The fractional viscoelastic response of human breast tissue cells. **Physical Biology**, IOP Publishing, v. 12, n. 4, 2015.

CATANIA, G.; SORRENTINO, S.; FASANA, A. A Condensation Technique for Finite Element Dynamic Analysis Using Fractional Derivative Viscoelastic Models. **Journal of Vibration and Control**, v. 14, n. 9-10, p. 1573–1586, 2008.

CAVALCANTE, G. C. et al. Development of radiofrequency ablation device for surgical hepatocellular carcinoma treatment in agreement with Brazilian standards. **Research on Biomedical Engineering**, v. 34, n. 2, p. 115–126, maio 2018. ISSN 2446-4740, 2446-4732.

CHAKRABORTY, S.; DEBBOUCHE, A.; ANTONOV, V. The role of diagnosis at early stages to control cervical cancer: A mathematical prediction. **European Physical Journal Plus**, Springer Berlin Heidelberg, v. 135, n. 10, p. 1–12, 2020.

CHAMSEDDINE, I. M.; REJNIAK, K. A. Hybrid modeling frameworks of tumor development and treatment. **Wiley Interdisciplinary Reviews: Systems Biology and Medicine**, n. June 2019, p. 1–16, 2019.

CHAUVIERE, A. H. et al. Mathematical oncology: How are the mathematical and physical sciences contributing to the war on breast cancer? **Current Breast Cancer Reports**, v. 2, n. 3, p. 121–129, 2010. ISSN 1943-4596 (Electronic)\n1943-4588 (Linking).

CHOLLET, F.; SAFARI, a. O. M. C. **Deep Learning with Python, Second Edition**. [S.l.: s.n.], 2021. ISBN 978-1-61729-686-4.

CLARK, K. et al. The Cancer Imaging Archive (TCIA): Maintaining and Operating a Public Information Repository. **Journal of Digital Imaging**, v. 26, n. 6, p. 1045–1057, dez. 2013. ISSN 0897-1889, 1618-727X.

COSTA, F. S.; CAPELAS DE OLIVEIRA, E. Fractional wave-diffusion equation with periodic conditions. **Journal of Mathematical Physics**, v. 53, n. 123520, p. 1–9, 2012. ISSN doi:10.1063/1.4769270.

COUSSOT, C. et al. Fractional derivative models for ultrasonic characterization of polymer and breast tissue viscoelasticity. **IEEE Transactions on Ultrasonics, Ferroelectrics, and Frequency Control**, IEEE, v. 56, n. 4, p. 715–725, 2009.

CRAIEM, D.; ARMENTANO, R. L. A fractional derivative model to describe arterial viscoelasticity. **Biorheology**, v. 44, n. 4, p. 251–63, 2007.

CRAIK, A.; HE, Y.; CONTRERAS-VIDAL, J. L. Deep learning for electroencephalogram (EEG) classification tasks: A review. **Journal of Neural Engineering**, v. 16, n. 3, p. 031001, jun. 2019. ISSN 1741-2560, 1741-2552.

CRISTINI, V.; KOAY, E. J.; WANG, Z. **An Introduction to Physical Oncology : How Mechanistic Mathematical Modeling Can Improve Cancer Therapy Outcomes**. First. Boca Raton, FL: CRC Press, 2017. 563 p. ISBN 978-1-4665-5136-7.

CROOKS, A. T.; HEPPENSTALL, A. J. Introduction to Agent-Based Modelling. In: HEPPENSTALL, A. J. et al. (Ed.). **Agent-Based Models of Geographical Systems**. Dordrecht: Springer Netherlands, 2012. p. 85–105. ISBN 978-90-481-8926-7 978-90-481-8927-4.

DAI, F.; LIU, B. Optimal control and pattern formation for a haptotaxis model of solid tumor invasion. **Journal of the Franklin Institute**, Elsevier Ltd, v. 356, n. 16, p. 9364–9406, 2019.

DAVID, S. et al. Fractional and fractal processes applied to cryptocurrencies price series. **Journal of Advanced Research**, jan. 2021.

DAVID, S. et al. A combined measure to differentiate EEG signals using fractal dimension and MFDFA-Hurst. **Communications in Nonlinear Science and Numerical Simulation**, v. 84, 2020.

DAVID, S.; VALENTIM, C. A. Fractional Euler-Lagrange Equations Applied to Oscillatory Systems. **Mathematics**, v. 3, n. 2, p. 258–272, 2015.

DAVID, S. A. et al. Fractional PID controller in an active image stabilization system for mitigating vibration effects in agricultural tractors. **Computers and Electronics in Agriculture**, v. 131, p. 1–9, dez. 2016.

DAVID, S. A.; KATAYAMA, A. Fractional Order for Food Gums: Modeling and Simulation. **Applied Mathematics**, Scientific Research Publishing, v. 04, n. 02, p. 305–309, 2013. ISSN doi:10.4236/am.2013.42046.

DAVID, S. A.; LINARES, J. L.; PALLONE, E. Fractional order calculus: Historical apologia, basic concepts and some applications. **Revista Brasileira de Ensino de Física**, v. 33, n. 4, p. 4302–4302, 2011.

DAVID, S. A. et al. A combined measure to differentiate EEG signals using fractal dimension and MFDFA-Hurst. **Communications in Nonlinear Science and Numerical Simulation**, v. 84, 2020.

DAVID, S. A. et al. Partial chaos suppression in a fractional order macroeconomic model. **Mathematics and Computers in Simulation**, Elsevier B.V., v. 122, p. 55–68, 2016. ISSN 0378-4754.

DAVID, S. A.; RABI, J. A. Can Fractional Calculus be Applied to Relativity? **Axiomathes**, Springer Netherlands, v. 30, n. 2, p. 165–176, abr. 2020. ISSN 0123456789.

DAVID, S. A.; VALENTIM, C. A.; DEBBOUCHE, A. Fractional Modeling Applied to the Dynamics of the Action Potential in Cardiac Tissue. **Fractal and Fractional**, v. 6, n. 3, p. 149, mar. 2022. ISSN 2504-3110.

DE ANDA-JÁUREGUI, G.; HERNÁNDEZ-LEMUS, E. Computational Oncology in the Multi-Omics Era: State of the Art. **Frontiers in Oncology**, v. 10, p. 423, abr. 2020. ISSN 2234-943X.

DEBBOUCHE, A. et al. On the stability of stationary solutions in diffusion models of oncological processes. **The European Physical Journal Plus**, Springer Berlin Heidelberg, v. 136, n. 1, p. 131–131, jan. 2021. ISSN 0123456789.

DEUTSCH, A.; DORMANN, S. Mathematical Modeling of Biological Pattern Formation. In: **Cellular Automaton Modeling of Biological Pattern Formation**. Boston, MA: Birkhäuser Boston, 2005. p. 45–56. ISBN 978-0-8176-4281-5 978-0-8176-4415-4.

DEUTSCH, A. et al. BIO-LGCA: A cellular automaton modelling class for analysing collective cell migration. **PLOS Computational Biology**, v. 17, n. 6, p. e1009066, jun. 2021. ISSN 1553-7358.

DEVELOPERS, T. **TensorFlow**. 2021. Zenodo.

DIETHELM, K.; FORD, N. J.; FREED, A. D. A Predictor-Corrector Approach for the Numerical. **Nonlinear Dynamics**, v. 29, n. 1, p. 3–22, 2002.

DIETHELM, K. et al. Algorithms for the fractional calculus: A selection of numerical methods. **Computer Methods in Applied Mechanics and Engineering**, v. 194, n. 6-8, p. 743–773, 2005.

DIETHELM, K.; GARRAPPA, R.; STYNES, M. Good (and Not So Good) practices in computational methods for fractional calculus. **Mathematics**, v. 8, n. 3, 2020.

DJURIC, U. et al. Precision histology: How deep learning is poised to revitalize histomorphology for personalized cancer care. **npj Precision Oncology**, v. 1, n. 1, p. 22, dez. 2017. ISSN 2397-768X.

DOLFIN, M.; LACHOWICZ, M.; SZYMA SKA, Z. A General Framework for Multiscale Modeling of Tumor–Immune System Interactions. In: **Mathematical Oncology 2013**. [S.l.: s.n.], 2014. p. 151–180.

DOMINGUES, J. C. SF Lacroix, Traité du calcul différentiel et du calcul intégral, (1797–1800). In: **Landmark Writings in Western Mathematics 1640-1940**. [S.l.: s.n.], 2005. p. 277–291.

D'ONOFRIO, A.; GANDOLFI, A. **Mathematical Oncology 2013**. First. New York, NY: Springer New York, 2014. 336 p. (Modeling and Simulation in Science, Engineering and Technology). ISBN 978-1-4939-0457-0.

DOROSHOW, J. H.; KUMMAR, S. Translational research in oncology - 10 years of progress and future prospects. **Nature Reviews Clinical Oncology**, Nature Publishing Group, v. 11, n. 11, p. 649–662, 2014.

D'OVIDIO, M.; LORETI, P. Solutions of fractional logistic equations by Euler's numbers. **Physica A: Statistical Mechanics and its Applications**, Elsevier B.V., v. 506, p. 1081–1092, 2018.

DU, M.; WANG, Z.; HU, H. Measuring memory with the order of fractional derivative. **Scientific Reports**, v. 3, n. 1, p. 1–3, 2013.

EASTON, D. F. et al. Gene-Panel Sequencing and the Prediction of Breast-Cancer Risk. **New England Journal of Medicine**, Massachusetts Medical Society, v. 372, n. 23, p. 2243–2257, jun. 2015.

ELADDADI, A.; KIM, P.; MALLET, D. **Mathematical Models of Tumor-Immune System Dynamics**. New York, NY: Springer New York, 2014. v. 107. 282 p. (Springer Proceedings in Mathematics & Statistics, v. 107). ISBN 978-1-4939-1793-8.

ELAZIZ, M. A. et al. New machine learning method for image-based diagnosis of COVID-19. **PLOS ONE**, v. 15, n. 6, p. e0235187, jun. 2020. ISSN 1932-6203.

ENDERLING, H. et al. Integrating Mathematical Modeling into the Roadmap for Personalized Adaptive Radiation Therapy. **Trends in Cancer**, Elsevier Inc., v. 5, n. 8, p. 467–474, 2019.

ENDERLING, H. et al. Paradoxical dependencies of tumor dormancy and progression on basic cell kinetics. **Cancer Research**, v. 69, n. 22, p. 8814–8821, 2009.

FARAYOLA, M. F. et al. Mathematical modeling of radiotherapy cancer treatment using Caputo fractional derivative. **Computer Methods and Programs in Biomedicine**, Elsevier B.V., v. 188, p. 105306–105306, 2020.

FASANO, A. et al. Conservation Laws in Cancer Modeling. In: D'ONOFRIO, A.; GANDOLFI, A. (Ed.). **Mathematical Oncology 2013**. First. New York, NY: Springer New York, 2014. p. 27–61. ISBN 978-1-4939-0457-0.

FLEURY ROSA, S. d. S. R.; ISHIHARA, J. Y.; GAIDOS ROSERO, O. F. Embedded System for Lighting Control of LED Light Source Applied to Therapy of Radiofrequency Ablation in Hepatocellular Carcinoma. **IEEE Latin America Transactions**, v. 17, n. 10, p. 1671–1677, out. 2019. ISSN 1548-0992.

FOLLAND, G. B. **Advanced Calculus**. [S.l.]: Pearson Education India, 2002. 473 p. ISBN 978-0-02-421411-9.

FRADKOV, A. L. Early History of Machine Learning. **IFAC-PapersOnLine**, v. 53, n. 2, p. 1385–1390, 2020. ISSN 24058963.

FRIEDMAN, N. et al. Using Bayesian Networks to Analyze Expression Data. **Journal of Computational Biology**, v. 7, n. 3-4, p. 601–620, ago. 2000. ISSN 1066-5277, 1557-8666.

FRITSCH, A. et al. Are biomechanical changes necessary for tumour progression? **Nature Physics**, Nature Publishing Group, v. 6, n. 10, p. 730–732, 2010.

FRUNZO, L. et al. Modeling biological systems with an improved fractional Gompertz law. **Communications in Nonlinear Science and Numerical Simulation**, Elsevier B.V., v. 74, p. 260–267, 2019.

GANGGAYAH, M. D. et al. Predicting factors for survival of breast cancer patients using machine learning techniques. **BMC Medical Informatics and Decision Making**, v. 19, n. 1, p. 48, dez. 2019. ISSN 1472-6947.

GATENBY, R. A.; MAINI, P. K. Mathematical oncology: Cancer summed up. **Nature**, v. 421, n. 6921, p. 321–321, 2003. ISSN 0028-0836 (Print)\r0028-0836 (Linking).

GÉRON, A. **Hands-on Machine Learning with Scikit-Learn, Keras, and TensorFlow: Concepts, Tools, and Techniques to Build Intelligent Systems**. Second edition. Beijing [China] ; Sebastopol, CA: O'Reilly Media, Inc, 2019. ISBN 978-1-4920-3264-9.

GHITA, M.; COPOT, D.; IONESCU, C. M. Lung cancer dynamics using fractional order impedance modeling on a mimicked lung tumor setup. **Journal of Advanced Research**, v. 32, p. 61–71, set. 2021. ISSN 20901232.

GOLUB, T. R. et al. Molecular Classification of Cancer: Class Discovery and Class Prediction by Gene Expression Monitoring. **Science**, v. 286, n. 5439, p. 531–537, out. 1999.

GONZALEZ-RODRIGUEZ, D. et al. Soft Matter Models of Developing Tissues and Tumors. **Science**, American Association for the Advancement of Science, v. 338, n. 6109, p. 910–917, nov. 2012.

GORENFLO, R. et al. **Mittag-Leffler Functions, Related Topics and Applications**. First. Berlin: Springer-Verlag, 2014. 443 p. ISBN 978-3-662-43930-2.

GORENFLO, R.; MAINARDI, F. Fractional diffusion Processes: Probability Distributions and Continuous Time Random Walk. In: RANGARAJAN, G.; DING, M. (Ed.). **Processes with Long-Range Correlations. Lecture Notes in Physics, Vol 621**. Berlin: Springer, 2003. p. 148–166. ISBN 978-3-540-44832-7.

GUIOT, C. et al. Does tumor growth follow a universal law ? **Journal of Theoretical Biology**, Academic Press, v. 225, n. 2, p. 147–151, nov. 2003.

HAMIS, S.; POWATHIL, G. G.; CHAPLAIN, M. A. Blackboard to Bedside: A Mathematical Modeling Bottom-Up Approach Toward Personalized Cancer Treatments. **JCO Clinical Cancer Informatics**, n. 3, p. 1–11, 2019.

HANAHAN, D.; WEINBERG, R. A. The Hallmarks of Cancer. **Cell**, v. 100, n. 1, p. 57–70, jan. 2000.

HANAHAN, D.; WEINBERG, R. A. Hallmarks of cancer: The next generation. **Cell**, Elsevier Inc., v. 144, n. 5, p. 646–674, 2011.

HARTUNG, N. et al. Mathematical modeling of tumor growth and metastatic spreading: Validation in tumor-bearing mice. **Cancer Research**, v. 74, n. 22, p. 6397–6407, 2014.

HASSANI, H.; TENREIRO MACHADO, J.; MEHRABI, S. An optimization technique for solving a class of nonlinear fractional optimal control problems: Application in cancer treatment. **Applied Mathematical Modelling**, v. 93, p. 868–884, maio 2021. ISSN 0307904X.

HASSANI, H. et al. Optimal solution of the fractional order breast cancer competition model. **Scientific Reports**, v. 11, n. 1, p. 15622, ago. 2021. ISSN 2045-2322.

HERNANDEZ, E.; O'REGAN, D.; BALACHANDRAN, K. On recent developments in the theory of abstract differential equations with fractional derivatives. **Nonlinear Analysis, Theory, Methods and Applications**, Elsevier Ltd, v. 73, n. 10, p. 3462–3471, 2010.

HERRMANN, R. **Fractional Calculus: An Introduction for Physicists**. Second. Singapore: World Scientific, 2014. 500 p. ISBN 978-981-4551-09-0.

HEY, A. J. G. (Ed.). **The Fourth Paradigm: Data-Intensive Scientific Discovery**. Redmond, Washington: Microsoft Research, 2009. ISBN 978-0-9825442-0-4.

HORMUTH, D. A. et al. Math, magnets, and medicine: Enabling personalized oncology. **Expert Review of Precision Medicine and Drug Development**, Taylor & Francis, v. 00, n. 00, p. 1–3, jan. 2021.

HORMUTH, D. A. et al. Biologically-Based Mathematical Modeling of Tumor Vasculature and Angiogenesis via Time-Resolved Imaging Data. **Cancers**, v. 13, n. 12, p. 3008, jun. 2021. ISSN 2072-6694.

HU, R.; RUAN, X. A simple cellular automaton model for tumor-immunity system. In: **International Conference on Robotics, Intelligent Systems and Signal Processing Vol. 2**. Changsha, China: IEEE, 2003. p. 1031–1035.

HUYNH, E. et al. Artificial intelligence in radiation oncology. **Nature Reviews Clinical Oncology**, v. 17, n. 12, p. 771–781, dez. 2020. ISSN 1759-4774, 1759-4782.

HWANG, K.-T. Clinical Databases for Breast Cancer Research. In: NOH, D.-Y.; HAN, W.; TOI, M. (Ed.). **Translational Research in Breast Cancer**. Singapore: Springer Singapore, 2021. v. 1187, p. 493–509. ISBN 978-981-329-619-0 978-981-329-620-6.

IBRAHIM, R. et al. Fractional Differential Texture Descriptors Based on the Machado Entropy for Image Splicing Detection. **Entropy**, v. 17, n. 7, p. 4775–4785, 2015.

INTERNATIONAL AGENCY FOR RESEARCH ON CANCER. **Global Cancer Observatory: Cancer Today**. 2020.

IOMIN, A. Toy model of fractional transport of cancer cells due to self-entrapping. **Physical Review E - Statistical, Nonlinear, and Soft Matter Physics**, v. 73, n. 6, p. 1–5, 2006.

IOMIN, A. Fractional kinetics under external forcing. **Nonlinear Dynamics**, Springer Netherlands, v. 80, n. 4, p. 1853–1860, 2014.

IONESCU, C. et al. The role of fractional calculus in modeling biological phenomena: A review. **Communications in Nonlinear Science and Numerical Simulation**, Elsevier, v. 51, p. 141–159, out. 2017.

IYIOLA, O. S.; ZAMAN, F. D. A fractional diffusion equation model for cancer tumor. **AIP Advances**, v. 4, n. 10, 2014.

JACKSON, T.; KOMAROVA, N.; SWANSON, K. Mathematical oncology: Using mathematics to enable cancer discoveries. **American Mathematical Monthly**, v. 121, n. 9, p. 840–856, 2014.

JAMALI, Y.; AZIMI, M.; MOFRAD, M. R. A sub-cellular viscoelastic model for cell population mechanics. **PLoS ONE**, v. 5, n. 8, 2010.

JEANQUARTIER, F. et al. In silico modeling for tumor growth visualization. **BMC Systems Biology**, BMC Systems Biology, v. 10, n. 1, p. 1–15, 2016.

KASHKOOLI, F. M. et al. Nexus between in silico and in vivo models to enhance clinical translation of nanomedicine. **Nano Today**, Elsevier, v. 36, p. 101057–101057, 2021.

KHAJANCHI, S.; NIETO, J. J. Mathematical modeling of tumor-immune competitive system, considering the role of time delay. **Applied Mathematics and Computation**, Elsevier Inc., v. 340, p. 180–205, 2019.

KHAJOTIA, R. et al. Unusually large breast tumour in a middle-aged woman. **Canadian Family Physician**, College of Family Physicians of Canada, v. 60, n. 2, p. 142–142, 2014.

KHOSHNEVISAN, D. **Multiparameter Processes**. New York, NY: Springer New York, 2002. (Springer Monographs in Mathematics). ISBN 978-1-4419-3009-5 978-0-387-21631-7.

KHOURY, M. J.; IOANNIDIS, J. P. A. Big data meets public health. **Science**, v. 346, n. 6213, p. 1054–1055, nov. 2014.

KILBAS, A. A. A.; SRIVASTAVA, H. M.; TRUJILLO, J. J. **Theory and Applications of Fractional Differential Equations**. [S.l.]: Elsevier Science Limited, 2006. v. 204.

KUMAR, D.; SINGH, J. **Fractional Calculus in Medical and Health Science**. First. Boca Raton, FL: CRC Press, 2020. ISBN 978-0-429-34056-7.

KUMAR, D. et al. An Efficient Computational Technique for Fractal Vehicular Traffic Flow. **Entropy**, Multidisciplinary Digital Publishing Institute, v. 20, n. 4, p. 259–259, abr. 2018.

KUMAR, S.; WEAVER, V. M. Mechanics, malignancy, and metastasis: The force journey of a tumor cell. **Cancer and Metastasis Reviews**, Springer US, v. 28, n. 1-2, p. 113–127, jun. 2009.

LAI, X. et al. A scalable solver for a stochastic, hybrid cellular automaton model of personalized breast cancer therapy. **International Journal for Numerical Methods in Biomedical Engineering**, v. 38, n. 1, jan. 2022. ISSN 2040-7939, 2040-7947.

LAIRD, A. K. Dynamics of Tumour Growth. **British journal of cancer**, Nature Publishing Group, v. 13, n. 3, p. 490–502, set. 1964.

LEE, R. S. et al. A curated mammography data set for use in computer-aided detection and diagnosis research. **Scientific Data**, v. 4, n. 1, p. 170177, dez. 2017. ISSN 2052-4463.

LEYDEN, K.; GOODWINE, B. Using fractional-order differential equations for health monitoring of a system of cooperating robots. **Proceedings of the IEEE International Conference on Robotics and Automation (ICRA)**, IEEE, p. 366–371, maio 2016. ISSN 978-1-4673-8026-3.

LOWENGRUB, J. S. et al. Nonlinear modelling of cancer: Bridging the gap between cells and tumours. **Nonlinearity**, v. 23, n. 1, p. 1–91, jan. 2010.

LUCHKO, Y.; KOCHUBEI, A. **Handbook of Fractional Calculus with Applications. Volume 2: Fractional Differential Equations**. First. Berlin/Boston: De Gruyter, 2019. ISBN 978-3-11-057166-0.

MACHADO, J. A. T. Entropy analysis of integer and fractional dynamical systems. **Nonlinear Dynamics**, v. 62, n. 1-2, p. 371–378, 2010. ISSN 0924-090X.

MACHADO, J. A. T. et al. Some Applications of Fractional Calculus in Engineering. **Mathematical Problems in Engineering**, Hindawi Publishing Corporation, v. 2010, p. 1–34, 2010.

MACHADO, J. T. A probabilistic interpretation of the fractional-order differentiation. **Fractional Calculus and Applied Analysis**, v. 6, p. 73–79, 2003.

MAGIN, R. L. Fractional Calculus in Bioengineering, Part 2. **Critical Reviews in Biomedical Engineering**, Begel House Inc., v. 32, n. 2, p. 105–194, 2004.

MAGIN, R. L. Fractional calculus models of complex dynamics in biological tissues. **Computers & Mathematics with Applications**, Pergamon, v. 59, n. 5, p. 1586–1593, mar. 2010.

MAGIN, R. L. Fractional calculus in bioengineering: A tool to model complex dynamics. **Proceedings of the 2012 13th International Carpathian Control Conference, ICCC 2012**, p. 464–469, 2012. ISSN 9781457718687.

MAGIN, R. L. et al. Anomalous diffusion expressed through fractional order differential operators in the Bloch–Torrey equation. **Journal of Magnetic Resonance**, Academic Press, v. 190, n. 2, p. 255–270, fev. 2008.

MAGIN, R. L. et al. Fractional Order Complexity Model of the Diffusion Signal Decay in MRI. **Mathematics**, Multidisciplinary Digital Publishing Institute, v. 7, n. 4, p. 348–348, abr. 2019.

MAINARDI, F. An historical perspective on fractional calculus in linear viscoelasticity. **Fractional Calculus and Applied Analysis**, Versita, v. 15, n. 4, p. 712–717, jan. 2012.

MAINARDI, F. Fractional Calculus: Theory and Applications. **Mathematics**, v. 6, n. 9, p. 145–145, ago. 2018. ISSN 9783038972068.

MANIMARAN, J. et al. Numerical Solutions for Time-Fractional Cancer Invasion System With Nonlocal Diffusion. **Frontiers in Physics**, v. 7, n. July, p. 1–16, 2019.

MARU' I , M. et al. Analysis of growth of multicellular tumour spheroids by mathematical models. **Cell Proliferation**, v. 27, n. 2, p. 73–94, 1994.

MATOZ-FERNANDEZ, D. A. et al. Nonlinear Rheology in a Model Biological Tissue. **Physical Review Letters**, American Physical Society, v. 118, n. 15, p. 158105–158105, abr. 2017.

MERAL, F.; ROYSTON, T.; MAGIN, R. Fractional calculus in viscoelasticity: An experimental study. **Communications in Nonlinear Science and Numerical Simulation**, v. 15, n. 4, p. 939–945, abr. 2010. ISSN 10075704.

MESCIA, L.; BIA, P.; CARATELLI, D. Fractional-Calculus-Based Electromagnetic Tool to Study Pulse Propagation in Arbitrary Dispersive Dielectrics. **physica status solidi (a)**, John Wiley & Sons, Ltd, v. 216, n. 3, p. 1–13, fev. 2019.

METZCAR, J. et al. A Review of Cell-Based Computational Modeling in Cancer Biology. **JCO Clinical Cancer Informatics**, n. 3, p. 1–13, 2019.

MEYER, A.-M. et al. Big Data for Population-Based Cancer Research. **North Carolina Medical Journal**, v. 75, n. 4, p. 265–269, jul. 2014. ISSN 9780444518323.

MILJKOVI , N. et al. ECG artifact cancellation in surface EMG signals by fractional order calculus application. **Computer Methods and Programs in Biomedicine**, v. 140, p. 259–264, 2017.

MITRI, Z. I. et al. Implementing a comprehensive translational oncology platform: From molecular testing to actionability. **Journal of Translational Medicine**, BioMed Central, v. 16, n. 1, p. 1–10, 2018.

MOHAMAD, A. A. **Lattice Boltzmann Method**. London: Springer London, 2019. v. 5. 9507 p. ISBN 978-1-4471-7422-6.

MURPHY, H.; JAAFARI, H.; DOBROVOLNY, H. M. Differences in predictions of ODE models of tumor growth: A cautionary example. **BMC Cancer**, BMC Cancer, v. 16, n. 1, p. 1–10, 2016.

NAMAZI, H.; KULISH, V. V.; WONG, A. Mathematical Modelling and Prediction of the Effect of Chemotherapy on Cancer Cells. **Scientific Reports**, Nature Publishing Group, v. 5, n. 1, p. 13583–13583, out. 2015.

NENOFF, L. et al. Deformable image registration uncertainty for inter-fractional dose accumulation of lung cancer proton therapy. **Radiotherapy and Oncology**, The Author(s), v. 147, p. 178–185, 2020.

NIU, H.; CHEN, Y.; WEST, B. J. Why Do Big Data and Machine Learning Entail the Fractional Dynamics? **Entropy**, v. 23, n. 3, p. 297, fev. 2021. ISSN 1099-4300.

NORTON, K. A. et al. Multiscale agent-based and hybrid modeling of the tumor immune microenvironment. **Processes**, v. 7, n. 1, p. 1–23, 2019.

NORTON, L. A Gompertzian Model of Human Breast Cancer Growth. **Cancer research**, v. 48, n. 24, p. 7067–7071, 1988.

OLDHAM, K. B.; SPANIER, J. **The Fractional Calculus - Theory and Applications of Differentiation and Integration to Arbitrary Order**. New York: Academic Press, 1974.

ORTIGUEIRA, M.; BENGOCHEA, G. A new look at the fractionalization of the logistic equation. **Physica A: Statistical Mechanics and its Applications**, Elsevier B.V., v. 467, p. 554–561, 2017.

ORTIGUEIRA, M.; MACHADO, J. Which Derivative? **Fractal and Fractional**, v. 1, n. 1, p. 3–3, jul. 2017.

ORTIGUEIRA, M. D.; VALÉRIO, D.; MACHADO, J. T. Variable order fractional systems. **Communications in Nonlinear Science and Numerical Simulation**, Elsevier B.V., v. 71, p. 231–243, 2019.

PANG, B.; NIJKAMP, E.; WU, Y. N. Deep Learning With TensorFlow: A Review. **Journal of Educational and Behavioral Statistics**, v. 45, n. 2, p. 227–248, abr. 2020. ISSN 1076-9986, 1935-1054.

PHAM, K. et al. Density-dependent quiescence in glioma invasion: Instability in a simple reaction-diffusion model for the migration/proliferation dichotomy. **Journal of Biological Dynamics**, v. 6, n. SUPPL. 1, p. 54–71, 2012.

PHILLIPS, C. M. et al. A hybrid model of tumor growth and angiogenesis: In silico experiments. **PLoS ONE**, v. 15, n. 4, p. 1–27, 2020. ISSN 1111111111.

PODLUBNY, I. Geometric and Physical Interpretation of Fractional Integration and Fractional Differentiation. **Fractional Calculus and Applied Analysis**, v. 5, n. 4, p. 367–386, out. 2001.

POLESZCZUK, J.; ENDERLING, H. A High-Performance Cellular Automaton Model of Tumor Growth with Dynamically Growing Domains. **Applied Mathematics**, v. 05, n. 01, p. 144–152, 2014.

POLOVINKINA, M. V. et al. Stability of stationary solutions for the glioma growth equations with radial or axial symmetries. **Mathematical Methods in the Applied Sciences**, p. 1–14, jan. 2021.

PORTA, C. L.; ZAPPERI, S. **The Physics of Cancer**. Cambridge: Cambridge University Press, 2017. 172 p. ISBN 978-1-316-27175-9.

QIU, S. et al. Characterizing viscoelastic properties of breast cancer tissue in a mouse model using indentation. **Journal of Biomechanics**, Elsevier Ltd, v. 69, p. 81–89, 2018.

RAMIÃO, N. G. et al. Biomechanical properties of breast tissue, a state-of-the-art review. **Biomechanics and Modeling in Mechanobiology**, Springer Berlin Heidelberg, v. 15, n. 5, p. 1307–1323, 2016.

RANGAYYAN, R. M. et al. Effect of Pixel Resolution on Texture Features of Breast Masses in Mammograms. **Journal of Digital Imaging**, v. 23, n. 5, p. 547–553, out. 2010. ISSN 0897-1889, 1618-727X.

REJNIAK, K. A. **Systems Biology of Tumor Microenvironment - Quantitative Modeling and Simulations**. [S.l.]: Springer International Publishing, 2016. v. 936. 249 p. (Advances in Experimental Medicine and Biology, v. 936). ISBN 978-3-319-42023-3.

REJNIAK, K. A.; ANDERSON, A. R. Hybrid models of tumor growth. **Wiley Interdisciplinary Reviews: Systems Biology and Medicine**, v. 3, n. 1, p. 115–125, 2011.

REN, G.; YU, Y.; CHEN, Y. Q. Fractional Dynamics for Coupled CTRW Optimal Random Search Algorithm. **SSRN Electronic Journal**, n. July 2019, 2018.

RICE, A.; DEL RIO HERNANDEZ, A. Biomechanics of cancer cells. In: LADAME, S.; CHANG, J. Y. H. (Ed.). **Bioengineering Innovative Solutions for Cancer**. [S.l.]: Elsevier, 2020. p. 327–361. ISBN 978-0-12-813886-1.

ROCKNE, R. C. et al. The 2019 mathematical oncology roadmap. **Physical Biology**, v. 16, n. 4, p. 041005, jun. 2019. ISSN 1478-3975.

ROCKNE, R. C.; SCOTT, J. G. Introduction to Mathematical Oncology. **JCO Clinical Cancer Informatics**, n. 3, p. 1–4, nov. 2019. ISSN 9781584889915.

RODRIGUEZ-BRENES, I. A.; KOMAROVA, N. L.; WODARZ, D. Tumor growth dynamics: Insights into evolutionary processes. **Trends in Ecology and Evolution**, Elsevier Ltd, v. 28, n. 10, p. 597–604, 2013.

ROSS, B. Fractional Calculus. **Mathematics Magazine**, v. 50, n. 3, p. 115–122, 1977.

SABATIER, J.; FARGES, C.; TARTAGLIONE, V. **Fractional Behaviours Modelling: Analysis and Application of Several Unusual Tools**. Cham: Springer International Publishing, 2022. v. 101. (Intelligent Systems, Control and Automation: Science and Engineering, v. 101). ISBN 978-3-030-96748-2 978-3-030-96749-9.

SACHS, R.; HLATKY, L.; HAHNFELDT, P. Simple ODE models of tumor growth and anti-angiogenic or radiation treatment. **Mathematical and Computer Modelling**, Pergamon, v. 33, n. 12-13, p. 1297–1305, jun. 2001.

SAGUY, I. S. Challenges and opportunities in food engineering: Modeling, virtualization, open innovation and social responsibility. **Journal of Food Engineering**, Elsevier, v. 176, p. 2–8, maio 2016.

SALES TEODORO, G.; TENREIRO MACHADO, J. A.; CAPELAS DE OLIVEIRA, E. A review of definitions of fractional derivatives and other operators. **Journal of Computational Physics**, Academic Press, v. 388, p. 195–208, jul. 2019.

SAMKO, S. G.; ROSS, B. Integration and differentiation to a variable fractional order. **Integral Transforms and Special Functions**, v. 1, n. 4, p. 277–300, 1993.

SANTOS, M. L. de Souza. **Analytical and Approximate Methods in Transport Phenomena**. First. Boca Raton, FL: CRC Press, 2007.

SARAPATA, E. A.; DE PILLIS, L. G. A Comparison and Catalog of Intrinsic Tumor Growth Models. **Bulletin of Mathematical Biology**, v. 76, n. 8, p. 2010–2024, 2014.

SARHADDI, M.; YAGHOOBI, M. A new approach in cancer treatment regimen using adaptive fuzzy back-stepping sliding mode control and tumor-immunity fractional order model. **Biocybernetics and Biomedical Engineering**, Nalecz Institute of Biocybernetics and Biomedical Engineering of the Polish Academy of Sciences, v. 40, n. 4, p. 1654–1665, 2020.

SAVAGEAU, M. A. Growth equations: A general equation and a survey of special cases. **Mathematical Biosciences**, Elsevier, v. 48, n. 3-4, p. 267–278, abr. 1980.

SAWYER-LEE, R. et al. **Curated Breast Imaging Subset of DDSM**. [S.l.]: The Cancer Imaging Archive, 2016.

SCHNECKENREITHER, G. Developing mathematical formalisms for cellular automata in modelling and simulation. TU Wien, p. 144 pages, 2014.

SINGH, J.; KUMAR, D.; BALEANU, D. On the analysis of chemical kinetics system pertaining to a fractional derivative with Mittag-Leffler type kernel. **Chaos: An Interdisciplinary Journal of Nonlinear Science**, AIP Publishing LLC, v. 27, n. 10, p. 103113–103113, out. 2017.

SOLÍS-PÉREZ, J.; GÓMEZ-AGUILAR, J.; ATANGANA, A. A fractional mathematical model of breast cancer competition model. **Chaos, Solitons & Fractals**, v. 127, p. 38–54, out. 2019.

SOWNDARRAJAN, P. T. et al. Distributed optimal control of a tumor growth treatment model with cross-diffusion effect. **European Physical Journal Plus**, v. 134, n. 9, 2019.

SPENCER, S. L. et al. An ordinary differential equation model for the multistep transformation to cancer. **Journal of Theoretical Biology**, v. 231, n. 4, p. 515–524, 2004.

SWEILAM, N. et al. Optimal control of variable-order fractional model for delay cancer treatments. **Applied Mathematical Modelling**, v. 89, p. 1557–1574, jan. 2021. ISSN 0307904X.

SWEILAM, N. et al. Optimal Control of Variable-Order Fractional Model for Delay Cancer Treatments. **Applied Mathematical Modelling**, Elsevier Inc., ago. 2020.

TALONI, A. et al. Mechanical Properties of Growing Melanocytic Nevi and the Progression to Melanoma. **PLoS ONE**, Public Library of Science, v. 9, n. 4, p. e94229–e94229, abr. 2014.

TALONI, A. et al. The role of pressure in cancer growth. **The European Physical Journal Plus**, Springer Berlin Heidelberg, v. 130, n. 11, p. 224–224, nov. 2015.

TARASOV, V. E. Rules for fractional-dynamic generalizations: Difficulties of constructing fractional dynamic models. **Mathematics**, v. 7, n. 6, p. 1–50, 2019.

TARASOV, V. E.; TARASOVA, V. V. Logistic equation with continuously distributed lag and application in economics. **Nonlinear Dynamics**, Springer Netherlands, v. 97, n. 2, p. 1313–1328, 2019. ISSN 1107101905.

TEODORO, G. S.; OLIVEIRA, D. S.; CAPELAS DE OLIVEIRA, E. de. Sobre derivadas fracionárias. **Revista Brasileira de Ensino de Física**, v. 40, n. 2, out. 2017.

TJØRVE, K. M. C.; TJØRVE, E. The use of Gompertz models in growth analyses, and new Gompertz-model approach: An addition to the Unified-Richards family. **PLOS ONE**, Public Library of Science, v. 12, n. 6, p. e0178691–e0178691, jun. 2017.

TRACQUI, P. Biophysical models of tumour growth. **Reports on Progress in Physics**, v. 72, n. 5, 2009.

TRUJILLO, J. J.; RIBERO, M.; BONILLA, B. On a Riemann – Liouville Generalized Taylor's Formula. **Journal of Mathematical Analysis and Applications**, v. 231, p. 255–265, 1999.

UCAR, E.; ÖZDEMIR, N.; ALTUN, E. Fractional order model of immune cells influenced by cancer cells. **Mathematical Modelling of Natural Phenomena**, v. 14, n. 3, 2019.

VALENTIM, C. A. **Generalização Da Termoacústica Linear de Rott a Partir de Um Modelo de Ordem Fracionária**. 2018. 117 p. Tese (Doutorado), 2018.

VALENTIM, C. A. **Code: Stochastic agent-based cellular automaton model for tumor dynamics**. 2022. <https://github.com/carlosvalentim/phd-published/blob/main/CBM-2022_Valentim-et-al_Cellular-automaton-model.py>. Made available on December 4, 2022.

VALENTIM, C. A.; INACIO, C. M. C.; DAVID, S. A. Fractal Methods and Power Spectral Density as Means to Explore EEG Patterns in Patients Undertaking Mental Tasks. **Fractal and Fractional**, v. 5, n. 4, p. 225, nov. 2021. ISSN 2504-3110.

VALENTIM, C. A. et al. Mathematical Epidemiology through Transport Phenomena Viewpoint: Generalized Coordinates to Categorize People and Preliminary Numerical Results towards COVID-19. **International Journal of Advanced Thermofluid Research**, v. 7, n. 1, p. 3–25, jun. 2021. ISSN 2455-1368.

VALENTIM, C. A. et al. Can fractional calculus help improve tumor growth models? **Journal of Computational and Applied Mathematics**, Elsevier B.V., v. 379, n. 112964, p. 112964–112964, dez. 2020.

VALENTIM, C. A.; RABI, J. A.; DAVID, S. A. Fractional modeling applied to tilting-pad journal bearings. **International Journal of Dynamics and Control**, Springer Berlin Heidelberg, 2020.

VALENTIM, C. A.; RABI, J. A.; DAVID, S. A. Fractional Mathematical Oncology: On the potential of non-integer order calculus applied to interdisciplinary models. **Biosystems**, v. 204, p. 104377, jun. 2021. ISSN 03032647.

VALENTIM, C. A.; RABI, J. A.; DAVID, S. A. Cellular-automaton model for tumor growth dynamics: Virtualization of different scenarios. **Computers in Biology and Medicine**, v. 153, p. 106481, fev. 2023. ISSN 00104825.

VALENTIM, C. A. et al. On multistep tumor growth models of fractional variable-order. **Biosystems**, v. 199, p. 104294, jan. 2021. ISSN 03032647.

VALÉRIO, D.; COSTA, J. S. D. Variable-order fractional derivatives and their numerical approximations. **Signal Processing**, v. 91, n. 3, p. 470–483, 2011.

VALÉRIO, D. et al. Fractional calculus: A survey of useful formulas. **The European Physical Journal Special Topics**, v. 222, n. 8, p. 1827–1846, out. 2013.

VARALTA, N.; GOMES, A. V.; CAMARGO, R. F. A Prelude to the Fractional Calculus Applied to Tumor Dynamic. **Tendências em Matemática Aplicada e Computacional**, v. 15, n. 2, p. 211–221, 2014.

VON BERTALANFFY, L. Principles and theory of growth. **Fundamental aspects of normal and malignant growth**, Elsevier, Amsterdam, v. 493, p. 137–259, 1960.

WANG, Z. et al. Simulating cancer growth with multiscale agent-based modeling. **Seminars in Cancer Biology**, Elsevier Ltd, v. 30, p. 70–78, 2015.

WEERASINGHE, H. N. et al. Mathematical Models of Cancer Cell Plasticity. **Journal of Oncology**, v. 2019, 2019.

WEST, B. J. Colloquium: Fractional calculus view of complexity: A tutorial. **Reviews of Modern Physics**, v. 86, n. 4, p. 1169–1184, 2014. ISSN 0034-6861\r1539-0756.

WEST, B. J. Fractional Calculus and the Future of Science. **Entropy**, v. 23, n. 12, p. 1566, nov. 2021. ISSN 1099-4300.

WEST, B. J. The Fractal Tapestry of Life: II Entailment of Fractional Oncology by Physiology Networks. **Frontiers in Network Physiology**, v. 2, p. 845495, mar. 2022. ISSN 2674-0109.

WEST, G. B.; BROWN, J. H.; ENQUIST, B. J. A general model for ontogenetic growth. **Nature**, Nature Publishing Group, v. 413, n. 6856, p. 628–631, out. 2001.

WIMAN, A. über den Fundamentalsatz in der Teorie der Funktionen Ea (x). **Acta Mathematica**, v. 29, n. 1, p. 191–201, 1905.

WODARZ, D.; KOMAROVA, N. L. **Dynamics of Cancer**. Singapore: World Scientific, 2014. 563 p. ISBN 978-981-4566-36-0.

WONG, K. C. et al. Tumor growth prediction with reaction-diffusion and hyperelastic biomechanical model by physiological data fusion. **Medical Image Analysis**, Elsevier, v. 25, n. 1, p. 72–85, out. 2015.

WORLD HEALTH ORGANIZATION. **Breast Cancer: Fact Sheet.** 2021.

WORSCHECH, A. et al. Systemic treatment of xenografts with vaccinia virus GLV-1h68 reveals the immunologic facet of oncolytic therapy. **BMC Genomics**, v. 10, 2009.

WU, E. Q. et al. Detecting Fatigue Status of Pilots Based on Deep Learning Network Using EEG Signals. **IEEE Transactions on Cognitive and Developmental Systems**, v. 13, n. 3, p. 575–585, set. 2021. ISSN 2379-8920, 2379-8939.

WU, G.-C. et al. Discrete fractional diffusion equation. **Nonlinear Dynamics**, Springer Netherlands, v. 80, n. 1-2, p. 281–286, abr. 2015.

XIE, J. et al. The Differential Feature Detection and the Clustering Analysis to Breast Cancers. In: FUJITA, H. et al. (Ed.). **Trends in Artificial Intelligence Theory and Applications. Artificial Intelligence Practices**. Cham: Springer International Publishing, 2020. v. 12144, p. 457–469. ISBN 978-3-030-55788-1 978-3-030-55789-8.

XU, J.; VILANOVA, G.; GOMEZ, H. A Mathematical Model Coupling Tumor Growth and Angiogenesis. **PLOS ONE**, Public Library of Science, v. 11, n. 2, p. e0149422–e0149422, fev. 2016.

YALA, A. et al. A Deep Learning Model to Triage Screening Mammograms: A Simulation Study. **Radiology**, v. 293, n. 1, p. 38–46, out. 2019. ISSN 0033-8419, 1527-1315.

YI, P. H. et al. DeepCAT: Deep Computer-Aided Triage of Screening Mammography. **Journal of Digital Imaging**, v. 34, n. 1, p. 27–35, fev. 2021. ISSN 0897-1889, 1618-727X.

YILDIZ, T. A.; ARSHAD, S.; BALEANU, D. Optimal chemotherapy and immunotherapy schedules for a cancer-obesity model with Caputo time fractional derivative. **Mathematical Methods in the Applied Sciences**, v. 41, n. 18, p. 9390–9407, dez. 2018.

ZANGOOEI, M. H.; HABIBI, J. Hybrid multiscale modeling and prediction of cancer cell behavior. **PLoS ONE**, v. 12, n. 8, p. 1–26, 2017. ISSN 1111111111.

ZHENG, X. et al. Ensemble deep learning for automated visual classification using EEG signals. **Pattern Recognition**, v. 102, p. 107147, jun. 2020. ISSN 00313203.

APPENDIX A PUBLISHED CONTENT, COLLABORATIONS AND AWARD

As the main text mentions, chapters 3, 4, 5, and 6 were fully published and made available to the research community as the following papers:

VALENTIM, C. A. et al. Can fractional calculus help improve tumor growth models? **Journal of Computational and Applied Mathematics**, Elsevier B.V., v. 379, n. 112964, p. 112964–112964, dez. 2020.

Impact Factor: 2.872. **Google Scholar Citations:** 35.

VALENTIM, C. A. et al. On multistep tumor growth models of fractional variable-order. **Biosystems**, v. 199, p. 104294, jan. 2021. ISSN 03032647.

Impact Factor: 1.957. **Google Scholar Citations:** 19.

VALENTIM, C. A.; RABI, J. A.; DAVID, S. A. Fractional Mathematical Oncology: On the potential of non-integer order calculus applied to interdisciplinary models. **Biosystems**, v. 204, p. 104377, jun. 2021. ISSN 03032647.

Impact Factor: 1.957. **Google Scholar Citations:** 11.

VALENTIM, C. A.; RABI, J. A.; DAVID, S. A. Cellular-automaton model for tumor growth dynamics: Virtualization of different scenarios. **Computers in Biology and Medicine**, v. 153, p. 106481, fev. 2023. ISSN 00104825.

Impact Factor: 6.698. **Google Scholar Citations:** –.

In addition, during the development of this thesis, the author has participated in other projects involving dynamic systems modeling applied to health-related applications. Despite not directly resulting from the doctorate, the following papers have also been produced and published in collaboration with the author:

DAVID, S. A.; VALENTIM, C. A.; DEBBOUCHE, A. Fractional Modeling Applied to the Dynamics of the Action Potential in Cardiac Tissue. **Fractal and Fractional**, v. 6, n. 3, p. 149, mar. 2022. ISSN 2504-3110.

Impact Factor: 5.400. **Google Scholar Citations:** 5.

VALENTIM, C. A.; INACIO, C. M. C.; DAVID, S. A. Fractal Methods and Power Spectral Density as Means to Explore EEG Patterns in Patients Undertaking Mental Tasks. **Fractal and Fractional**, v. 5, n. 4, p. 225, nov. 2021. ISSN 2504-3110.

Impact Factor: 5.400. **Google Scholar Citations:** 8.

VALENTIM, C. A. et al. Mathematical Epidemiology through Transport Phenomena Viewpoint: Generalized Coordinates to Categorize People and Preliminary Numerical Results towards COVID-19. **International Journal of Advanced Thermofluid Research**, v. 7, n. 1, p. 3–25, jun. 2021. ISSN 2455-1368.

Impact Factor: –. **Google Scholar Citations:** 1.

DEBBOUCHE, A. et al. On the stability of stationary solutions in diffusion models of oncological processes. **The European Physical Journal Plus**, Springer Berlin Heidelberg, v. 136, n. 1, p. 131–131, jan. 2021. ISSN 0123456789.

Impact Factor: 3.400. **Google Scholar Citations:** 17.

DAVID, S. et al. A combined measure to differentiate EEG signals using fractal dimension and MFDFA-Hurst. **Communications in Nonlinear Science and Numerical Simulation**, v. 84, 2020.

Impact Factor: 4.186. **Google Scholar Citations:** 28.

The author has also participated in the following conferences:

VALENTIM, C.A.; RABI, J.A.; DAVID, S.A., Cellular-automaton simulation of tumor growth dynamics: from computational implementation to case analysis. In: **XLI National Conference in Applied and Computational Mathematics (CNMAC 2022)**, 2022, Campinas, Brazil on September 25-29.

VALENTIM, C.A.; RABI, J.A.; DAVID, S.A., Stochastic cellular automaton for modeling benign and invasive tumor dynamics. In: **International Conference on Mathematical Analysis and Applications in Science and Engineering-ICMAS2SC'22**, 2022, Porto, Portugal on June 27-29.

VALENTIM, C.A.; RABI, J.A.; DAVID, S.A. Fractional mathematical oncology: cancer-related dynamics under an interdisciplinary view. In: **First Online Conference on Modern Fractional Calculus and Its Applications (OCMFCA I)**, 2020, Istanbul, Turkey. Online.

VALENTIM, C. A.; DE OLIVEIRA, N. A.; RABI, J. A.; DAVID, S. A. Tumor tissue as soft matter – computational modeling based on fractional calculus. In: **International Symposium in Material Science and Engineering (SICEM XX)**, 2019, São Carlos, Brazil, on November 19.

Finally, the author was awarded with honorable mention in "2021 TV Cultura Video Contest for Graduate Students" sponsored by the University of São Paulo, for which a short video was produced to explain and publicize the research theme of this doctorate. The video can be found at University of São Paulo's official Youtube page.

Note: Impact Factors and citations counted as of July 2, 2023.